A STATISTICAL ANALYSIS OF THE TRANSITION ZONE OF THE S-N CURVE FOR AISI 4340 STEEL

by

Neal Robert Kennedy

A Thesis Submitted to the Faculty of the

DEPARTMENT OF AEROSPACE AND MECHANICAL ENGINEERING

In Partial Fulfillment of the Requirements
For the Degree of

MASTER OF SCIENCE
WITH A MAJOR IN MECHANICAL ENGINEERING

In the Graduate College

THE UNIVERSITY OF ARIZONA

1 9 7 0

STATEMENT BY AUTHOR

This thesis has been submitted in partial fulfillment of the requirements for an advanced degree at The University of Arizona and is deposited in the University Library to be made available to borrowers under rules of the Library.

Brief quotations from this thesis are allowable without special permission, provided that accurate acknowledgement of source is made. Requests for permission for extended quotation from or reproduction of this manuscript in whole or in part may be granted by the copyright holder.

SIGNED: 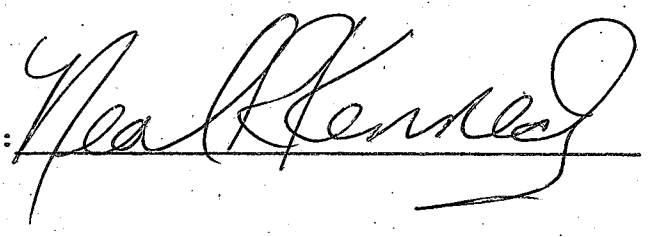

APPROVAL BY THESIS DIRECTOR

This thesis has been approved on the date shown below.

Edward B. Haugen
Professor of Engineering

July 22, 1970
Date

ACKNOWLEDGMENTS

The author would like to express his appreciation to Professor Edward B. Haugen of the Aerospace and Mechanical Engineering Department for his aid in the preparation of this thesis. Without his help in the development of the problem and its solution the thesis would not have been possible.

The author would also like to thank Dr. H. D. Christensen and Mr. Duane Dietrich for reading this report and offering suggestions and criticism.

TABLE OF CONTENTS

TABLE OF CONTENTS--Continued

LIST OF ILLUSTRATIONS

LIST OF ILLUSTRATIONS--Continued

LIST OF ILLUSTRATIONS--Continued

LIST OF TABLES

ABSTRACT

The principle objective of this thesis was to define the transition zone of the S-N curve for cold drawn and annealed AISI 4340 steel by statistical fatigue testing. The results are correlated with recent fatigue theory in an effort to analyze the phenomena, with estimates made of the relationship between elastic and plastic strain and cycle life. An introduction to fatigue is presented to give the reader more insight into the area of interest.

The testing methods are detailed and the fatigue testing equipment used is described. Data was generated to give strain distributions at a series of cycle lives. The reduced data is shown to agree with recent theory and a procedure is outlined to develop a cyclic stress range-strain range curve. The strain distributions were converted to stress using this estimated cyclic stress range-strain range curve. The final result is the desired statistical S-N surface defining the transition and endurance regions applicable to probabilistic design methods.

CHAPTER 1

INTRODUCTION

In the literature of mechanical and structural design, the S-N curve is the generally accepted representation when plotting fatigue data for reversed bending or reversed torsion loading. Each S-N curve is a plot of stress intensity versus cycles to failure for a particular material and condition. Recently developed theory postulates that at the upper end of the S-N curve (for steels) where the stress levels are high and approach yield intensity, plastic strain is the dominant factor in fatigue. Near the transition zone, where the S-N curve begins to flatten out and where stress intensities are of the order of the endurance level or slightly larger, elastic strains are dominant in the total strain makeup. Thus, it is conjectured that the failure mechanism undergoes a change in the transition area.

It is these fatigue failure phenomena that are the subjects of investigation in this study. An extensive program of testing was planned and carried out to thoroughly investigate the transition zone of the S-N curve and determine its shape for one ferrous alloy, cold drawn and annealed AISI 4340 steel. The results and findings, as well as the methods by which they were obtained are presented later in this thesis. Comparisons and analyses will be made between the experimental data and the latest theory that is to be found in the literature.

In the field of machine design, the design of civil structures, etc., the trend in recent years has been more and more toward the consideration of probabilistic methods in design. The concept of safety factor has been shown to be limited in that it cannot answer the question, "How safe?" Instead, because most engineering variables are statistical functions and are characterized by a distribution of values, probabilistic methods are used to determine the probability of failure which, in each case, is related to the reliability of the final design. See Figure 1-1.

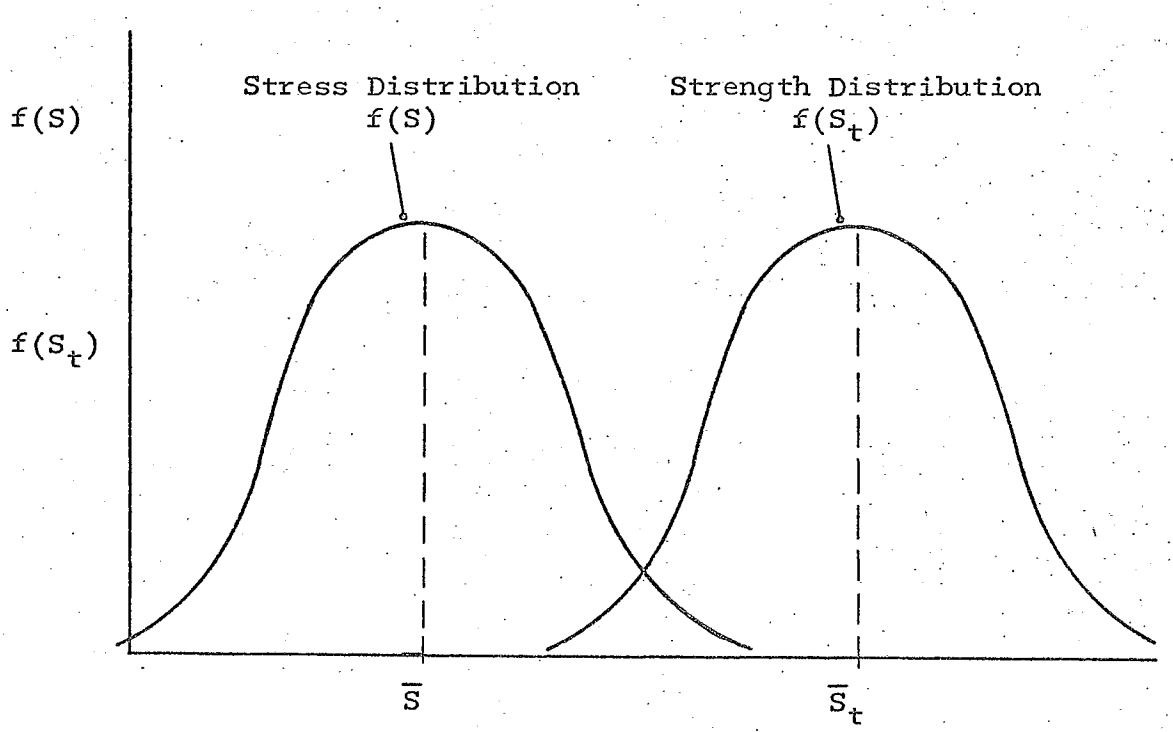

Figure 1-1. Graphical Relationship between Stress and Strength Distributions (1, p. 5).

The area of overlap of the stress and strength distributions (due to the ranges of both) indicates the finite probability of failure, which can be expressed as a function of the mean values and the standard deviations of the stress and strength (1, p. 5).

The problem, then, is to find these stress and strength distributions. The stress distribution is dependent, of course, on the loading conditions of the member in question and supposedly the designer would have some knowledge of this, either from previous conditions on similar equipment or because he has chosen the conditions in the first place. Finding the strength distribution is quite another problem. The strength of the material can depend on many things: the nature of the material itself, size, and the number of expected load cycles if the loading is not static, to mention a few. The only way to determine basic strength properties is through rather extensive testing, and recently there has begun to be an accumulation of the data that can be useful to the average designer. Even so, fatigue test data is still fairly scarce for many commonly used materials.

As mentioned, loading conditions need not be static and, in fact, frequently are not. When a member is expected to operate without failure for a minimum number of cycles under given loads, the problem of fatigue must be considered. The strength of a material decreases considerably as the number of cycles that it must endure increases. This decrease in strength is attributed to

the phenomenon of fatigue. The relationship between stress intensity and cycle life is plotted and, the result is the familiar S-N curve. An example of the S-N curve is shown in Figure 1-2.

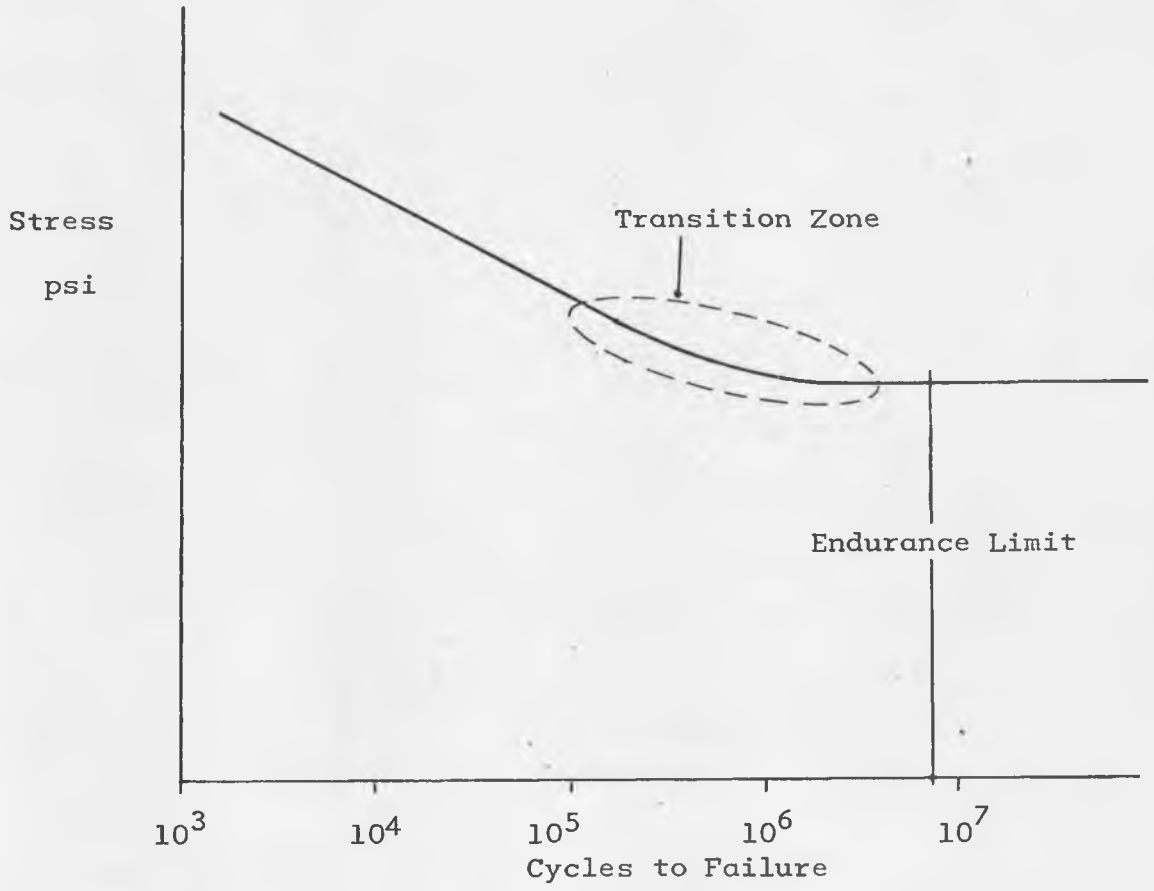

Figure 1-2. Example of an S-N Curve for Ferrous Materials Showing the Transition Zone and Endurance Limit.

1-1. Background on Fatigue

Before discussing the transition zone or the endurance limit in detail, the fatigue phenomenon will be reviewed. The

review is not presented as an authoratative dissertation on the subject but as an introduction to the problem with which this paper is concerned.

Fatigue is a progressive cracking in a material that is the result of repeated cyclic loading which, unless detected, will eventually end in complete rupture. The loads required for the fatigue fracture of a structural member are less intense than those required under static conditions, i.e., less than yield. This is immediately evident from the example S-N curve shown in Figure 1-2. Fatigue failure is dependent upon the interaction of cyclic stress, tensile stress and plastic strain. There will be no fatigue failure without these conditions (2, p. 2). Without cyclic loading or repeated stochastic loading, the concern is with a static problem. Compressive loads are not conducive to crack formation or growth, and therefore it is the tensile stress that is required for crack formation and propagation. Theoretically, also, there is no fatigue damage unless plastic strain is present (3, p. 134).

The first stage of fatigue starts with individual atoms in the material crystal grains. This is due to the fact that no materials are perfectly homogeneous. Fatigue is primarily a property of crystalline solids wherein the dislocations originally present in the crystals multiply rapidly even when cycled just a few times (2, p. 107). Eventually in the first stage of fatigue, the crystals are strain hardened to saturation and then dislocation

motion may be fully reversed with each cycle. This phenomenon, called cold-working, can sometimes lead to the annihilation of dislocations and relief of lattice strains, i.e., strain softening.

The second stage in the fatigue process involves the formation of submicroscopic intrusions as a result of loss of ductility. The intrusions are actually fissures that develop along the persistent slip planes. The actual cracks initiate in these intrusions.

In the final stage of fatigue the submicroscopic cracks concentrate stress, with subsequent growth, until macroscopic cracks appear finally leading to failure (2, p. 107; 4, p. 51; 5, p. 161). As much as 99 percent of the fatigue life of a member can be spent in the first two stages (2, p. 107). All of these phenomena are related to plastic deformation, and not to ideal elastic strain. Except when obviously otherwise, fatigue is considered a surface phenomenon.

Since it is unlikely that the designer will know the complete internal structure of the material, it is important that he be able to determine where a fatigue crack will probably start and that he attempt to design to avoid such crack initiation. A common point of crack initiation is at a stress concentration.

Stress concentrations in engineering materials can be traced to many causes, such as particles of foreign matter or voids in the material. They also occur at the surface as the result of scratches, corrosion, press-fit assemblies, and the more obvious sharp corners and other geometric discontinuities (2, p. 4; 6, p. 330).

The effect of minute imperfections is dependent on material grain size (7, p. 94). When stress concentrations cannot be avoided, it is important to take into consideration their possible consequences. Although stress raisers sometimes can be ignored in static loading of ductile materials, this is not true of structural and machine elements subject to repeated loading and consequent stresses.

Testing results show that ductile materials fail in the same manner as brittle materials when subjected to cyclic loading (2, p. 3; 6, p. 331). The fracture surface usually can be divided into two distinct zones: (1) the fatigue zone and (2) the rupture zone. The fatigue zone is distinguished by a series of concentric concave marks called stop marks which indicate variations in the rate of crack propagations and herringbone patterned granular traces which show the origin of the original crack. The rupture zone is similar in appearance to that in static failure, i.e., it is characterized by a very rough material surface (2, p. 3).

1-2. The S-N Curve

To determine the fatigue behavior of any material, we must resort to experimental testing. When the results of simple reversed bending tests are plotted, they are usually the same basic S-N curves that have been used since Wöhler first started fatigue testing in 1858 (as shown in Figure 1-2). However, to produce data that is usable in the field of probabilistic design,

the testing is not as simple as might appear from the conventional single line S-N curve which is usually plotted. Fatigue, being statistical in nature (a random pheonomenon), requires that the S-N curve be regarded as a surface made up of a series of distributions, each of which defines a definite probability versus frequency relationship, e.g., not by a single line (4, p. 51). That is, the correct and complete representation resembles that shown in Figure 1-3. The conventional S-N curve becomes the 50 percent probability locus or mean line on the statistical S-N

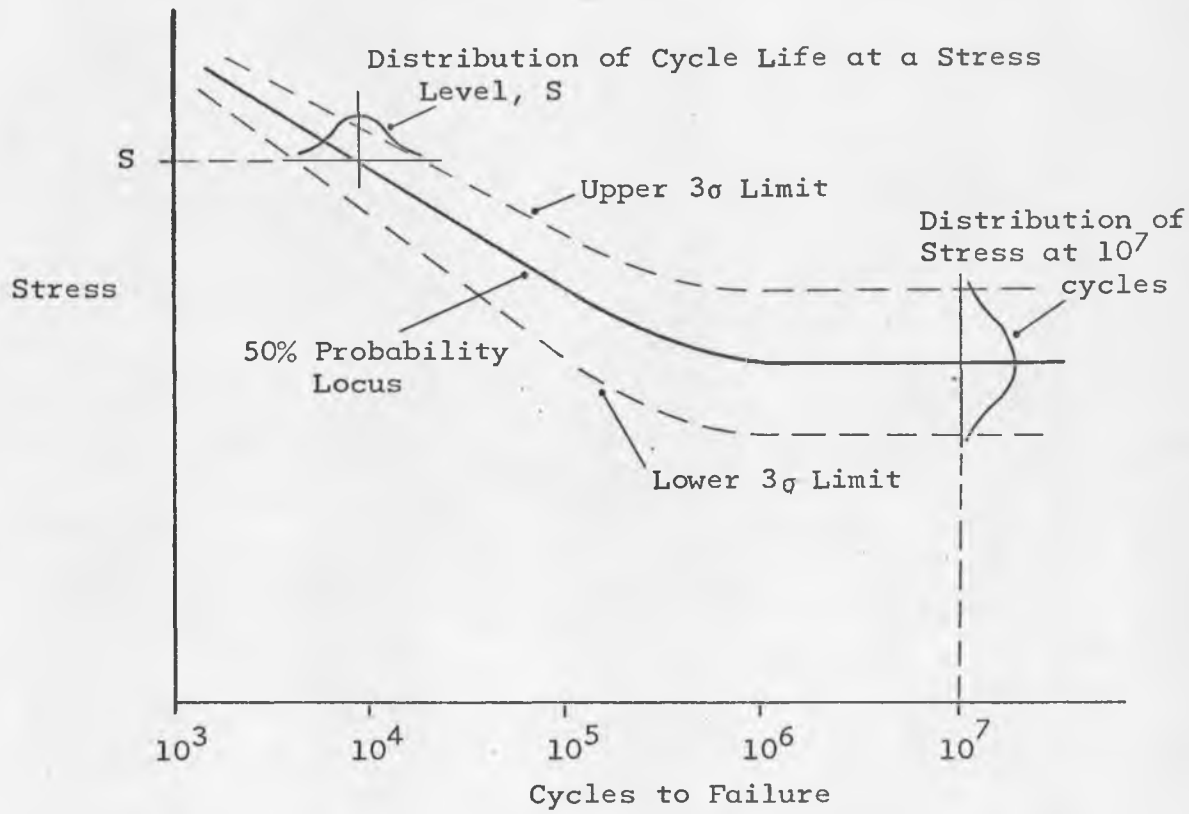

Figure 1-3. Example of a Statistical S-N Surface for Ferrous Materials.

Surface. The dashed lines shown in Figure 1-3 represent the upper and lower three standard deviation lines. At the right end of the curve, a distribution of stress for a particular cycle life is drawn. This distribution is usually assumed to be a normal distribution, based on studies by Stulen, Cummings, and Schulte as reported by Juvinall (8, p. 351). The distribution of cycles to failure found at a specified stress level is most often assumed to be log-normal with respect to cycles, based on investigations by Freudenthal and Gumbel (9, p. 317). The abscissa is almost always plotted as logarithmic but the ordinate, or stress axis, is plotted either as a log scale or linearly, depending on the way the data plots best. Whichever scale is used, the distributions described above are generally considered to hold. Obviously from this, one can see that designing a structural or mechanical component for a precise deterministic life or stress level is not only incorrect but could be catastrophic.

The S-N curve given in Figure 1-2 shows a horizontal line starting at approximately 10^6 cycles. It can be seen that theoretically if a member is stressed at a level below this line it will never fail, regardless of the number of cycles (6, p. 333; 10, p. 160). The stress level indicated by the horizontal line is called the endurance limit. The endurance limit is usually considered to be a characteristic property of ferrous metals

although similar behavior has been observed in some strain-aging aluminum alloys, superpure aluminum, some titanium alloys, and some magnesium alloys (11, p. 336). Generally, however, in non-ferrous metals the S-N curve will appear as shown in Figure 1-4, where the curve continues to fall with increasing cycles, at least as far as experimentation has been carried out. In such cases the designer utilizes the (so-called) "fatigue strength" value, which is the allowable stress level, for the number of cycles life required in his design (11, p. 336).

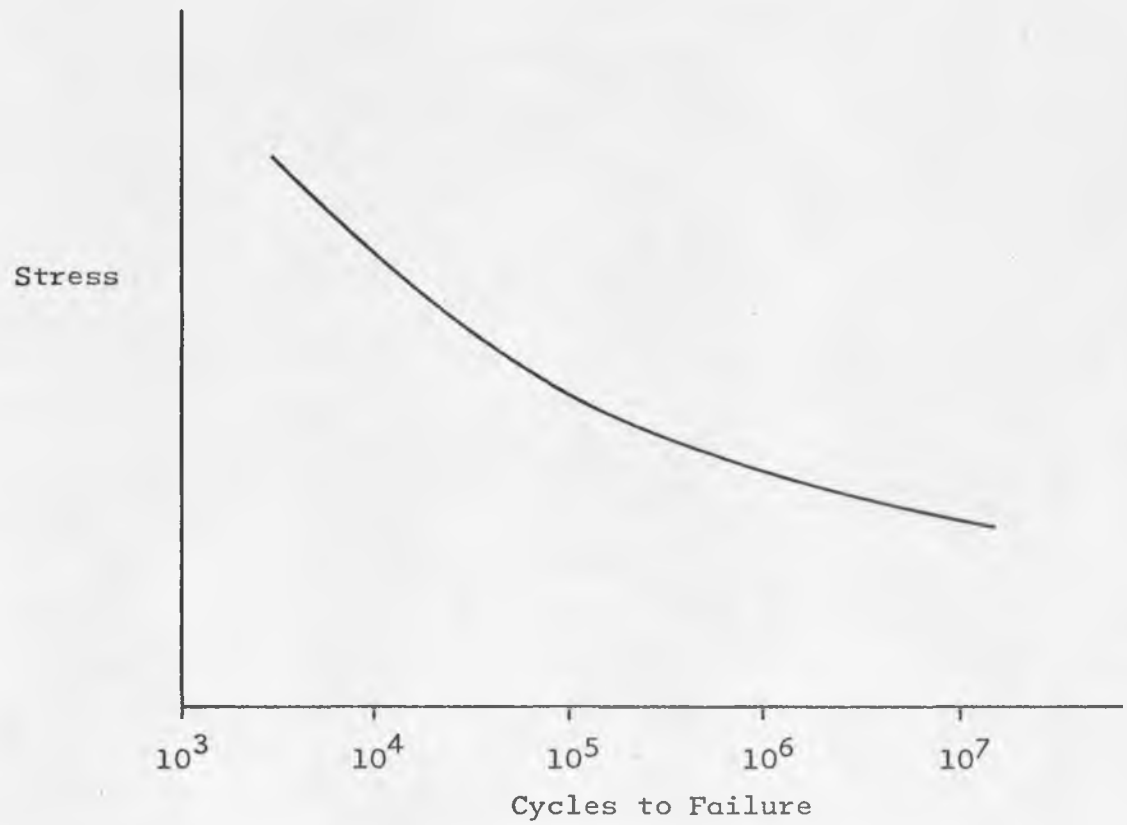

Figure 1-4. Example of an S-N Curve for Non-ferrous Materials.

Why a definite endurance or fatigue limit exists (as with ferrous materials) is a phenomenon which is not completely understood. Some theories postulate that it is a result of "coaxing", in which the alternating stress is supposed to gradually increase in the early part of the test (11, p. 337; 12, p. 114). This, then, changes the S-N curve such that the horizontal line appears rather than a curve as that shown in Figure 1-4. Coaxing is the process of applying successive periods of stress cycling beginning just below the endurance limit and raising the stress in small increments with a resulting increase in the endurance limit (8, p. 219). Figure 1-5 shows two examples of coaxing for AISI 1045 steel. The first of these is for 10^7 cycle increments and the second showing a smaller increase in the endurance limit is for increments of 2×10^6 cycles. The dashed line in the figure represents the normal S-N curve (8, p. 218). Coaxing is a phenomenon limited to materials that have a definite endurance limit so far as is known (12, p. 114).

The endurance limit will almost always be in the range of 40 to 60 percent of the ultimate tensile stress for steels up to 200,000 psi (10, p. 160). Joseph E. Shigley (10) gives the following method of estimating the S-N curve: for ultimate strengths below 200,000 psi the endurance limit is assumed to be approximately 50% of the ultimate tensile strength at 10^6 cycles; for ultimate tensile strength values above 200,000 psi the endurance limit is assumed to be 100,000 psi at 10^6 cycles. The horizontal endurance strength

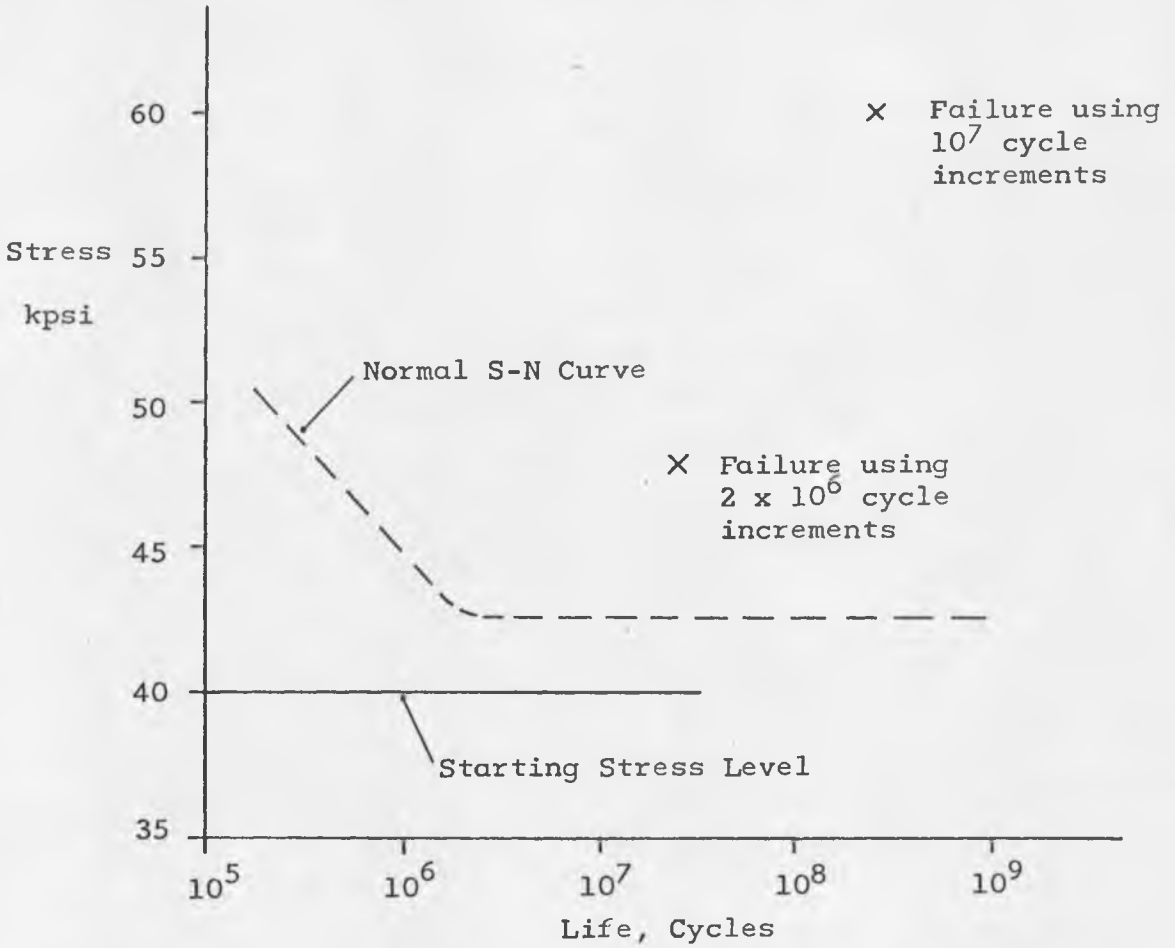

Figure 1-5. Results of Coaxing AISI 1045 Steel (8, p. 219).

line is then intersected at 10^6 cycles with another straight line (on a log-log plot) which starts at $0.9S_{ut}$ at 10^3 cycles (10, p. 162). The S-N curve estimate, using this method, will next be developed for the material used in the testing reported in this thesis, i.e., cold drawn and annealed AISI 4340 steel wire with a diameter of 0.0625 $\pm$ 0.0005 inches. From previous work by another University of Arizona graduate student, it is known that the mean ultimate tensile strength for this material is 113,000 psi (13, p. 87). Therefore, the stress value at 10^3 cycles would be

$0.9S_{ut}$ = 101,700 psi and the stress values at 10^6 cycles would be $0.5S_{ut}$ = 56,500 psi. The resulting estimated S-N curve is shown in Figure 1-6.

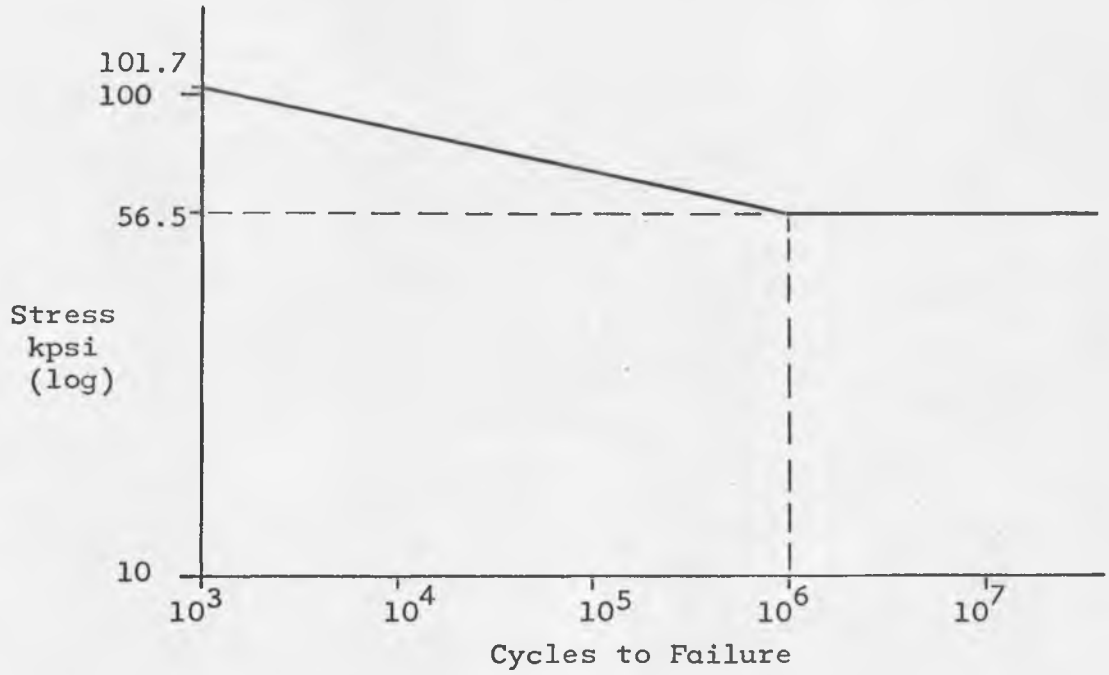

Figure 1-6. Estimated S-N Curve for Cold Drawn and Annealed AISI 4340 Steel Wire.

It is obvious from Figure 1-6 that the transition of slopes (knee of the curve) is assumed to be a sharp corner. Many S-N curves appear in the literature, and it should be noted that in few of these has there been an attempt to define the knee of the curve in great detail. In fact, most representations show a sharp corner. A typical S-N diagram, for annealed 1040 steel, is shown in Figure 1-7 (10, p. 160). This curve is plotted as a log-log relationship. Figure 1-8 shows a simple S-N curve for

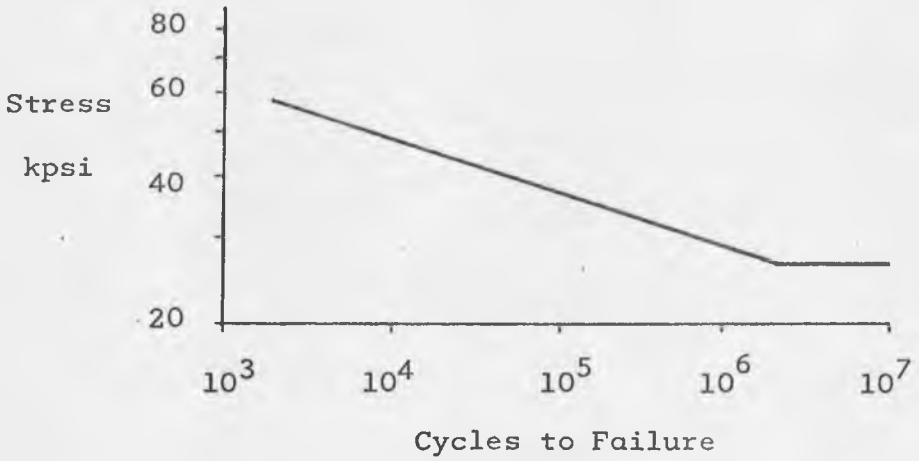

Figure 1-7. S-N Curve for Annealed 1040 Steel (10, p. 160).

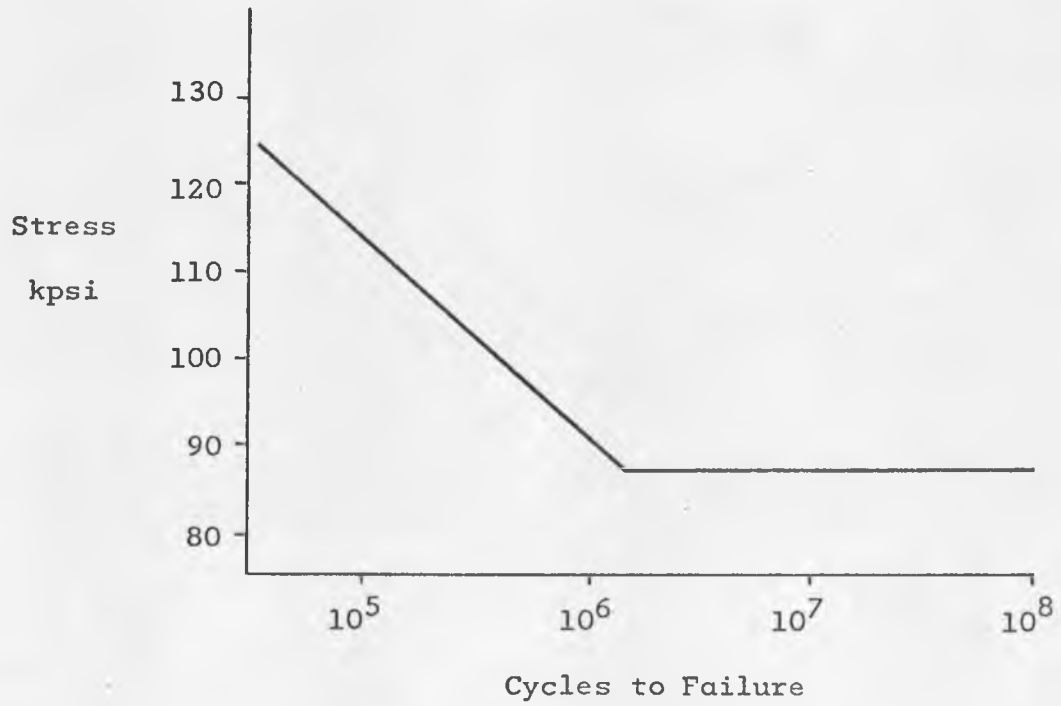

Figure 1-8. S-N Curve for AISI 4340 Steel, Unknown Heat Treat (4, p. 55).

4340 steel, which has a considerably higher endurance limit, and apparently a higher ultimate tensile strength, than that of the estimated curve of Figure 1-6. Obviously, these two materials have different properties, and were heat treated in different manners (4, p. 55). Note that the S-N curve in Figure 1-8 is plotted with the stress axis linear. Another S-N diagram for 4340 steel is given in Figure 1-9, and in this case the specimens came from hot-worked bar stock (5, p. 161). This curve also shows a higher endurance limit than the estimated curve.

There have been numerous interesting studies showing size effect on fatigue strength as well as fatigue differences (strength and/or cycle life) as a result of temperature, surface conditions, and notches in specimens. Figure 1-10 shows the change in fatigue behavior comparing notched and smooth specimens for 4340 steel (2, p. 112). This figure shows the relationship for two values of static tensile ultimate strength, 210,000 psi and 290,000 psi. While the purpose of Figure 1-10 is not to define the transition zone of the curve, it does not have the unrealistic sharp corner, and would seem to indicate that the curves were derived from more extensive data than usual.

Fatigue properties vary with the size of the original material body from which the test specimens were taken. The series of curves in Figure 1-11 clearly shows this (2, p. 334). This indicates that fatigue data obtained from small diameter specimens must be used with a degree of caution when extrapolating to the

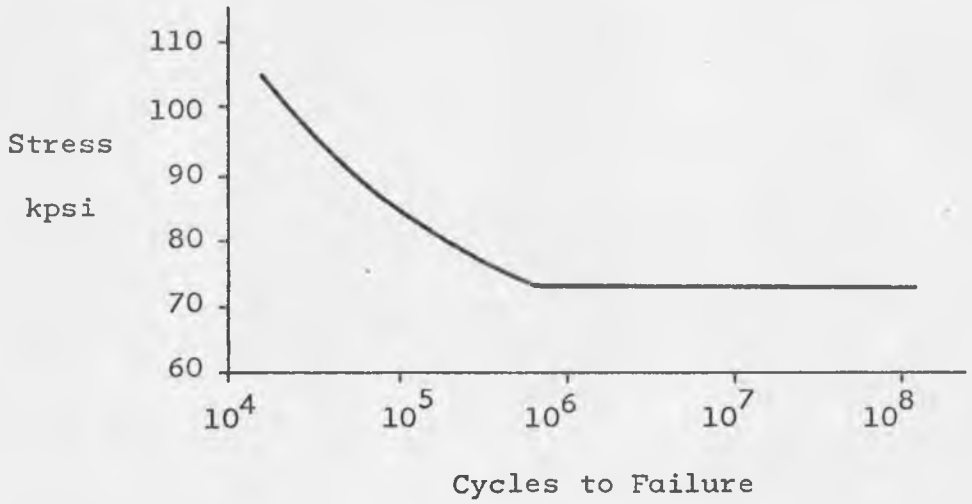

Figure 1-9. S-N Curve for AISI 4340 Steel, Hot-worked Bar Stock (5, p. 161).

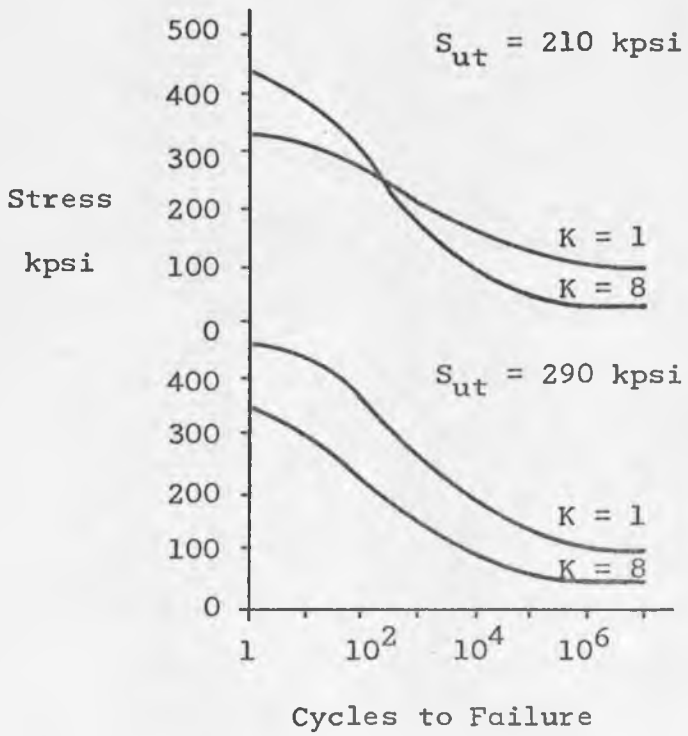

Figure 1-10. S-N Curves for Smooth and Notched Rotating Beam Specimens of 4340 Steel (2, p. 112).

design of larger components (2, p. 333). As will be seen later, this is true of the data presented in this thesis.

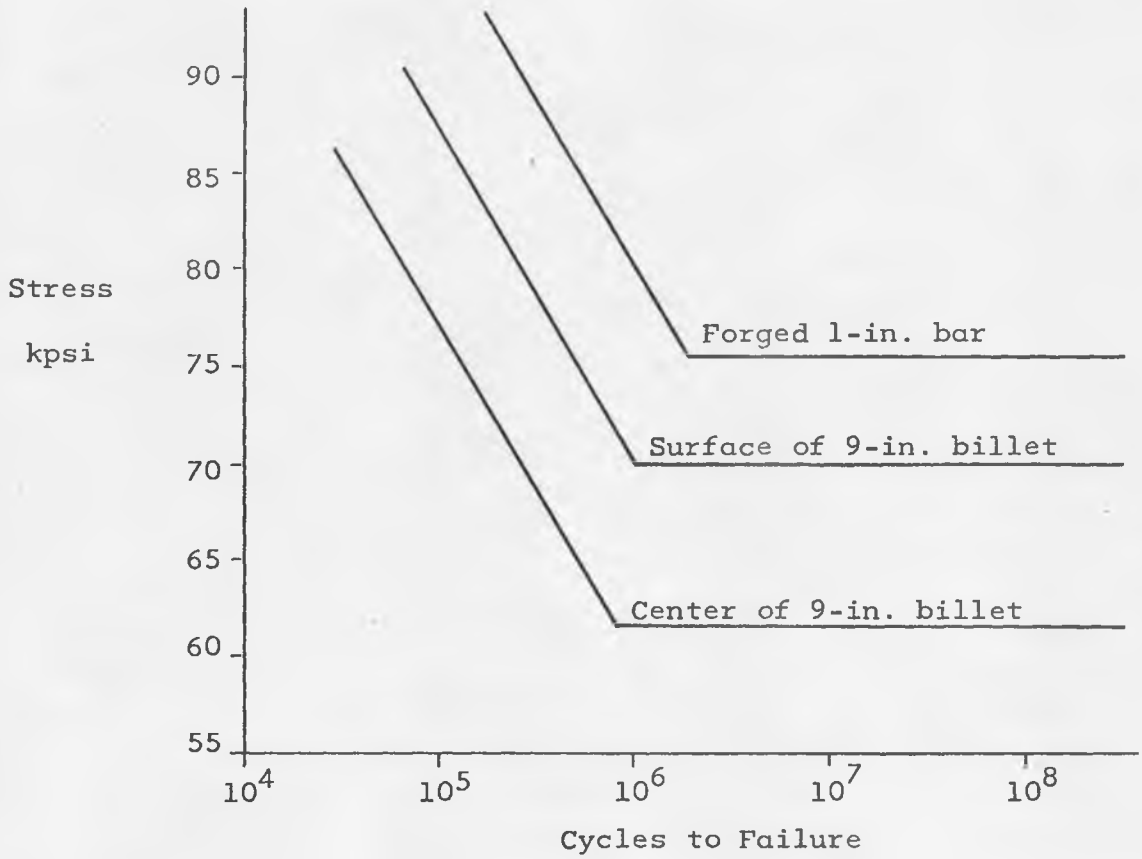

Figure 1-11. Size Effect on Fatigue Strengths of 4340 Steel Specimens (2, p. 334).

As has been stated, because of the fact that fatigue is statistical in nature (a random phenemon) it is desirable to develop an S-N surface, and one of the objectives of this report is to develop such a surface for cold drawn and annealed AISI 4340 steel in the transition zone. Data of this kind is very scarce in the literature. Frequently, a series of data is generated and

an envelope is drawn around the points perhaps indicating the 1 percent and 99 percent probabilities of failure as shown in Figure 1-12 (8, p. 210). Figure 1-12 is a generalized S-N curve for wrought steel, and thus, the ordinate is not specific. A well defined S-N surface, or composite S-N curve as it is sometimes called, was found for 75S-T aluminum alloy shown in Figure 1-13. It is also a good example of the fact that nonferrous materials do not exhibit the phenomenon of a fatigue limit (4, p. 50). Even though the experimentation was carried out to the order of 10^8 cycles, the curves continued to drop as a function of cycles.

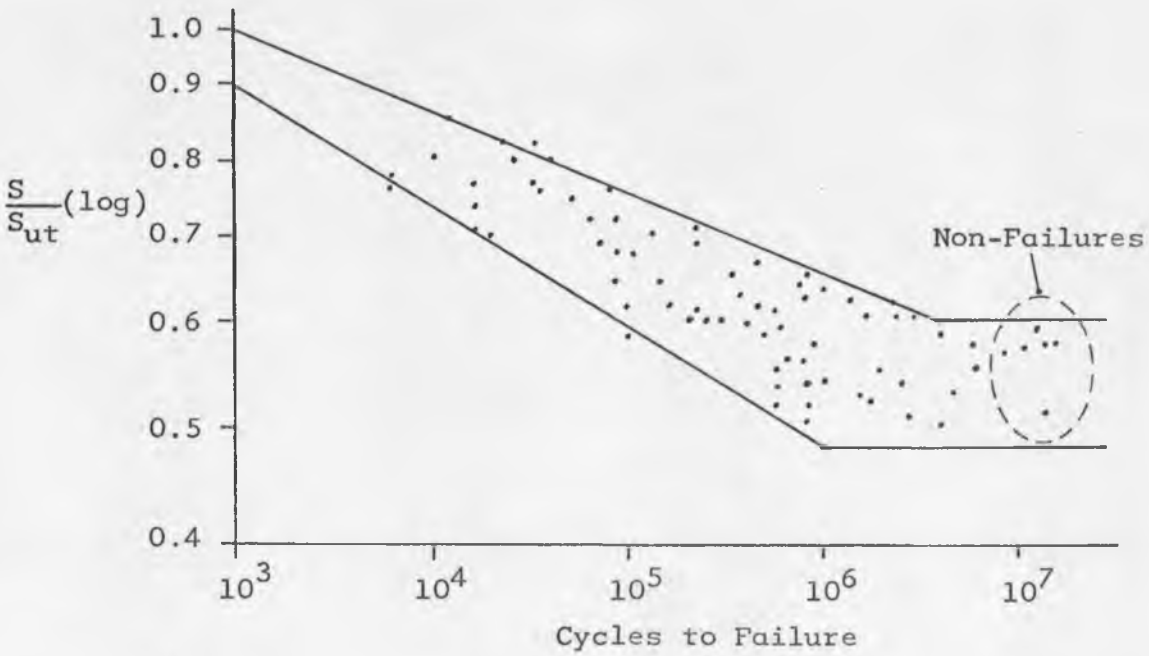

Figure 1-12. Approximation of an S-N Surface for Wrought Steel (8, p. 210).

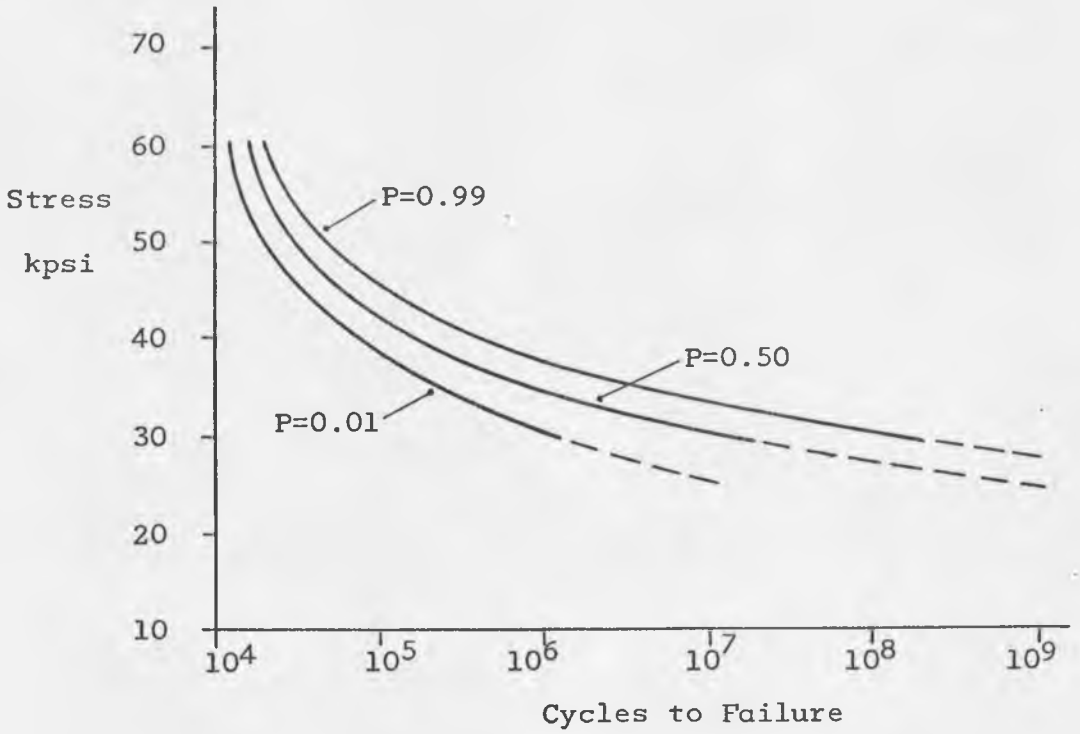

Figure 1-13. Statistical S-N Surface for Aluminum Alloy 75S-T (4, p. 50).

With a few more assumptions we can estimate an S-N surface for our test material, based on Shigley's method of constructing S-N curves (see Figure 1-6). It has been stated earlier that the endurance limit will almost always fall in the range of 40 to 60 percent of the ultimate tensile strength, and it would not be illogical to assume that this range corresponds to the $+3\sigma$ and -3σ limits in a normal distribution with a mean value at 50 percent of the ultimate tensile strength. All that is

needed then, to plot an S-N surface, is the standard deviation of the ultimate tensile strength. This is known from previous tests of 4340 wire specimens to have a value of 1,600 psi (13, p. 87). If it is assumed that this standard deviation is approximately unchanged at 10^3 cycles, where the stress is $0.9S_{ut}$, we have all of the data necessary to estimate an S-N surface, with a mean line and a $+3\sigma$ to -3σ envelope. The curve is shown in Figure 1-14.

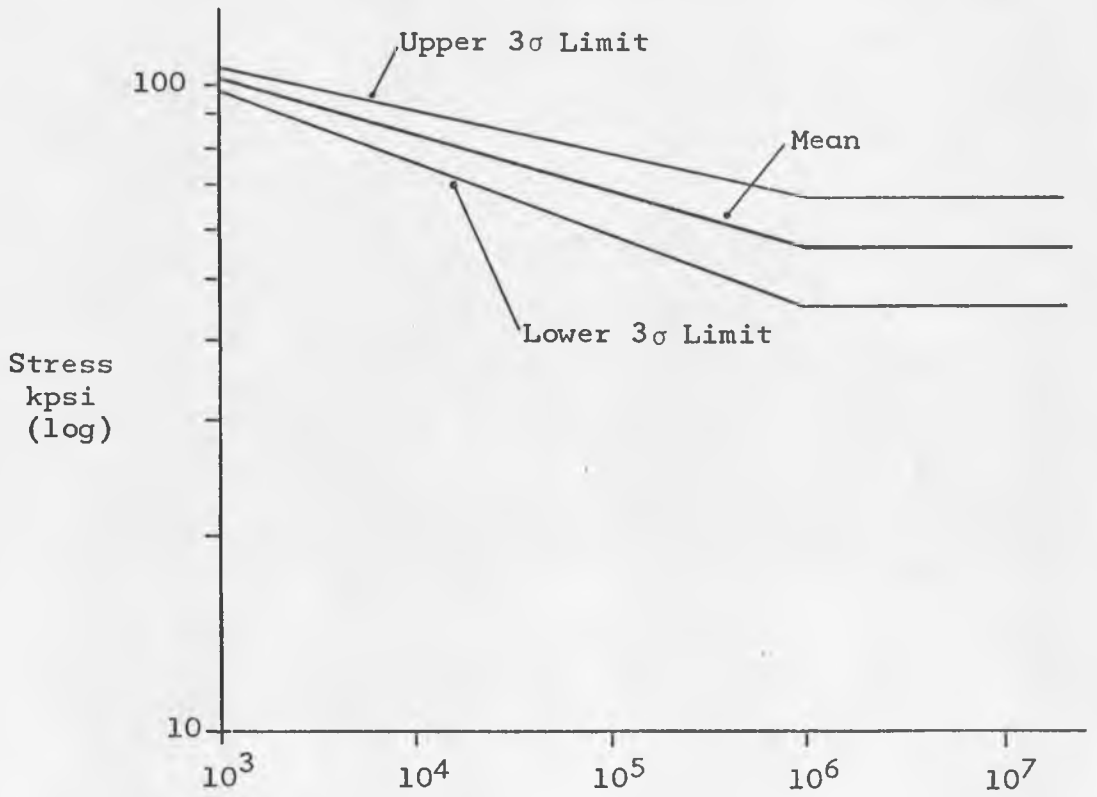

Figure 1-14. Estimated S-N Surface Showing $+3\sigma$ to -3σ Envelope for 4340 Steel Wire.

1.3 Mathematical Theory

Although fatigue is usually analyzed from statistical information, several attempts have been made to express the S-N curve in the form of generalized equations which were derived empirically.

Weibull presents the following equation:

$$(S - S_e)(N + C)^a = b \qquad (1.1)$$

Where S and N are the stress and cycles to failure respectively and S_e is the endurance limit; a, b, and C are material constants (2, p. 110).

Another such equation developed is Equation 1.2 (2, p. 110):

$$N = \frac{2}{C} \frac{\ln(S_{ut}/S) \ln\left[(S - S_i)/K\right]}{\left[(S - S_i)/E\right]^2 \left[(S - S')/S_i\right]^2} \qquad (1.2)$$

where S = maximum cyclic stress

S' = minimum cyclic stress

S_{ut} = Ultimate Tensile Strength

S_i = Internal Stress $\approx$ Endurance Limit

K, C = Material Constants

E = Modulus of Elasticity

Both Equations 1.1 and 1.2 are based on a linear stress versus log cycles plot, and neither has really tried to relate theory to what is actually happening to the material under the cyclic loading. Hence, we will not discuss them further.

There has been one recent attempt to relate theory to the observed phenomena, i.e., by Mr. S. S. Manson in his book, Thermal Stress and Low-Cycle Fatigue (3, Ch. 4). His theories are quite involved and will be presented in some detail in the following pages. One basic problem that will become more evident to the reader is that the data that was taken could only be measured in terms of strain and therefore relating this to stress under cyclic conditions is difficult. Mr. Manson's theories, if applicable in this case, will allow us to find this relationship. In this thesis an attempt is made to correlate actual experimental results obtained at The University of Arizona to Mr. Manson's hypotheses.

Even though most problems of interest, including the problem studied and reported here, for ductile materials involve inelasticity, it is possible to solve these problems by assuming that a universal relationship exists between stress and strain. This takes on the form of the familiar stress-strain curve obtained in the uniaxial tensile test, where inelasticity is evident when the stress is no longer proportional to strain (3, p. 127). A typical example of a static stress-strain curve is shown in Figure 1-15.

The variables that Manson finds most convenient to relate to the strain cycling characteristics are the stress range and the strain range. The stress range is defined as the difference between the maximum stress incurred and the minimum stress. The

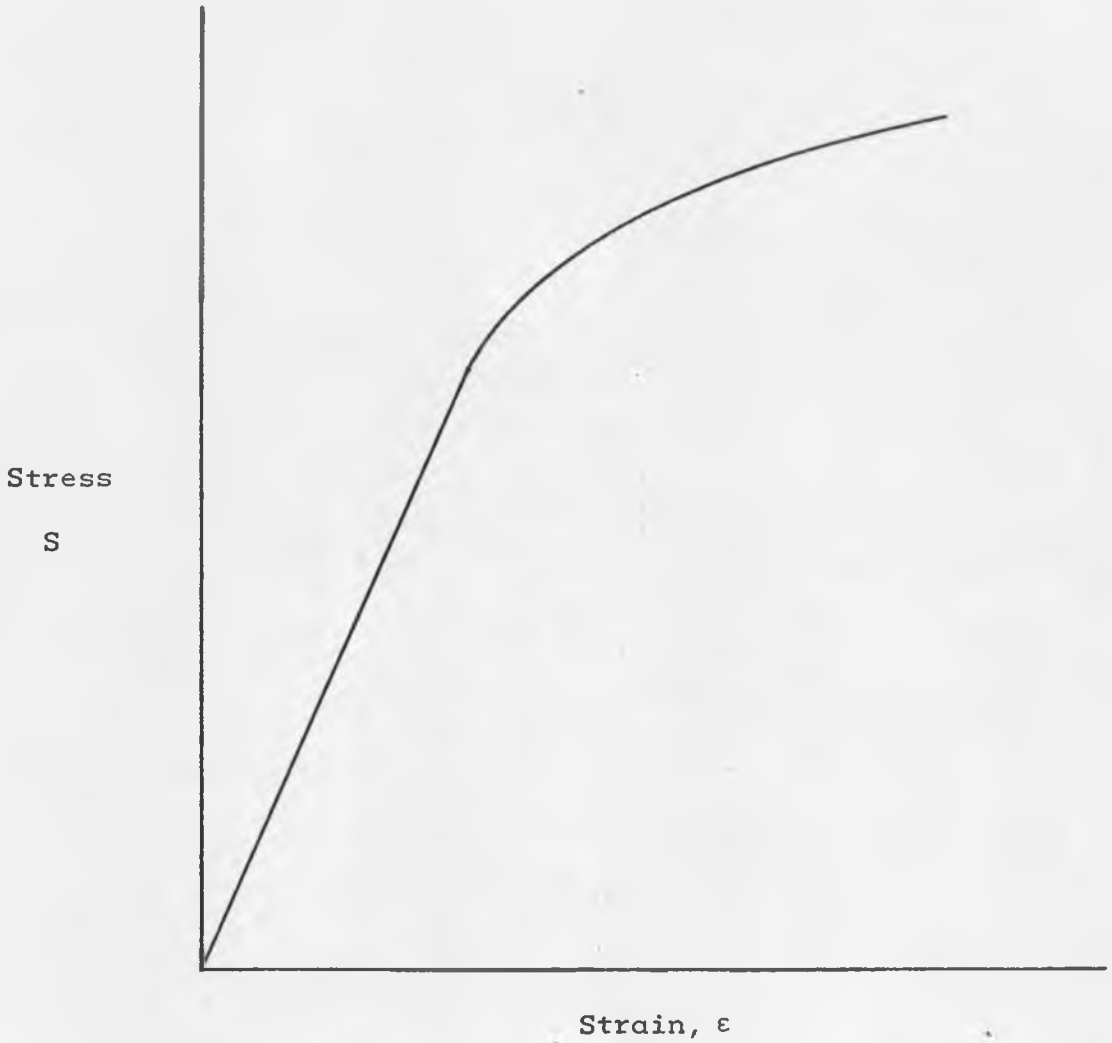

Figure 1-15. Example of a Static Stress-Strain Curve.

strain range follows the same reasoning. In the case of simple bending in a member, this would appear to indicate that the stress range is simply twice the maximum stress and the strain range is twice the maximum strain in the member. Under more complex loading this may not be true. The static relationship between stress range and strain range is, therefore, similar to

Figure 1-15 and takes on the form drawn in dashed lines in Figure 1-16. Note that the departure from the ideal elastic line is shown at the endurance limit, S_{end}, and the stress range is thus 2 S_{end}.

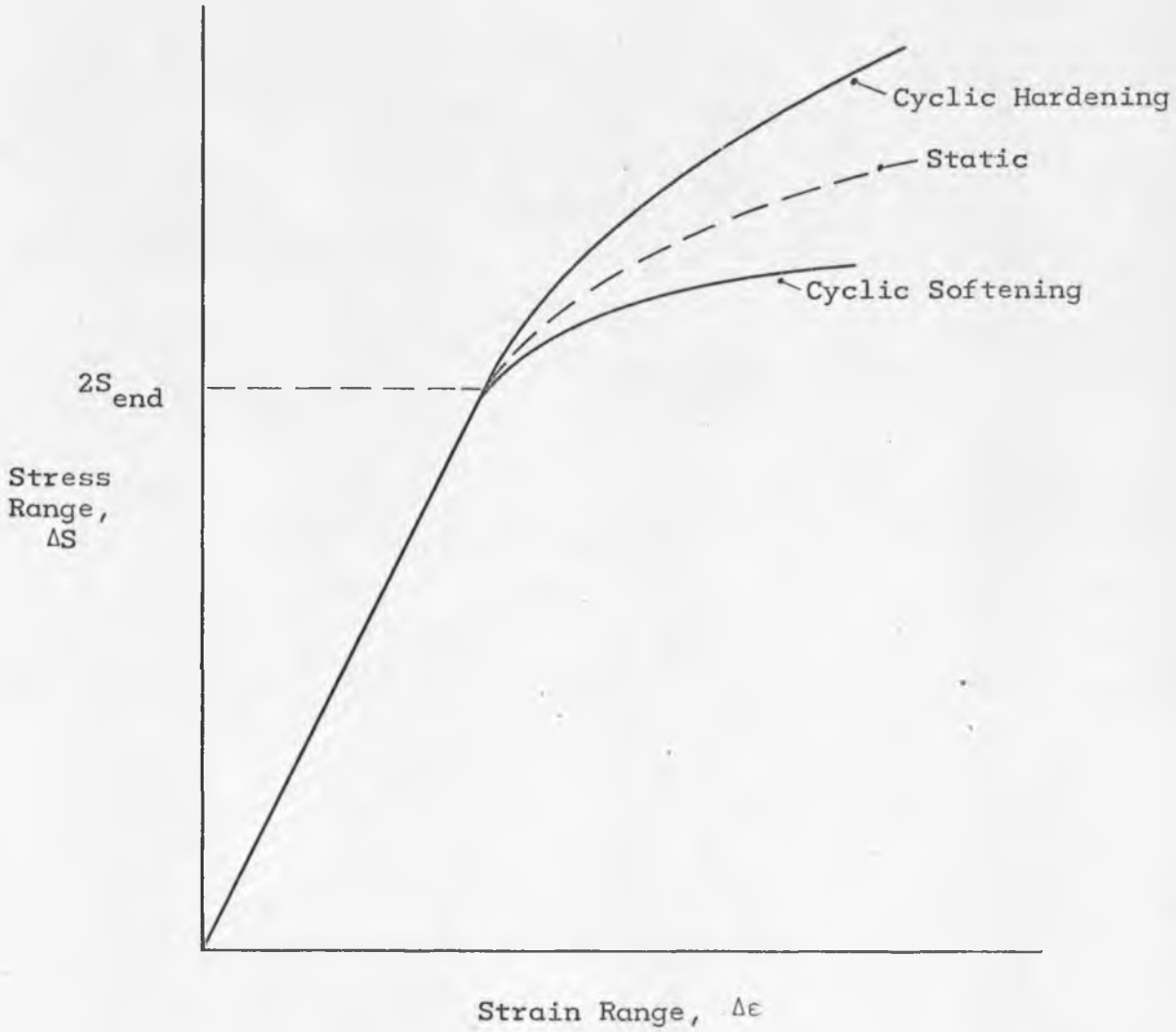

Figure 1-16. Example of a Stress Range-Strain Range Curve Showing Comparison of Static with Characteristics of Cyclic Hardening and Cyclic Softening.

Also shown in Figure 1-16 are two solid line curves designated as cyclic hardening and cyclic softening. Under cyclic conditions like those considered in fatigue, a material will usually either cyclicly strain soften or strain harden (3, p. 129). In such cases the stress range-strain range curve, as well as the stress-strain curve, will exhibit change (from the static curve) like that indicated in Figure 1-16. The test material in this study, being cold drawn and annealed AISI 4340 steel, is of the cyclic strain hardening class, thus the cyclic stress range-strain range curve will be above the static curve. In the early cycles, the stress range-strain range curve changes constantly, but after a few thousand cycles will appear as depicted in Figure 1-16 (3, p. 128).

Referring now to Figure 1-17, which typifies the case in this study, Manson states that the total strain range at any point "A" can be broken down into two components: the plastic strain range, ε_p, and the elastic strain range, ε_{el}, which is equal to $\Delta S_A/E$, the corresponding stress range divided by the modulus of elasticity (3, p. 132).

As postulated by Manson, these two elements, constituting the total strain range, can be individually related to cycle life.

After some testing Manson found that for most materials, including annealed 4340 steel, the plot of plastic strain range versus cycles to failure is a nearly straight line if the plot is log-log. The line can be defined by an equation, therefore, of the

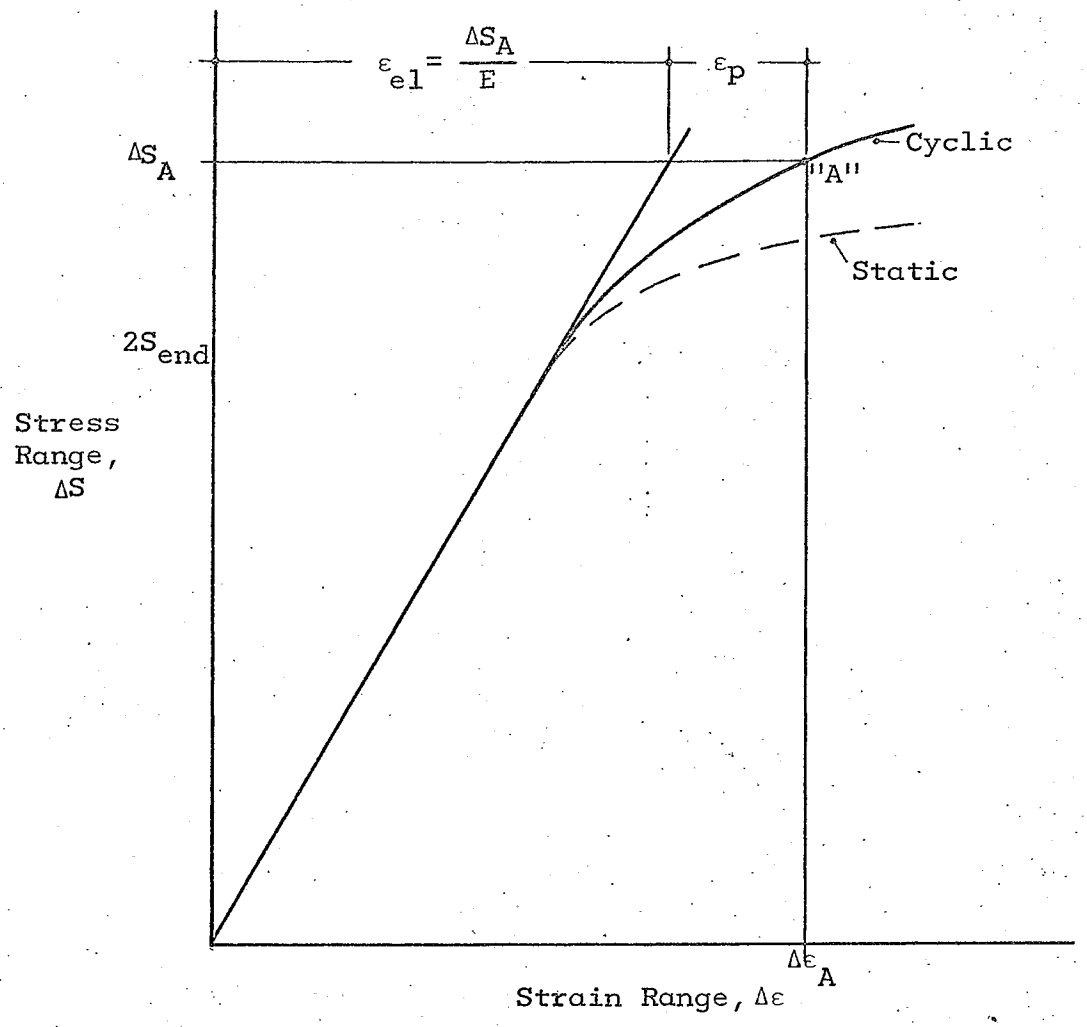

Figure 1-17. Stress Range-Strain Range Curve for Cyclic Hardening Material.

form:

$$\varepsilon_p = MN^z \tag{1.3}$$

where M and z are material constants and N is the number of cycles to failure. When plotted, the relationship will resemble that shown in Figure 1-18 (3, p. 132-133).

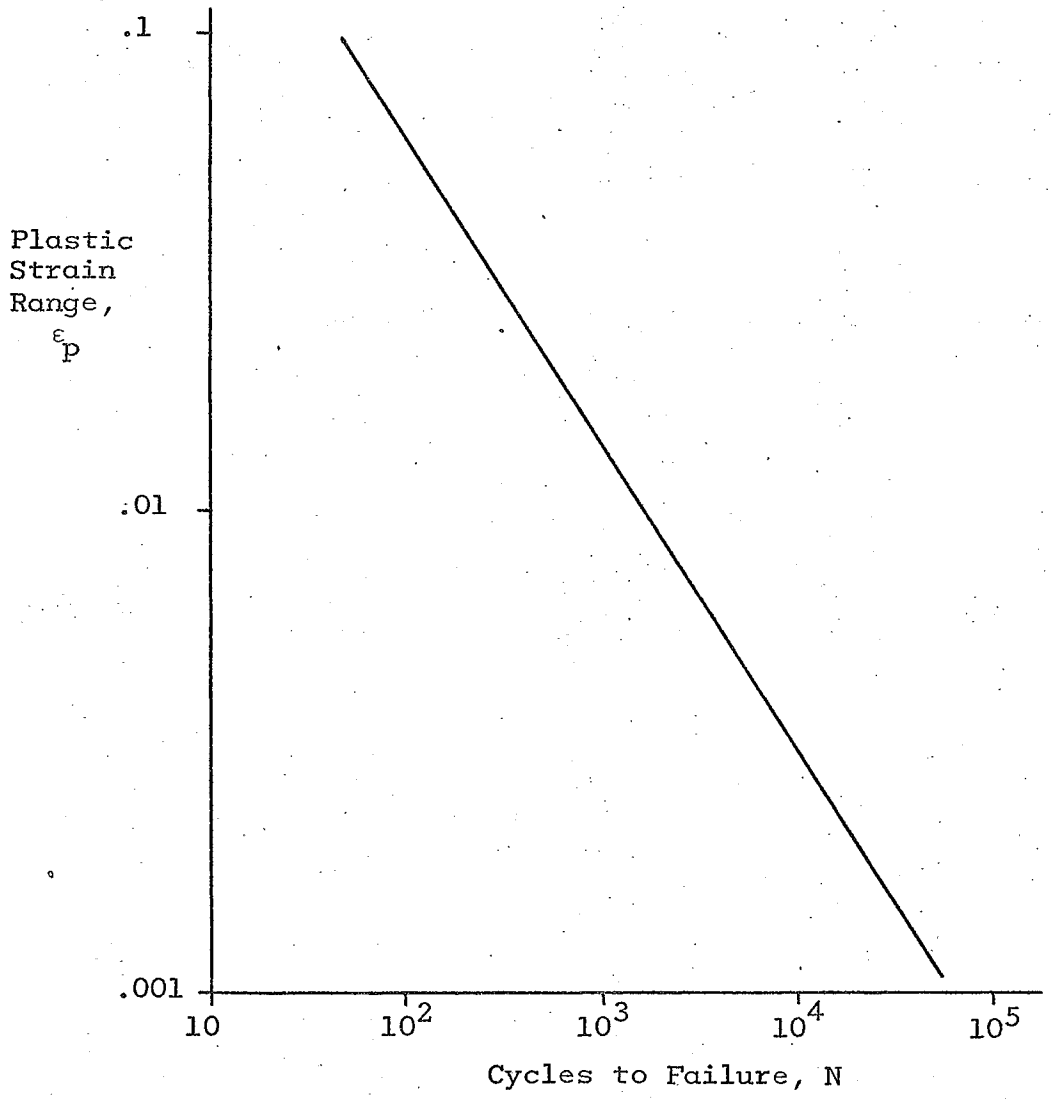

Figure 1-18. Relation Between Plastic Strain Range and Cycle Life for 4130 Steel (3, p. 133).

Similarly, the elastic strain range, ε_{el}, versus cycles to failure has been shown to follow a straight line relationship on a log-log plot (3, p. 134). The equation for this line is given as:

$$\varepsilon_{el} = \frac{\Delta S}{E} = \frac{G}{E} N^{\gamma} , \qquad (1.4)$$

where G and γ are material constants and E is the modulus of elasticity. Graphically, the plot will appear as that in Figure 1-19. Notice that the slope of this line is much less steep than that of the plastic strain range, Figure 1-18. This should be no surprise, because as has already been stated, the elastic strain is dominant at the higher cycle lives.

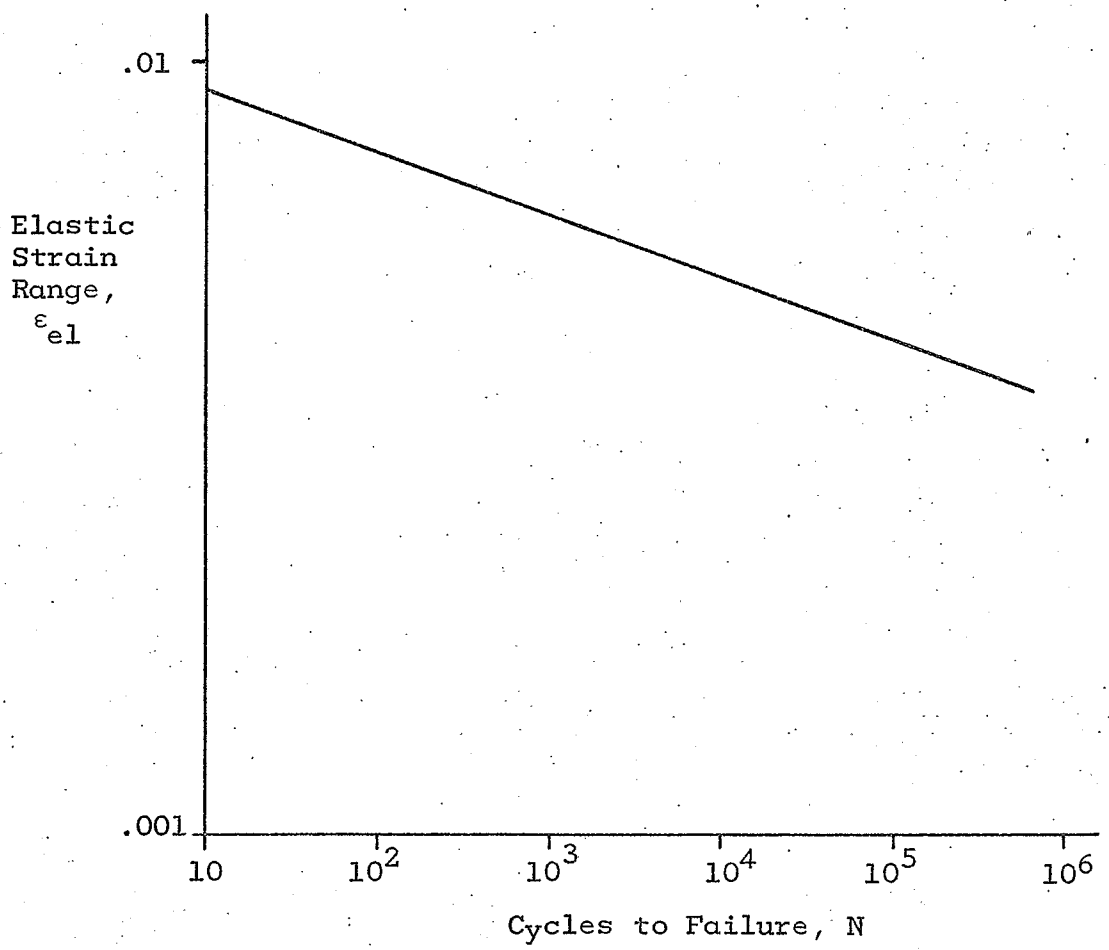

Figure 1-19. Relation Between Elastic Strain Range and Cycle Life for 4130 Steel (3, p. 134).

Equation 1.4 can be considered valid (based on available data) for cycle lives up to 10^6, and sometimes higher. The equation for ε_{el} does not take into consideration a definite endurance limit below which the life is essentially infinite, since the line in Figure 1-19 relates elastic strain range with cycle life. Manson has developed equations which include the endurance limit but he states that the numerical difference is negligable (3, p. 135) so we will use the more simple Equations 1.3 and 1.4.

Assuming that the relationships between plastic strain range and elastic strain range and cycle life are valid then it is a simple matter to determine the total strain range by adding Equations 1.3 and 1.4 (3, p. 141). This is seen by referring to Figure 1-17. For total strain range as a function of cycles to failure we have:

$$\begin{aligned} \Delta\varepsilon &= \varepsilon_p + \varepsilon_{el} = \varepsilon_p + \frac{\Delta S}{E} \\ &= MN^Z + \frac{G}{E} N^Y \end{aligned} \tag{1.5}$$

Figure 1-20 shows Equation 1.5 in graphical form. From this figure it can be seen that at the high cycle lives the total strain range curve is almost assymptotic to the elastic strain range line, and the curve is nearly assymptotic to the plastic strain range at the low cycles. This corresponds to the general theory, as stated in the first paragraph of this chapter.

There are methods by which the plastic strain range line of Figure 1-18 and the elastic strain range line of Figure 1-19 can be estimated, knowing a few material properties. These methods,

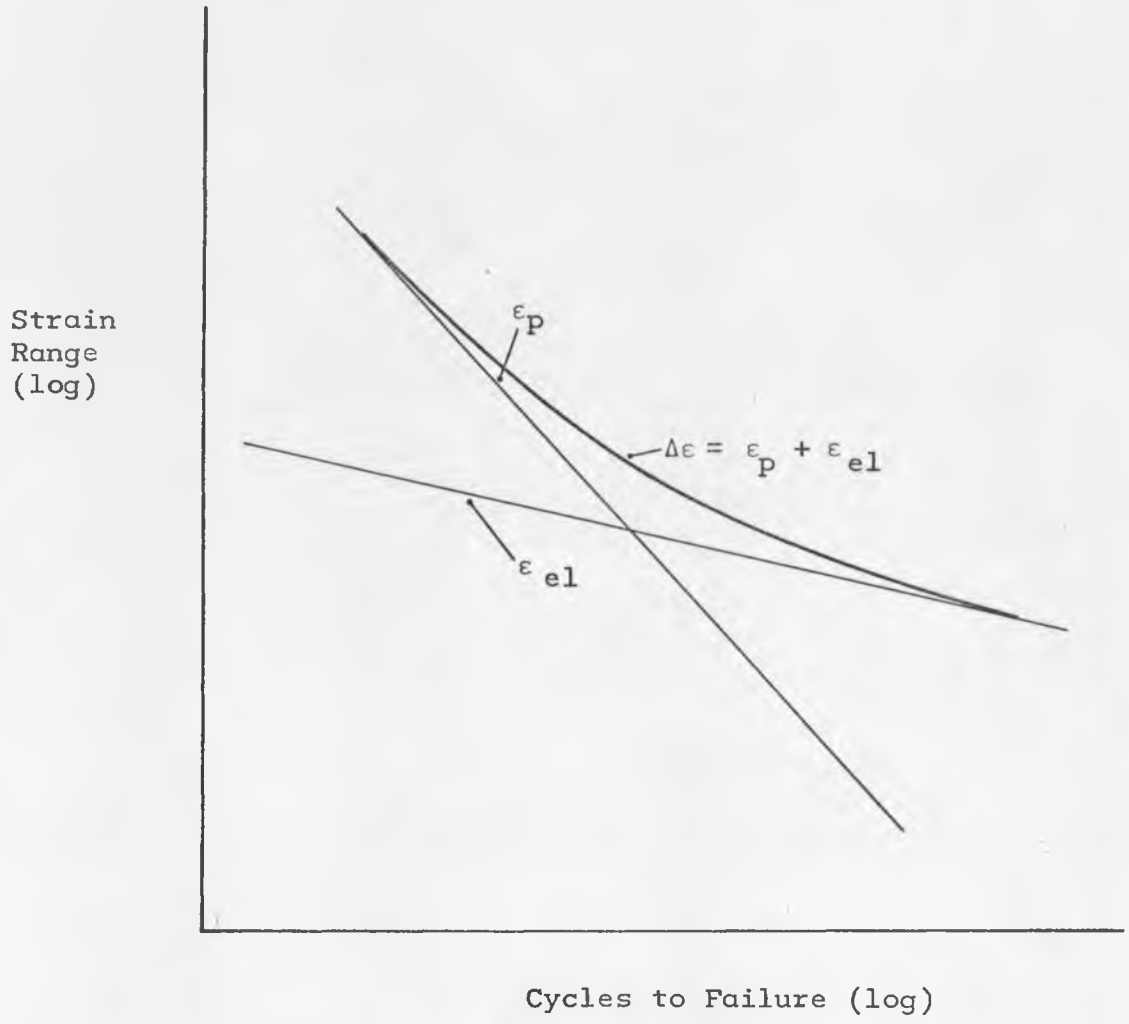

Figure 1-20. Relationship Between Total Strain Range and Cycle Life.

explained by Manson, are described in detail in Chapter 4. For the moment assume that these estimations have been made. Therefore, the relationship between total strain range and the cycle life is known, i.e., known are all of the constants M, z, G, γ,

as well as the modulus of elasticity, E. If the data from this study relates well with this approximate total strain range curve, then it can be assumed that Equation 1.5 holds in the case examined and tends to verify Mr. Manson's theories.

The main purpose of this report is to define the S-N curve statistically in the region of the transition. From strain data it is necessary to develop a relationship to calculate the corresponding stress. That is cyclic stress range-strain range curve must be constructed, similar to that presented in Figure 1-17. This is a cyclic relationship and, knowing the strain range at various cycle lives from our data, we very easily obtain the stress range at the same cycle lives. With the stress range we immediately know the maximum bending stress and we have all of the information necessary to plot the S-N curve. The mathematical relationship between stress range and strain range is found without much difficulty by eliminating N from Equations 1.3 and 1.4 and then combining with Equation 1.5. The result which defines a curve such as Figure 1-17 is given as Equation 1.6 (3, p. 144):

$$\Delta\varepsilon = \frac{\Delta S}{E} + M\left(\frac{\Delta S}{G}\right)^{z/\gamma} \qquad (1.6)$$

The methods of approximating the plastic and elastic strain range lines will, as already stated, appear in Chapter 4, as will the final results of these approximations and the comparison with the data that was generated. Before analyzing these results there must first be a discussion of the equipment used to obtain this data and the statistical methods used in reducing the data to summarizing constants.

CHAPTER 2

TEST EQUIPMENT AND MATERIALS

As was stated earlier, fatigue is of a statistical nature and extensive experimentation is required to determine truly representative fatigue strength values of materials. To get the stress or strain distribution at any particular cycle life, for instance, requires that a great number of nominally identical test specimens be run at that cycle life. Fatigue specimens can be quite costly, and it is obvious that economics is of some concern. Also, in the determination of the fatigue limit the experimenter is faced with having to run fatigue tests for high cycle lives, often in excess of 10^6 cycles. It would be helpful, then, to have a method of producing data rapidly and to produce it inexpensively. H. T. Corten and G. M. Sinclair have written a paper describing such a method. They have proposed a machine which tests wire specimens (14).

2-1. Wire Fatigue Testing Machines

The wire fatigue testing machine is very simple in principal and can be modified easily to test various diameter wires. Wire fatigue machines were used to generate all fatigue data for this paper. The wire machines in the Reliability Research Laboratory at The University of Arizona were patterned after the original

Corten machine. The basic configuration of the University of Arizona machines is shown in Figure 2-1.

The wire specimen is held on one end by a Jacobs chuck mounted directly on the shaft of the motor, which in this case operated at a speed of 17,000 revolutions per minute. The other end of the specimen slips into a bushing which is pressed into the inner race of a miniature ball bearing. This assembly rides in a carriage which can be moved along a circular arc track and set at any angle indicated with a pointer, thereby varying the maximum stress in the wire specimen itself, by varying the amount of bending. The bearing housing pivots in the carriage, self-adjusting for each angle. Behind the motor, the shaft connects to a gear reducer, driving a counter, which records the number of cycles the specimen has experienced.

The motor turns the chucked end and the other end is free to rotate as the wire turns; the wire remains in the same plane in which it was originally bent, barring any undue vibration. The curved track theoretically imposes the appropriate shortening of the distance between the ends of the wire necessary to subject the specimen to zero moment at both ends (14, p. 1125). The wire must be long in relation to its diameter, and the region of maximum stress must be located away from each end, so that undesired stress concentrations, as a result of the method of holding the ends, will be eliminated (14, p. 1125).

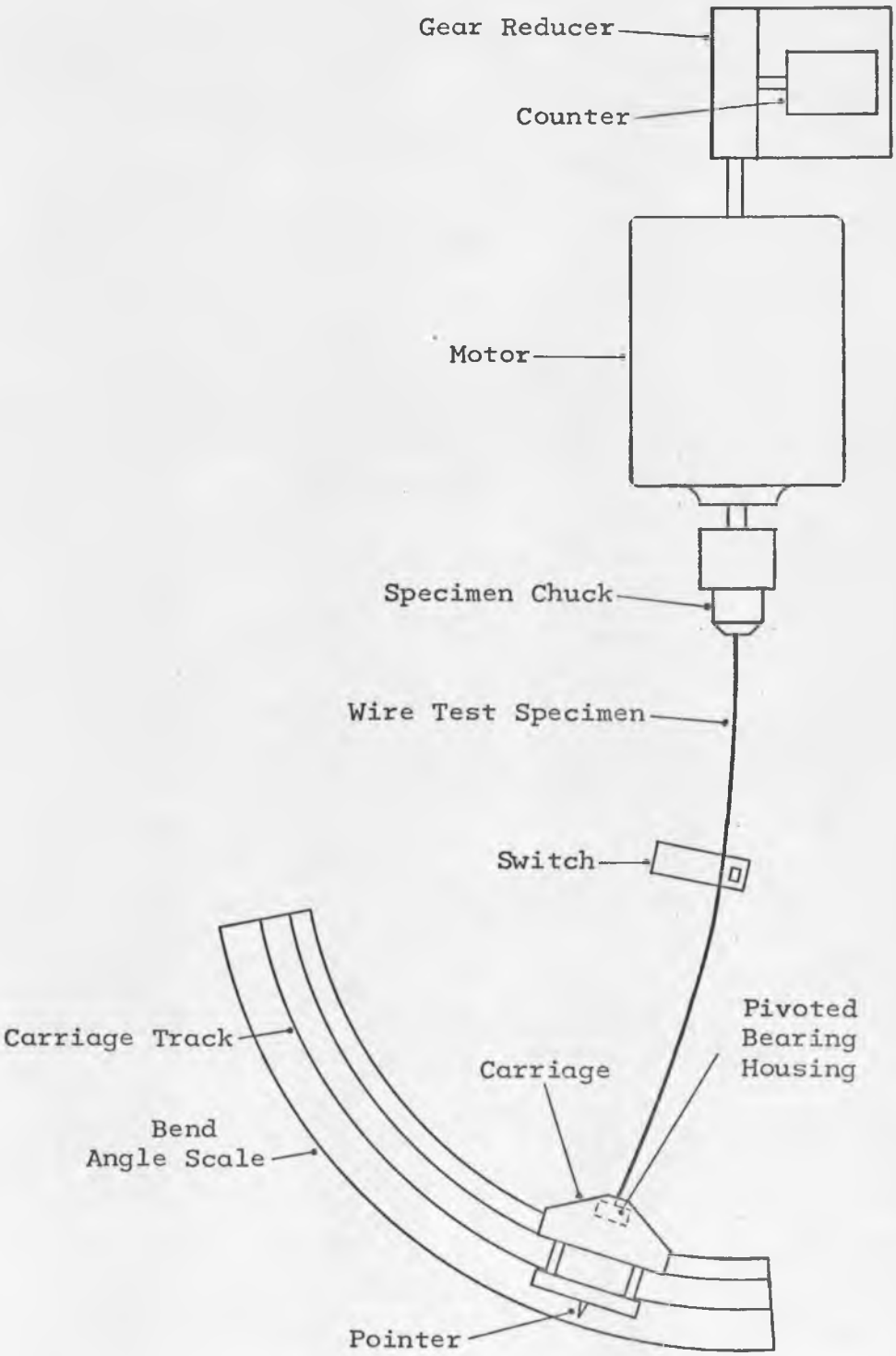

Figure 2-1. Schematic of Wire Fatigue Testing Machine.

Figure 2-2 shows a deflected wire specimen loaded and with zero moment at the ends (14, p. 1125). There is an angle, α, which corresponds to any deflected length, L. The equation for the maximum stress which occurs in the exact center for any angle, α, can be developed from the basic equation for a member subjected to bending.

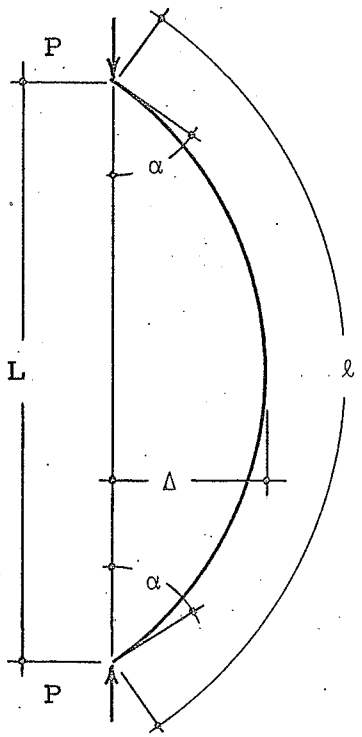

Figure 2-2. Loaded Wire Specimen Subjected to Zero Moment at Ends.

That is:

$$S = \frac{mc}{I} + \frac{P}{Area} \qquad (2.1)$$

where c is the distance from the neutral axis which in this case equals the wire radius, I is the moment of inertia, m is the moment at the center of the span, and P is the axial load which is small. In this case Equation 2.1 becomes

$$S = \frac{P \Delta c}{I} + \frac{P}{Area} \tag{2.2}$$

Using the theory of elastica, the equation is finally found in terms of known parameters (13, p. 19):

$$S = \frac{4Ec}{\ell} (\sin \alpha/2) K(\sin \alpha/2, \pi/2) \tag{2.3}$$

where $K(\sin \alpha/2, \pi/2)$ is the complete elliptic integral of the first kind (15, p. 205). E is the modulus of elasticity.

The theoretical track that would load the member with zero moment at the ends calculated if the values of L are known for each angle, α. Again, by using the theory of elastica, these values can be found from Equation 2.4 (13, p. 19):

$$\frac{\ell - L}{\ell} = 2 \left[1 - \frac{E(\sin \alpha/2, \pi/2)}{K(\sin \alpha/2, \pi/2)} \right] . \tag{2.4}$$

In Equation 2.4 $K(\sin \alpha/2, \pi/2)$ and $E(\sin \alpha/2, \pi/2)$ are the complete elliptic integrals of the first and second type. Rearranging the equation to find L:

$$L = \ell \left[2 \frac{E(\sin \alpha/2, \pi/2)}{K(\sin \alpha/2, \pi/2)} - 1 \right] \tag{2.5}$$

The values of α and L are given in Table 2-1 below.

Table 2-1. Theoretical Track Length for Values of Bend Angle, α.

α, degrees	L, inches	α, degrees	L, inches
0	10.0000	20	9.6980
2	9.9974	22	9.6360
4	9.9878	24	9.5654
6	9.9740	26	9.4896
8	9.9518	28	9.4104
10	9.9236	30	9.3214
12	9.8808	32	9.2232
14	9.8502	34	9.1356
16	9.8410	36	9.0324
18	9.7544	38	8.9250
		40	

2-2. Calibration of Wire Machines

As might be clear it would pose a difficult task to physically manufacture such a track without rather sophisticated equipment. However, the ideal track can be very closely approximated by a circular arc track whose location can be determined experimentally if its center of curvature is known. The final radius was obtained by trial and error by Corten and Sinclair and their value of 6.592 inches was also used in the manufacture of the University of Arizona machines.

Using the circular track introduces a problem, of course, and that is the fact that Equation 2.3 is no longer valid. Therefore, manual calibration of the wire machine was necessary. This calibration was performed for each University of Arizona machine.

The first step in the calibration was to measure the strain versus the bend angle of the machine, as read on the scale shown in Figure 2-1. This is the angle, α, in Figure 2-2. A type C6-1X1-M15E (120 $\pm$ 0.5 ohms, 2.08 $\pm$ 2% gage factor, 1/64 inch gage length) variable resistance strain gage manufactured by Automation Industries, Inc., was mounted on a wire specimen like those used in the fatigue tests. This active strain gage was mounted on the test specimen, in the center, where the theoretical maximum stress is located. A similar strain gage was mounted on another specimen of the same material and approximately the same mass as the test wire to act as a temperature compensation. Both were connected to the bridge circuit of a B.L.H. Strain Indicator, Model 120C with a digital readout in micro-inches per inch (13, p. 64).

Ten strain readings were taken starting with $\alpha = 0^{\circ}$ and going up to $\alpha = 12^{\circ}$ in increments of 2°. A mean strain was then calculated for each angle and these values are presented in Table 2-2 for wire machines #3 and #4, the machines used to generate most of the data used in this thesis. The original data from which Table 2-2 was derived is presented in Appendix A. For calibration information on machines #1 and #2 see reference 13.

Table 2-2. Mean Strain as a Function of Bend Angle, α for Wire Fatigue Machines #3 and #4.

Bend Angle, α, in degrees	Mean Strain in Micro-in/in for Machine #3	Mean Strain in Micro-in/in for Machine #4
0	0.0	0.0
2	154.4	137.5
4	401.0	334.6
6	749.9	650.1
8	1116.7	985.4
10	1461.7	1330.7
12	1806.7	1694.8

A static stress versus strain curve for the elastic region of strain has been developed for the wire specimens by performing an axial load test on the same test piece as was used in the angle-strain calibration. Known calibrated weights were loaded onto the test wire and then the corresponding strains were read out on the strain indicator. The results proved that our material has a modulus of elasticity equal to 30×10^6 psi, the most commonly used value for steel (13, p. 68).

Using the values presented in Table 2-2 calibration charts for each machine were constructed. These resulting curves for strain versus bend angle, α, are shown in Figures 2-3 and 2-4

for wire machines #3 and #4 respectively. The non-linearity at the lower angles is probably due to error in measuring very small amounts of strain. These curves are very important as will become evident, and they will be referred to frequently in Chapter 3. Since we can only measure strain and not stress, to find the stress requires use of a cyclic stress-strain curve. The approximate cyclic stress range-strain range curve, that was described in the latter part of Chapter 1, will suffice providing that it can be shown to be valid.

2-3. Testing Materials

All of the calibration procedures were based on a wire diameter of 0.0625 $\pm$ 0.005 inches, which is the same wire size used in all of the experimentation. The material follows a MIL-S-5000 military specification for cold drawn and annealed AISI 4340 steel. The effective length, ℓ , for the wires on the machines is 10.000 inches, but the wires are actually 10.5 inches long. This allows approximately one quarter inch for supporting the wire on each end in the bushing and the motor chuck. All of the specimens were cold drawn, annealed and then straightened. A copy of the manufacturer's material certification appears in Figure 2-5.

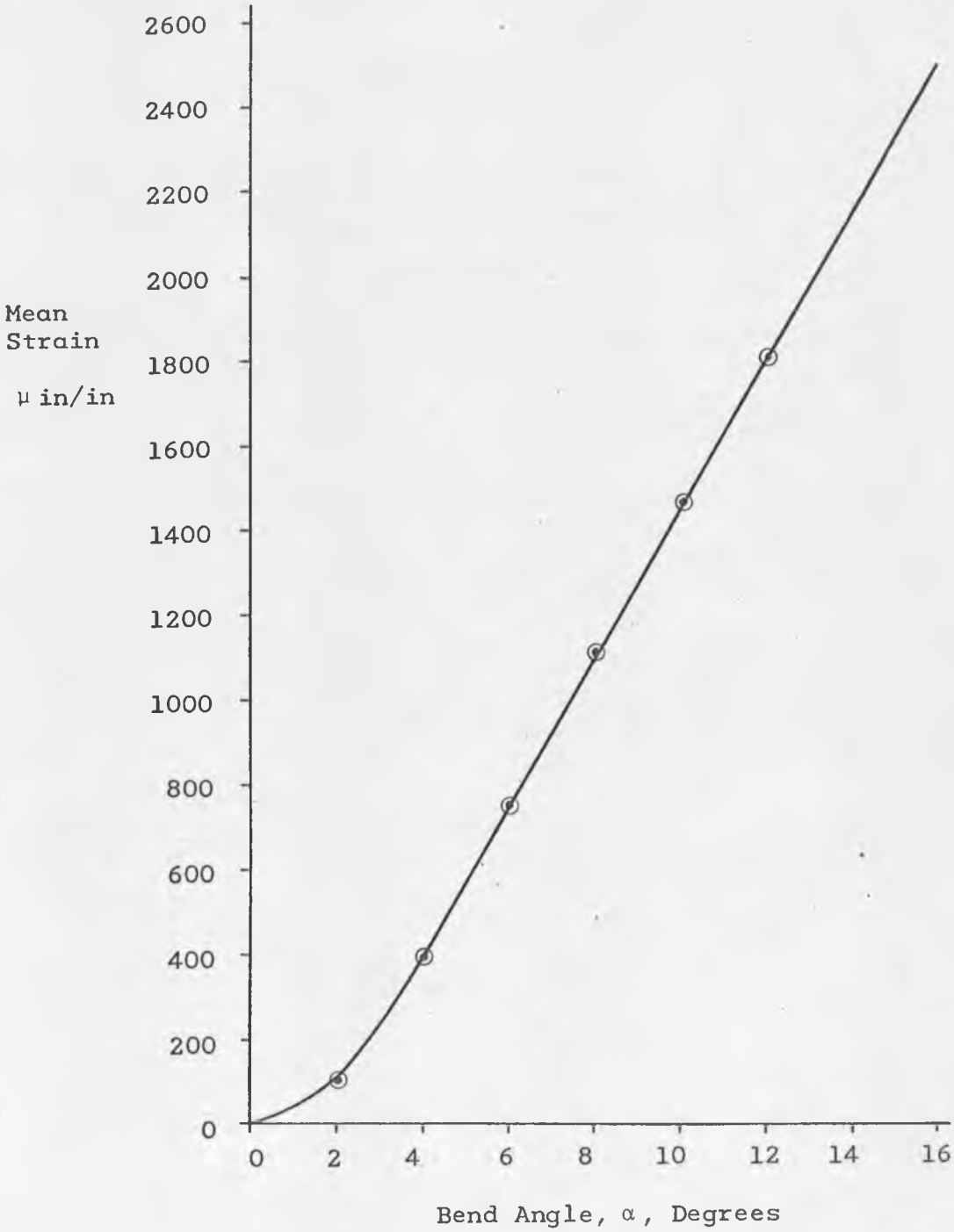

Figure 2-3. Calibration Chart for Machine #3.

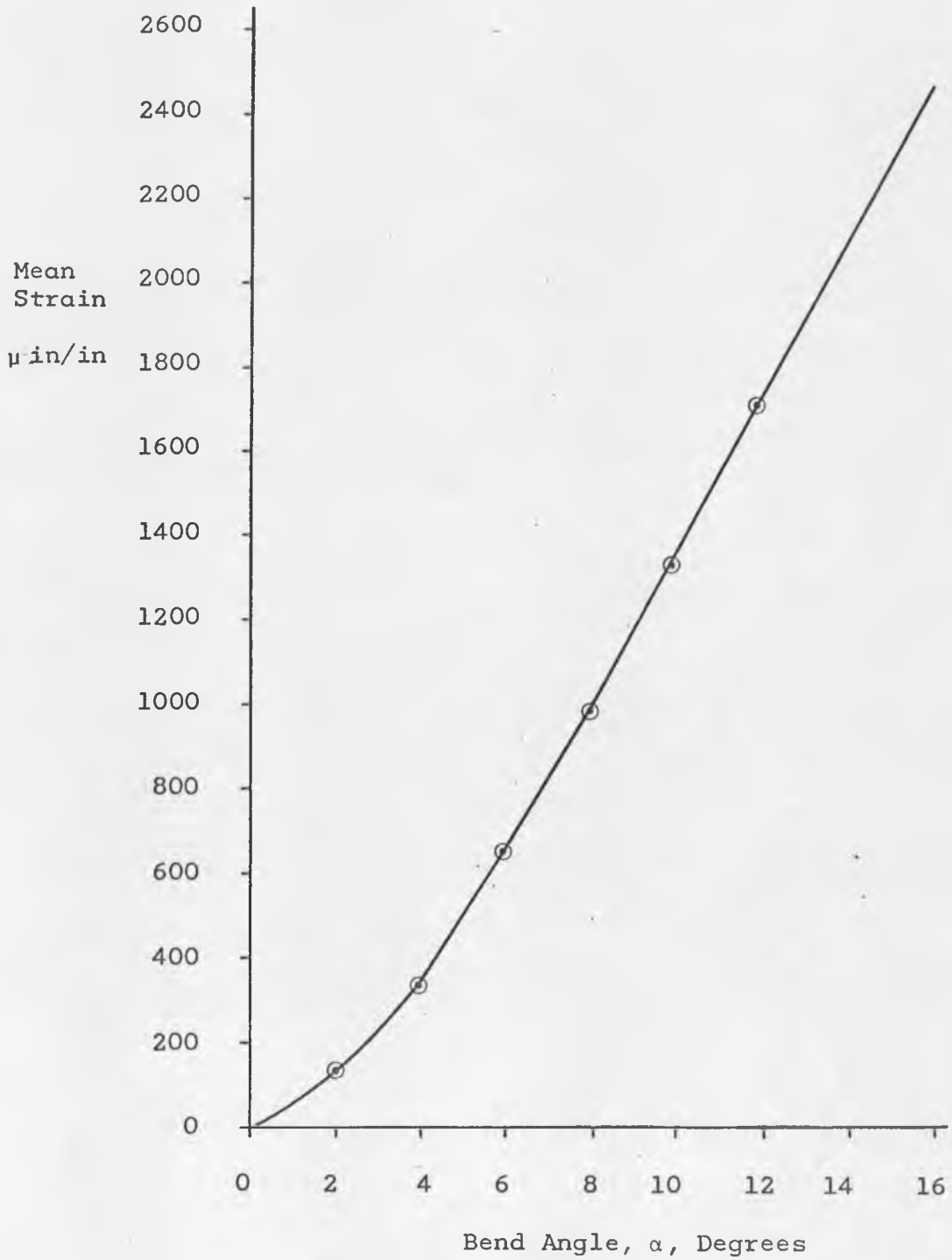

Figure 2-4. Calibration Chart for Machine #4.

MANUFACTURERS OF TECHNICALLY CONTROLLED WIRE, ROD, ALLOY STEELS FOR COLD HEADING AND OTHER APPLICATIONS.

TECHALLOY INC. CALIF.*

15100 EAST NELSON AVENUE

CITY OF INDUSTRY, CALIFORNIA

213-EDgewood 0-2211, TWX 910-584-1301

CUSTOMER'S ORDER NO.	TECHALLOY ORDER NO.	DATE SHIPPED	SPECIFICATION
VERBAL	C59225	6/3/68	MIL-S-5000

SHIPPED TO: Axvall Inst

WT.	DESCRIPTION
77#	.0625 Dia., 4340

GENTLEMEN: WE HEREBY CERTIFY THAT MATERIAL REFERRED TO ABOVE CONFORMS TO THE PHYSICAL AND CHEMICAL TESTS AS FOLLOWS AND IS IN ACCORDANCE WITH SPECIFICATIONS:-

HEAT	C.	MN.	P.	S.	SI.	NI.	CR.	MO.	VA.	AL.	TI.	ELEMENTAL	CO.	CU.
38043	.41	.70	.013	.015	.30	1.54	.89	.22						

ITEM	TENSILE	YIELD	% ELONG	% R.A.	HARDNESS	GRAIN SIZE	DECARB.	JOMINY 20/16	JOMINY 7/16	JOMINY 7/16
1					98RB	7/8		52		

OFFICIAL SEAL
VERNARD KENNAN
NOTARY PUBLIC - CALIFORNIA
PRINCIPAL OFFICE IN
LOS ANGELES COUNTY

Very truly yours,
TECHALLOY, INC., CALIF.

AUTHORIZED OFFICIAL

Figure 2-5. Material Certification for Wire Specimens.

CHAPTER 3

TESTING PROCEDURE AND DATA

It was stated in the previous chapter that the strain can be measured but not the stress. This could present a problem in the determination of the S-N surface in that we do not really know the distribution of strain at a particular cycle life. We do know that the stress at any cycle life is generally considered to be a normal distribution, however. Because the area of concern in this thesis is the transition zone, where the elastic strain becomes dominant, we can make a reasonable assumption of this distribution. In elastic strain, the stress is directly proportional to the strain by the factor of the modulus of elasticity. Thus, it seems a reasonable first assumption that the strain and therefore the strain range is also a normal distribution at a specified cycle life. All that remains in the determination of this distribution, i.e., finding the mean and standard deviation, is a method of testing.

In most fatigue testing, once a test has been performed on a specimen, the specimen is physically changed so that it is not suitable for a second test. There is just one observation for each experiment. Even if a specimen is not run to failure, after a test, it has a completely different stress history. This is certainly true in the fatigue testing that was utilized for this paper.

3-1. Staircase Testing Method

A method of obtaining data that is applicable in this study was developed and used in explosives research at the Explosive Research Laboratory in Bruccton, Pennsylvania in 1943 and is described in detail in a paper written by W. J. Dixon and A. M. Mood (16). They call this type of testing the "up and down" method. It has since become known also as the "staircase" method. This is used extensively in fatigue testing where it is desirable to determine the fatigue limit, or endurance limit, of the test material. The general area of interest of this thesis is the transition zone and the endurance region of the S-N curve, so the "up and down" test method was adopted. The method will be described along with the more important underlying assumptions and basic equations. The advantages and disadvantages will be noted, but there will be no attempt to develop the theory that supports the method.

The "staircase" method is quite simple to use. In fatigue testing, a specimen will be tested at an increment, in our case in terms of strain, immediately below the previous test level if that specimen failed within the preselected number of cycles or, it will be tested at an increment immediately above the previous test if that specimen was a run-out or non-failure for the same chosen number of cycles.

After a test series of this kind, by two very simple equations, an estimate for the mean and standard deviation of strain (at that preselected number of cycles) can be determined. The

series of data for a certain cycle life is usually plotted for convenience, as shown in Figure 3-1, with the test levels being ordinate values and the specimen number the abcissa. The curve has a sawtooth appearance, hence the name "staircase".

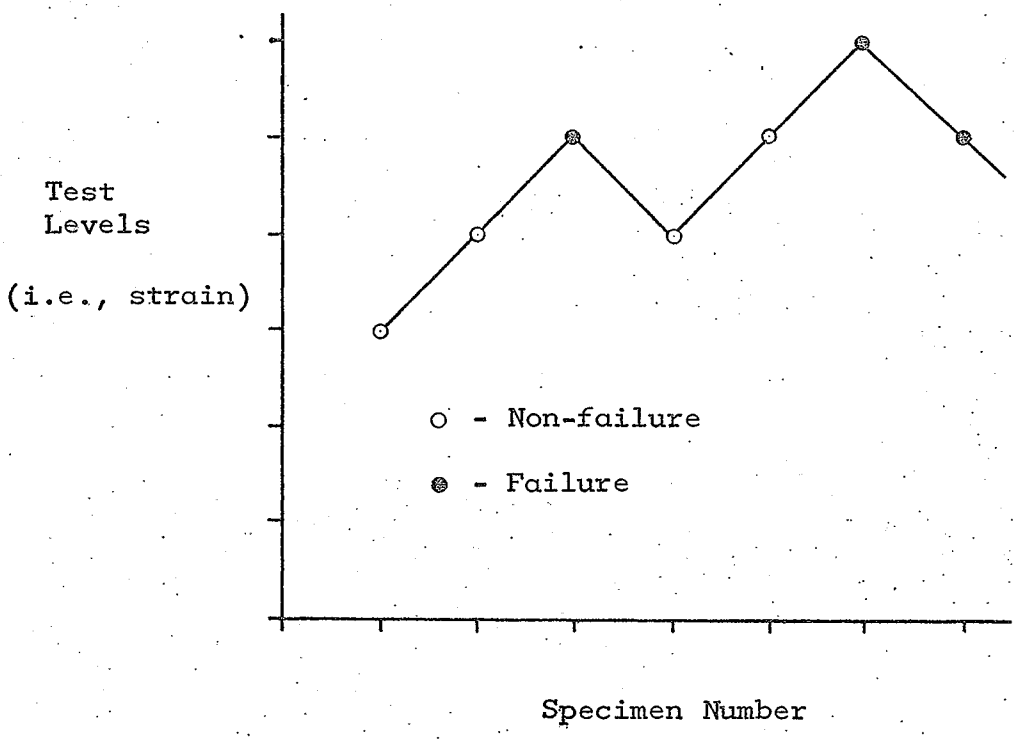

Figure 3-1. Example of Plotted Data from the Staircase Method.

The staircase method has several advantages, the most important of which is that the testing is automatically concentrated about the mean value, which is where the observations are most valuable (16, p. 110; 17, p. 231). The mean can therefore be rather accurately estimated (16, p. 110). Another important advantage is that the statistical analysis is simple, as opposed to some other methods of data reduction.

Using the simple analysis method requires the assumption that the variate be normally distributed, which is not strictly true in practice. Sometimes transformation of variables becomes necessary (16, p. 111). This could be considered a disadvantage of the method, but it is not often serious. However, for this study, we have assumed that the strain is approximately normally distributed at any cycle life, since in the elastic region it is very close to a linear function of stress.

A notable disadvantage is that the staircase method is not very accurate in determining the values at the extreme tails of the normal distribution curve except possibly for very large samples. If it is of primary interest to obtain precise values of the standard deviation of the distribution, then this is not the method to use (16, p. 112). The standard deviation is of interest in the study of the transition zone of the S-N curve, and the staircase method was used as the best that was available.

A second condition for the statistical analysis to yield meaningful results is that the sample size be large (16, p. 112). As will be seen, only about one half of the total test points are used, and the values obtained in the analysis may be incorrect or misleading if no more than forty or fifty specimens are tested (16, p. 112). When possible sample sizes of one hundred were employed in this study.

The test increment should be a rough approximation of the standard deviation of the population and should be less than twice

the standard deviation. Therefore, it is necessary to be able to make a reasonable estimate of the standard deviation before the testing begins (16, p. 112).

If d is the preliminary estimate for the standard deviation, σ, and if y_o is the first level of testing, then the following points in the test will be $y_o \pm d$, $y_o \pm 2d$, $y_o \pm 3d$, etc.

In each experiment, the total number of successes is nearly equal to the total number of failures. In estimating the sample mean and standard deviation, only the successes or failures are used, depending on which has the smaller total. This eliminates any bias incurred in the data as a result of starting the test at a value that is extremely high or low, which would cause an excess of failures or non-failures respectively. Since the test starts at an approximation to the fatigue strength at the specified cycle life of the test, the first guess is very likely different from the mean. Figure 3-2 illustrates this test situation for a case of a test that was started too low.

Let N denote the smaller total, and let n_o, n_1, n_2 . . ., n_k indicate the frequencies at each level of the less frequent (successes or failures) in the test where n_o is the lowest level and n_k is the highest level on which this even occurs; that is

$$\sum_{i=0}^{k} n_i = N$$

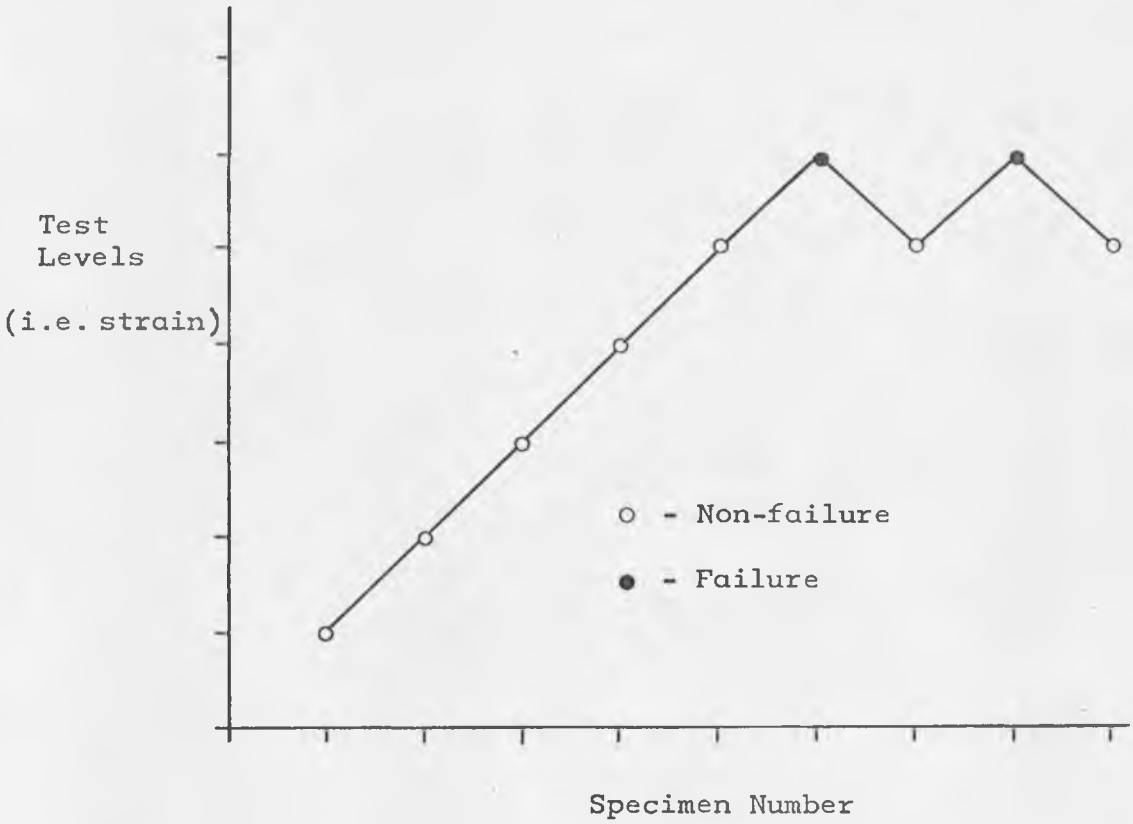

Figure 3-2. Staircase Plot for Data with Low Initial Value.

The estimates of μ and σ are based on the first two moments of the y values using the frequencies n_i. Since the levels are evenly divided, the moments can easily be computed using the sums A and B in Equations 3.1 and 3.2 (16, p. 113):

$$A = \sum_{i=0}^{k} in_i \qquad (3.1)$$

$$B = \sum_{i=0}^{k} i^2 n_i \qquad (3.2)$$

The relationship for the estimate of μ, called $\bar{y}$, is given as Equation 3.3.

$$\bar{y} = y' + d\left(\frac{A}{N} \pm \tfrac{1}{2}\right) \qquad (3.3)$$

In Equation 3.3, y' is the lowest value at which the less frequent event occurs. The plus sign in the parenthesis is used when the analysis is based on non-failures and the minus sign is used when based on failures (18, p. 48).

After a rather complicated derivation the estimate for the standard deviation is found (16, p. 113). It is denoted as s:

$$s = 1.62d\left(\frac{NB - A^2}{N^2} + 0.029\right) \qquad (3.4)$$

This formula is supposed to be accurate when the term $\left(\frac{NB - A^2}{N^2}\right)$ is greater than 0.3 but the equation breaks down rapidly when this term falls below 0.3. In the latter case a much more complex relationship must be used which is described in Reference 16.

The remaining portion of this chapter will be concerned with the actual data generated to determine the transition zone of the S-N curve. Copies of the original data sheets and staircase plots are given in Appendix B, but the reduced data and calculations for each cycle life will be presented next.

3-2. Reduction of Data

Staircase data plots were developed at eight different cycle lives: 10^5, 3×10^5, 5×10^5, 7.5×10^5, 10^6, 1.5×10^6,

2×10^6, and 10^7 cycles. Except when noted otherwise, one hundred specimens were run at each specified cycle life. All but the tests at 7.5×10^5 and 1.5×10^6 cycles were carried out by the author utilizing University of Arizona wire fatigue machines #3 and #4. These tests at 7.5×10^5 and 1.5×10^6 cycles were made by another University of Arizona graduate student, Robert Huball, on machines #1 and #2, and these data were used in the writing of this report. The calculated results from the data reduction are given in terms of strain and strain range.

The calculations to find the estimates for the mean and standard deviation from Equations 3.3 and 3.4 were made quite simple by tabulating the data. A column was needed for the approximate strain; bend angle, α ; the ranking subscript, i; the frequency, n_i; and the first two moments of the frequency, in_i and i^2n_i. The last three columns were then summed to give the values for N, A, and B, respectively. Table 3-1 shows this procedure, and contains the data for 10^5 cycles, which was run on machine #3.

Table 3-1. Staircase Data - 10^5 Cycles

Approx. Strain, μ in/in	α, degrees	i	n_i failures	in_i	i^2n_i
2690	17.0	3	12	36	108
2600	16.5	2	25	50	100
2510	16.0	1	11	11	11
2420	15.5	0	1	0	0
			N=49	A=97	B=219

The less frequent event at 10^5 cycles was failures, as it turned out to be for all other data. The lowest test level, y', was 15.5 degrees which corresponds to a value of 2420 micro in/in, from Figure 2-3. The increment d, was 0.5 degrees, equivalent to 86.3 micro in/in. The estimate for the mean was found from Equation 3.3 for failures:

$$\bar{y} = y' + d\left(\frac{A}{N} - \tfrac{1}{2}\right) \qquad (3.3a)$$

Substituting the data from Table 3-1 the equation becomes:

$$\bar{y} = 2420 + 86.3\left(\frac{97}{49} - \tfrac{1}{2}\right)$$

$$= 2548 \ \mu \text{in/in} \qquad (3.5)$$

The estimated standard deviation was obtained by using Equation 3.4 and in this case:

$$s = 1.62(86.3)\left[\frac{(49)(219) - (97)^2}{(49)^2} + .029\right]$$

$$= 80.4 \ \mu \text{ in/in} \qquad (3.6)$$

To find the distribution for the strain range, the Algebra of Normal Functions was used (7, Chap. 3). The strain range distribution being twice the strain distribution, the relationships between the means and standard deviations of these distributions were as follows (1, p. 123):

$$\text{Mean Total Strain} = 2(\text{Mean Maximum Strain})$$

$$\sigma_{(\text{Total Strain})} = 2\sigma_{(\text{Maximum Strain})}$$

Therefore, the estimate of the mean of the total strain range, $\bar{y}_t$, was twice $\bar{y}$ and the estimate of the standard deviation of the total strain range, s_t, was equal to $\sqrt{2}$ s.

For 10^5 cycles the total strain range distribution was defined by:

$$\bar{y}_t = 5096 \ \mu in/in \tag{3.7}$$

and

$$s_t = 160.8 \ \mu \ in/in \tag{3.8}$$

The next set of data to be considered was from tests at 3×10^5 cycles. This is presented in Table 3-2.

Table 3-2. Staircase Data - 3×10^5 Cycles

Approx. Strain, μ in/in	α, degrees	i	n_i failures	in_i	$i^2 n_i$
2510	16.0	4	1	4	16
2420	15.5	3	19	57	171
2340	15.0	2	14	28	56
2250	14.5	1	13	13	13
2160	14.0	0	2 N=49	0 A=102	0 B=256

Here, y' = 14.0 degrees which was equivalent to 2160 micro in/in and in this case d had a value of 86.3 micro in/in. This information came from Figure 2-3 since the data was run on machine #3. Therefore,

$$\bar{y} = 2296 \text{ μin/in} \quad (3.9)$$

$$s = 129.4 \text{ μin/in} \quad (3.10)$$

and the corresponding values for the strain range were

$$\bar{y}_t = 4592 \text{ μin/in} \quad (3.11)$$

$$s_t = 258.8 \text{ μin/in} \quad (3.12)$$

Table 3-3 gives the data for the life of 5×10^5 cycles which was run also on machine #3 so that d remained 86.3 micro in/in.

Table 3-3. Staircase Data - 5×10^5 Cycles

Approx. Strain, μ in/in	α , degrees	i	n_i failures	in_i	i^2n_i
2420	15.5	5	1	5	25
2340	15.0	4	8	32	128
2250	14.5	3	17	51	153
2160	14.0	2	12	24	48
2070	13.5	1	4	4	4
1985	13.0	0	7	0	0
			N=49	A=116	B=358

From Figure 2-3 the strain value at 13.0 degrees was found for y'; it was 1985 micro in/in. Substituting into Equations 3.3a and 3.4 resulted in:

$$\bar{y} = 2146\ \mu\text{in/in} \quad (3.13)$$

$$s = 244\ \mu\text{in/in} \quad (3.14)$$

and the strain range was defined by

$$\bar{y}_t = 4292\ \mu\text{in/in} \quad (3.15)$$

$$s_t = 488\ \mu\text{in/in} \quad (3.16)$$

At this writing only forty-three data points were available at 7.5×10^5 cycles of which twenty-one were failures. This is shown in Table 3-4 below. Machine #2 was used.

Table 3-4. Staircase Data - 7.5×10^5 Cycles

Approx. Strain, μ in/in	α, degrees	i	n_i failures	in_i	i^2n_i
2510	15.5	4	1	4	16
2415	15.0	3	1	3	9
2320	14.5	2	3	6	12
2225	14.0	1	6	6	6
2130	13.5	0	10 N=21	0 A=19	0 B=43

Using calibration charts similar to those presented in Figures 2-3 and 2-4 gave y' and d in terms of strain (13, pp. 65, 74, and 75). In this case y' is 2130 micro in/in and d is found to be 94 micro in/in. Therefore,

$$\bar{y} = 2168\ \mu\text{ in/in} \quad (3.17)$$

$$d = 191.2\ \mu\text{in/in} \quad (3.18)$$

and for the strain range

$$\bar{y}_t = 4336 \ \mu in/in \qquad (3.19)$$

$$s_t = 382.4 \ \mu in/in \qquad (3.20)$$

Machine #3 was used for the testing done at 10^6 cycles and then reduced data is in the now familiar form in Table 3-5. The value for d was unchanged, and y' = 13.5 degrees was equivalent to 2070 micro in/in.

Table 3-5. Staircase Data - 10^6 Cycles

Approx. Strain, μ in/in	α, degrees	i	n_i failures	in_i	$i^2 n_i$
2340	15.0	3	1	3	9
2250	14.5	2	16	32	64
2160	14.0	1	24	24	24
2070	13.5	0	7	0	0
			N=48	A=59	B=97

It can be easily shown that

$$\bar{y} = 2133 \ \mu in/in \qquad (3.21)$$

$$s = 75.8 \ \mu in/in \qquad (3.22)$$

For the corresponding strain range

$$\bar{y}_t = 4266 \ \mu in/in \qquad (3.23)$$

$$s_t = 151.6 \ \mu in/in \qquad (3.24)$$

Seventy-three data points were available for the cycle life of 1.5×10^6 and there were thirty-five failures. This is given in Table 3-6. Machine #1 was used in this case and the

value for d was 96 micro in/in and the strain value for y' = 13.5 degrees was 1890 micro in/in (13, pp. 65, 74, and 75).

Table 3-6. Staircase Data - 1.5 x 10^6 Cycles

Approx. Strain, μ in/in	α, degrees	i	n_i failures	in_i	i^2n_i
2270	15.5	4	2	8	32
2175	15.0	3	7	21	63
2080	14.5	2	14	28	56
1985	14.0	1	10	10	10
1890	13.5	0	2	0	0
			N=35	A=67	B=161

Computing for the estimates of the mean and standard deviation of the distribution the results were:

$$\bar{y} = 2026 \text{ μin/in} \quad (3.25)$$

$$s = 149.2 \text{ μin/in} \quad (3.26)$$

and for the strain range at 1.5 x 10^6 cycles

$$\bar{y}_t = 4052 \text{ μin/in} \quad (3.27)$$

$$s_t = 298.4 \text{ μin/in} \quad (3.28)$$

Two complete sets of data were made at 2 x 10^6 cycles. These were actually the first series of specimens run on the machines after they were calibrated so to get a comparison of the data between the machines data was generated at 2 x 10^6 cycles on both machines #3 and #4. It was hoped, of course, that the

results would be close, thereby giving strength to the method of calibration. Tables 3-7 and 3-8 show the reduced data.

Table 3-7. Staircase Data - 2 x 10^6 Cycles, Machine #3

Approx. Strain μ in/in	α, degrees	i	n_i failures	in_i	$i^2 n_i$
2250	14.5	5	1	5	25
2160	14.0	4	2	8	32
2070	13.5	3	6	18	54
1985	13.0	2	21	42	84
1900	12.5	1	11	11	11
1810	12.0	0	3	0	0
			N=44	A=84	B=206

As before, the value for d on machine #3 was 86.3 micro in/in, and 12.0 degrees was equivalent to 1810 micro in/in for y'. We get the following results:

$$\bar{y} = 1932 \ \mu in/in \tag{3.29}$$

$$s = 149.2 \ \mu in/in \tag{3.30}$$

The increment on Machine #4 was 0.5 degrees, as on the others; referring to Figure 2-4 it can be seen this d was 90 micro in/in. From the same figure, y' = 13.0 degrees corresponded to 1875 micro in/in.

Table 3-8. Staircase Data - 2 x 10^6 Cycles, Machine #4

Approx. Strain μ in/in	α, degrees	i	n_i failures	in_i	i^2n_i
2145	14.5	3	3	9	27
2055	14.0	2	10	20	40
1965	13.5	1	17	17	17
1875	13.0	0	15 N=45	0 A=46	0 B=84

Therefore,

$$\bar{y} = 1922 \ \mu \text{ in/in} \tag{3.31}$$

$$s = 123.8 \ \mu \text{ in/in} \tag{3.32}$$

Before finding the estimates of the mean and standard deviation of the distribution of the total strain range at 2 x 10^6 cycles the reduced data from machines #3 and #4 was averaged. That is,

$$\bar{y} = \frac{1932 + 1922}{2} = 1927 \ \mu\text{in/in} \tag{3.33}$$

$$s = \frac{149.2 + 123.8}{2} = 136.5 \ \mu \text{ in/in} \tag{3.34}$$

The values for the total strain range distribution that will be used in the final plot of the data were:

$$\bar{y}_t = 3854 \ \mu \text{ in/in} \tag{3.35}$$

$$s_t = 273 \ \mu \text{ in/in} \tag{3.36}$$

It is obvious from comparing Equations 3.29 and 3.31 that the mean values for the strain distribution are quite close, tending to

indicate that the calibration was performed satisfactorily. It follows then, that there should be no problem in using data obtained from different machines. Looking at Equations 3.30 and 3.32 we see that the estimates for the standard deviations of the distribution do not compare as well as the estimates for the mean. However, the difference is not very great and may just be due to the characteristics of the machines. It should be repeated, though, that the staircase method of fatigue testing is not the most reliable for finding the standard deviation.

The last set of data to be considered was run at 10^7 cycles and due to the fact that it takes so much longer to run this large number of cycles only fifty-three points were available for reduction. These were run on machine #4 so that again d had a value of 90 micro in/in. See Table 3-9 below.

Table 3-9. Staircase Data - 10^7 Cycles

Approx. Strain μ in/in	α, degrees	i	n_i failures	in_i	i^2n_i
2055	14.0	3	3	9	27
1965	13.5	2	10	20	40
1875	13.0	1	9	9	9
1785	12.5	0	2	0	0
			N=24	A=38	B=76

From Figure 2-4 we can find that y' = 12.5 was the equivalent of 1785 micro in/in on machine #4. In the same manner as before the calculations were performed to find:

$$\bar{y} = 1822.5 \ \mu in/in \tag{3.37}$$

$$s = 100.5 \ \mu in/in \tag{3.38}$$

And the strain range in this case became defined by:

$$\bar{y}_t = 3765 \ \mu in/in \tag{3.39}$$

$$s_t = 201 \ \mu in/in \tag{3.40}$$

This completes the reduction of the data that was generated to determine the transition zone of the S-N curve for cold drawn and annealed AISI 4340 steel. The data will be plotted and compared with the theories of Manson in the next chapter of this thesis. Before going on to this it would be convenient for the reader to have all of this data in one place and so the estimates of the means and standard deviations of the distributions of the strain and total strain range are consolidated in Table 3-10.

Table 3-10. Reduced Data for All Cycle Lives

Cycle Life	Maximum Strain (μ in/in)		Total Strain Range (μin/in)	
	$\bar{y}$	s	$\bar{y}_t$	s_t
10^5	2548	80.4	5096	160.8
3×10^5	2296	129.4	4592	258.8
5×10^5	2146	244.0	4292	488.0
7.5×10^5	2168	191.2	4336	382.4
10^6	2133	75.8	4266	151.6
1.5×10^6	2026	149.2	4052	298.4
2×10^6	1927	136.5	3854	273.0
10^7	1882.5	100.5	3765	201.0

CHAPTER 4

DATA REDUCTION RESULTS

As was stated in Chapter 1, there are several methods by which the elastic strain range line and the plastic strain range line can be approximated, thereby giving an estimated dynamic total strain range curve. Before plotting the reduced data discussed in Chapter 3, consider the approximate curves that are found by Manson's methods.

4-1. Approximation of Elastic Strain Range Line

First, the elastic strain range line will be found. All that is needed to define the line are two points. Testing has shown that the following relationship holds true for most materials, and is valid for annealed AISI 4340 steel (3, p. 154):

$$(\varepsilon_{el})_{1/4} = (\frac{\Delta S}{E})_{1/4} = 2.5 \frac{S_f}{E} \qquad (4.1)$$

This means that the elastic strain range, ε_{el}, at 1/4 cycles is equal to 2.5 times the tensile fracture stress, S_f, divided by the modulus of elasticity. Tensile fracture stress is defined as the load just prior to fracture in a static tensile test divided by the cross-sectional area just after fracture (3, p. 154). For the material in question the tensile fracture stress has a value of approximately 170,000 psi (3, p. 155). Because of the fact that this property is found using the cross-sectional area after fracture (which is smaller that the original area) it has a value

higher than the ultimate tensile strength. The modulus of elasticity has been shown to be very close to 30 x 10^6 psi for our wire specimens (13, p. 68). Equation 4.1 then becomes:

$$(\varepsilon_{el})_{1/4} = 2.5 \left(\frac{170{,}000}{30 \times 10^6}\right) = 0.01417 \text{ in/in} \qquad (4.1a)$$

The other point on the elastic strain range curve is calculated from the data itself. Theoretically the total strain at the endurance limit should be entirely elastic strain. Therefore, knowing the total strain range at the endurance limit from the reduced data, we can use this value to find the second point on the elastic strain range line. As will be shown later in this chapter, the endurance limit was found to be approximately equal to 0.00388 in/in at about 2.5 x 10^6 cycles. This was used as the second point to establish the elastic strain range line. That is,

$$(\varepsilon_{el})_{2.5 \times 10^6} = 0.00388 \text{ in/in} \qquad (4.2)$$

Beyond the endurance limit the author has assumed that the elastic strain range maintains a nearly constant value of 0.00388 in/in. The log-log plot for elastic strain range versus cycles to failure is shown in Figure 4-1.

From Chapter 1, it is known that the relationship between elastic strain range and cycles to failure is given by Equation 1.4, which is:

$$(\varepsilon_{el}) = \frac{G}{E} N^{\gamma} \quad . \qquad (1.4)$$

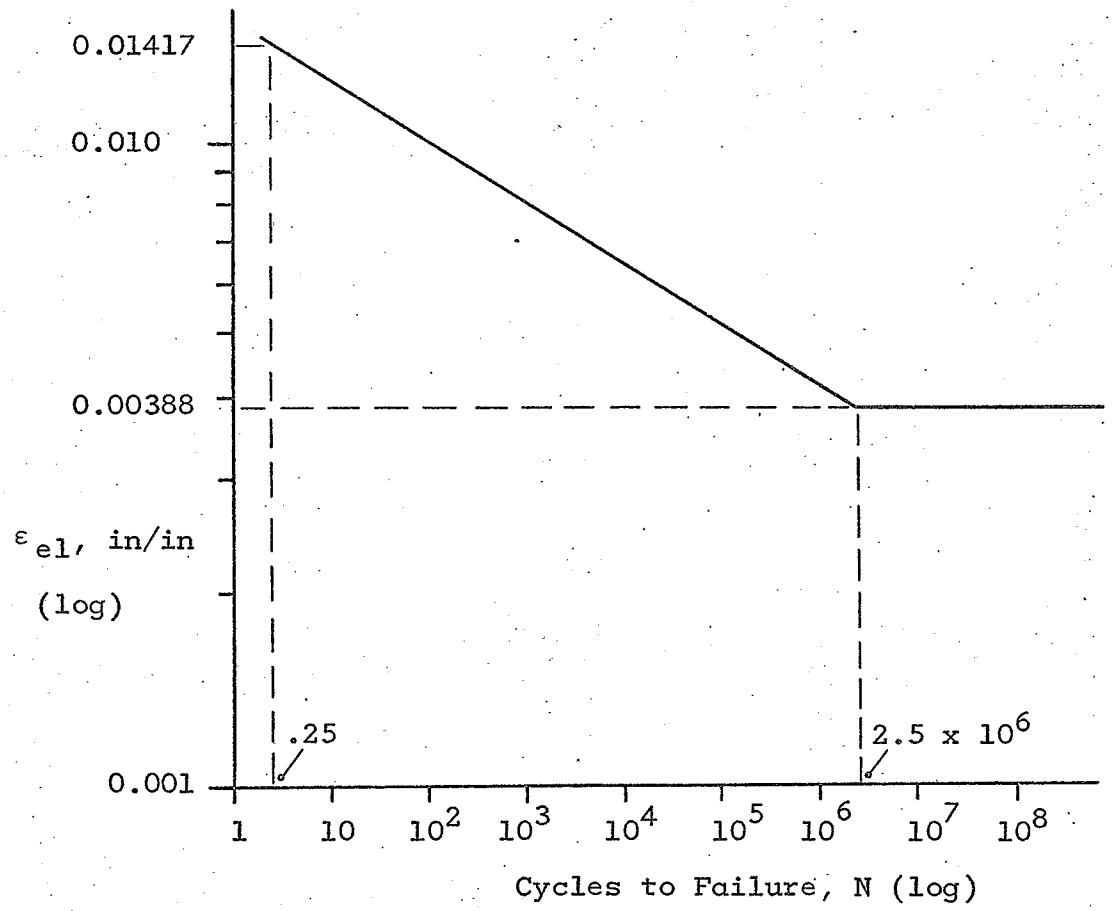

Figure 4-1. Elastic Strain Range Versus Cycles to Failure for Cold Drawn and Annealed AISI 4340 Steel.

Knowing two points on the line, we solve for the constants G and γ, which yields the equation for the line. A computer program was written in Focal-8 Language to find these constants, on the PDP-8 Computer; the program is presented in Appendix C. The results for this example were:

$$G = 380{,}200 \text{ psi}$$

$$\gamma = -0.08035$$

Substituting the above values into Equation 1.4, produces the following relationship between elastic strain range and cycles to failure:

$$\varepsilon_{el} = 0.01267N^{-0.08035} \tag{4.3}$$

4-2. Approximation of Plastic Strain Range Line

Similarly, an approximation can be found for the plastic strain range line, knowing two points on the line. In his experimentation, Manson has determined that the following equation was valid for most materials (3, p. 152):

$$(\varepsilon_p)_{10} = 0.25D^{0.75} \tag{4.4}$$

where D is the ductility of the material, defined by (3, p. 152):

$$D \equiv -\ln(1 - R.A.)$$

R.A. is the fractional reduction in area in a static tensile test. For 4340 steel with an ultimate tensile strength close to that of the wires, the reduction in area is 0.42 of the original (10, p. 600). Then, D is:

$$D = \doteq \ln(1.00 - 0.42) = 0.544$$

Using the ductility in Equation 4.4 we find the plastic strain range at ten cycles:

$$(\varepsilon_p)_{10} = 0.25(0.544)^{0.75} = 0.1585 \text{ in/in} \tag{4.4a}$$

Again through experimentation, Manson showed that this relationship is often true (3, p. 156):

$$(\varepsilon_p)_{10^4} = \frac{0.0132 - (\varepsilon_{el})_{10^4}}{1.91} \tag{4.5}$$

Evaluating the elastic strain range at 10^4 cycles and substituting into Equation 4.5 yields the second plastic strain range value required to quantify the equation of the line:

$$(\varepsilon_{el})_{10^4} = 0.01267(10{,}000)^{-.08035} = 0.00605 \text{ in/in}$$

Therefore, the corresponding plastic strain range is

$$(\varepsilon_p)_{10^4} = \frac{0.0132 - 0.00605}{1.91} = 0.00374 \text{ in/in} \qquad (4.5a)$$

There is now enough information to plot, on log-log coordinates, the straight line relationship between plastic strain range and cycles to failure. This is given in Figure 4-2.

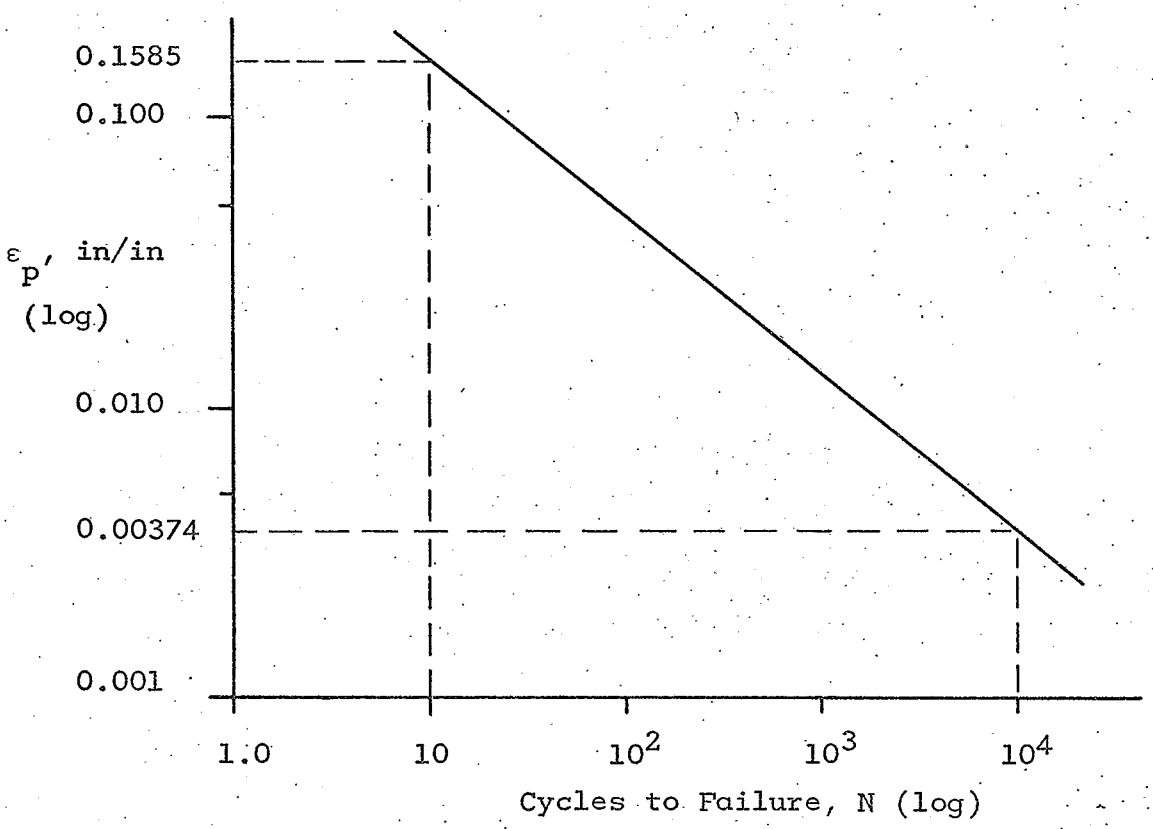

Figure 4-2. Plastic Strain Range Versus Cycles to Failure for Cold Drawn and Annealed AISI 4340 Steel.

This line is defined by Equation 1.3 which is:

$$\varepsilon_p = MN^z \tag{1.3}$$

where M and z are material constants that can be evaluated, knowing the two points on the line (that have been calculated above). To find the two constants, the same computer program (mentioned before) was used. For the wire material of this study, the unknowns were found to have the following values:

$$M = 0.5524$$

$$z = -0.5422$$

Equation 1.3 now has known terms:

$$\varepsilon_p = 0.5524N^{-0.5422} \tag{4.6}$$

4-3. Total Strain Range Curve

As was demonstrated in the discussion of Manson's theories in Chapter 1, the relationship between the total strain range and cycles to failure is obtained by adding Equations 1.3 and 1.4. In general terms, this was represented by Equation 1.7:

$$\Delta\varepsilon = \varepsilon_p + \varepsilon_{el}$$

$$= MN^z + \frac{G}{E}N^\gamma \quad , \tag{1.7}$$

and was shown graphically in Figure 1-9.

Now, having approximate values for the elastic and plastic strain ranges, we also have an approximate value for the total strain range for any cycle life. This can then be compared with our test results, to determine if Manson's theories appear to

apply in our area of interest. Adding Equations 4.3 and 4.6 yields this desired expression, designated as Equation 4.7:

$$\Delta\varepsilon = 0.5524N^{-0.5422} + 0.0126N^{-0.08035} . \quad (4.7)$$

Once again resorting to the computer program, the value of total strain range for any desired cycle life can be calculated. The total strain range and the elastic and plastic strain ranges, approximated by Manson's methods, are plotted for the spectrum of cycle lives from about .25 cycles to 10^7 cycles in Figure 4-3. In this thesis, however, the zone of particular interest is the endurance region. Therefore, the cycle range from 10^4 cycles to 10^7 cycles is developed in detail in Figure 4-4. It is evident from Figure 4-3 that at the lower cycle lives plastic strain constitutes nearly all of the total strain range. At the higher cycle lives, that are of interest here, the plastic strain is not a dominant factor. If our data and Manson's approximation are in agreement, then we can develop the formula that relates total strain range with stress range. Using this, the final S-N surface can be obtained, as described in detail in the latter part of Chapter 1.

The results of data reduction are presented in graphical form in Figure 4-5. In this figure are given the mean locus and the upper and lower three standard deviation limits. Thus, we have a complete strain range versus cycle life surface.

In Figure 4-5 the points that were generated, by applying the staircase method described in Chapter 3, are shown with circles. The upper and lower three standard deviation limits, that were

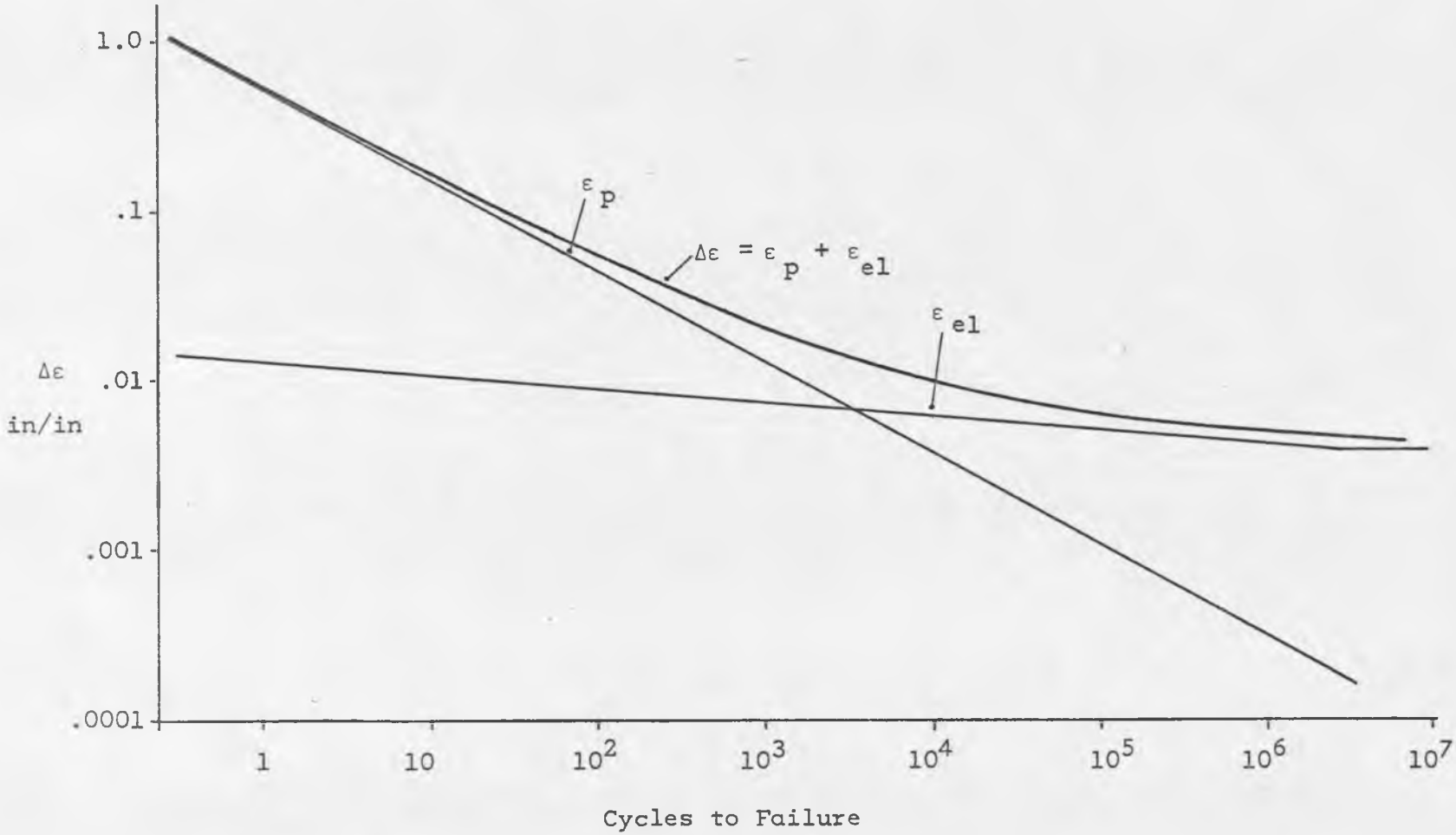

Figure 4-3. Complete Total Strain Range Versus Cycles to Failure for Cold Drawn and Annealed AISI 4340 Steel.

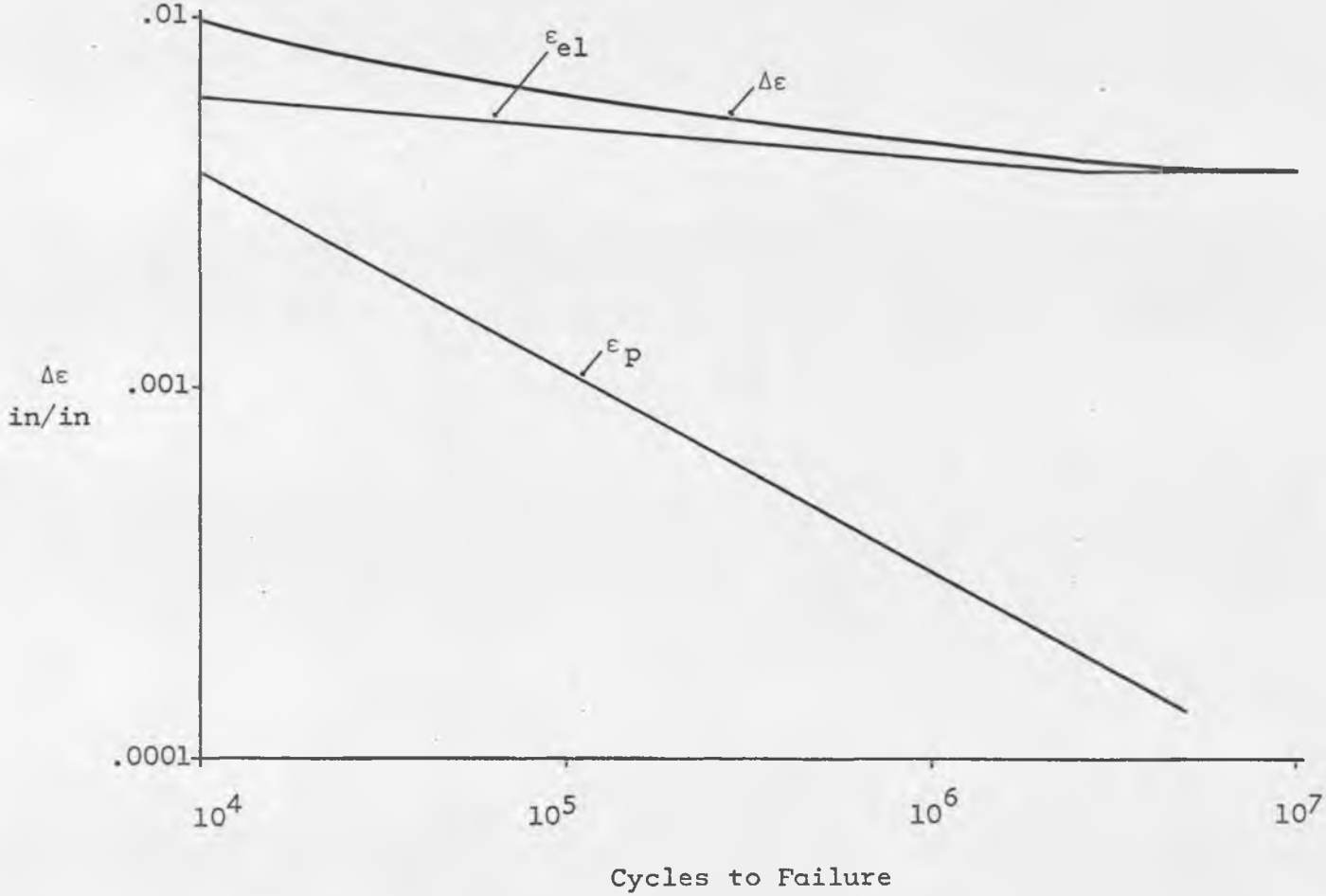

Figure 4-4. Total Strain Range Versus Cycles to Failure in Transition Zone for Cold Drawn and Annealed AISI 4340 Steel.

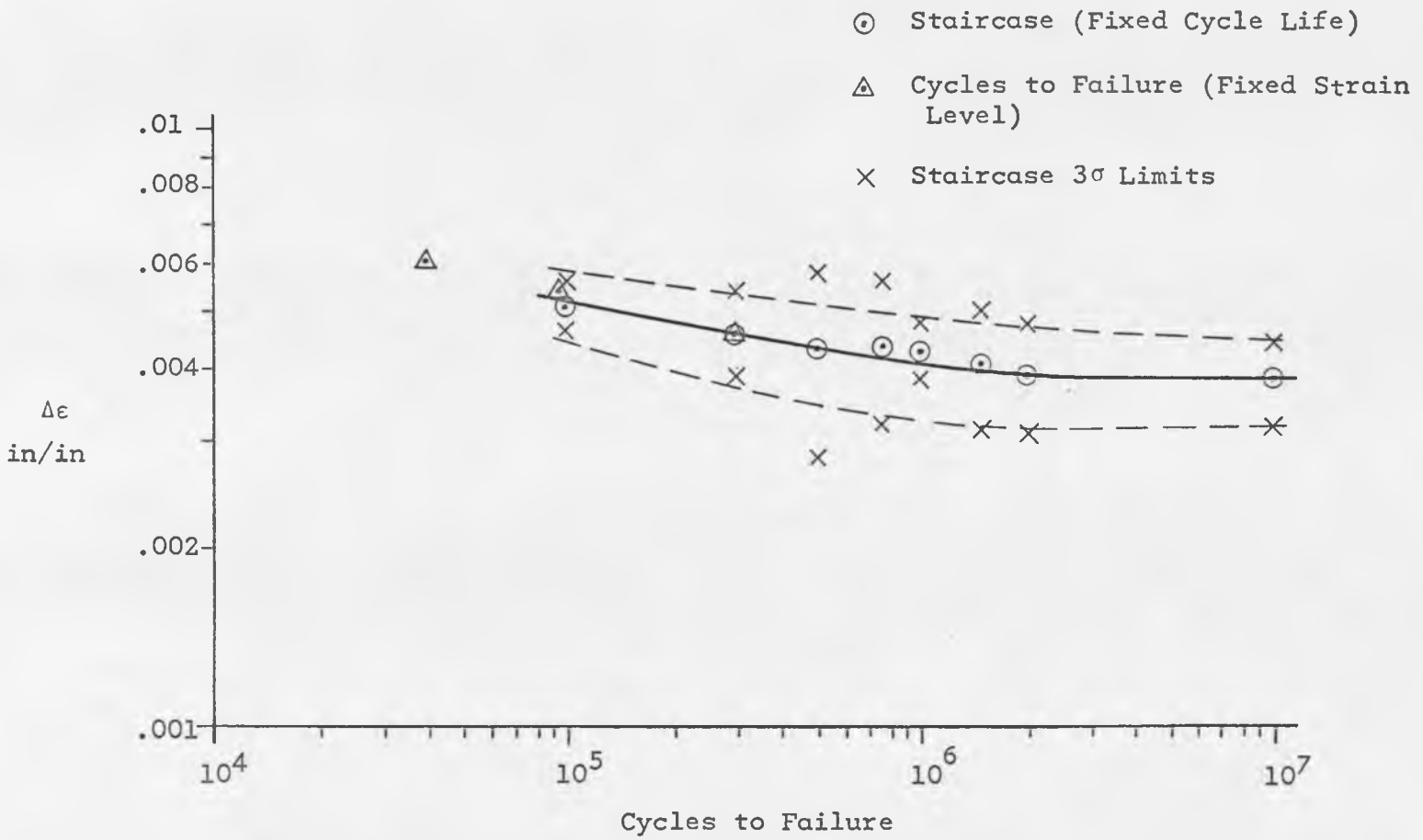

Figure 4-5. Statistical Total Strain Range Versus Cycles to Failure Surface.

calculated along with the mean value estimates, are indicated by x's in the plot. This plot indicates a distribution of strain for a fixed cycle life. As was stated earlier in this report one of the objectives was to compare the staircase results with available data that was found for a distribution of cycle life for a fixed stress or strain level. Data for fixed stress levels have been run on the University of Arizona wire fatigue machines, utilizing the same type of wire specimens that this author used. This data was run by another graduate student, Gary Peterson, whose Master's Report has been referred to before (13). Some of his results are shown in Figure 4-5. These points are represented by small triangles. Notice that for the two overlapping points, near 10^5 and 3×10^5 cycles, the mean values correspond very closely. This would seem to indicate that the testing produces consistant results, whichever method is used.

It was previously noted that the staircase method is not the most accurate method for obtaining the standard deviation estimates of the distribution. As a result, there was a considerable amount of scatter in the staircase results. However, the results do indicate one thing: the standard deviations as you approach either end of the cycle range become smaller, indicating that the greatest scatter, and therefore the most uncertain range, is the transition zone. This does not seem unreasonable. Most S-N surfaces show more narrow distributions at the lower cycle lives (See Figure 1-3), and it would follow that this would be true

also in the strain-cycles curve since the stress and strain are related. The fact that the strain distribution narrows immediately after the endurance limit would seem to indicate that at the higher cycle lives there is more certainty of actually being at the endurance level. It is this author's opinion, however, that the distribution would probably become constant beyond 10^7 cycles, at least for the material that was used in our testing.

Figure 4-6 shows the reduced data superimposed over the approximated curve of Manson (given before in Figures 4-3 and 4-4). Once again, the staircase results are represented by circles and the cycles to failure reduced data by triangles. Judging from Figure 4-6, which indicates that Manson's curve is a good approximation of our reduced data, it would seem reasonable to assume that our material behavior is defined by Equation 4.7. There is some difference between Manson's curve and the mean reduced data points, but this agrees with some of Manson's testing results. He has shown (in the range in which we are interested for 4340 hard steel) that the approximation was a little above the reduced data points. However, for low cycle lives, i.e., from 1 to 10^4 cycles the data falls somewhat above the approximation (3, p. 162). In these cases as in ours, the difference is small. Therefore, we will assume that Equation 4.7 holds for the test results.

4-4. Cyclic Stress-Strain Curve

It follows that we can develop the relation between total strain range and total stress range for our test material.

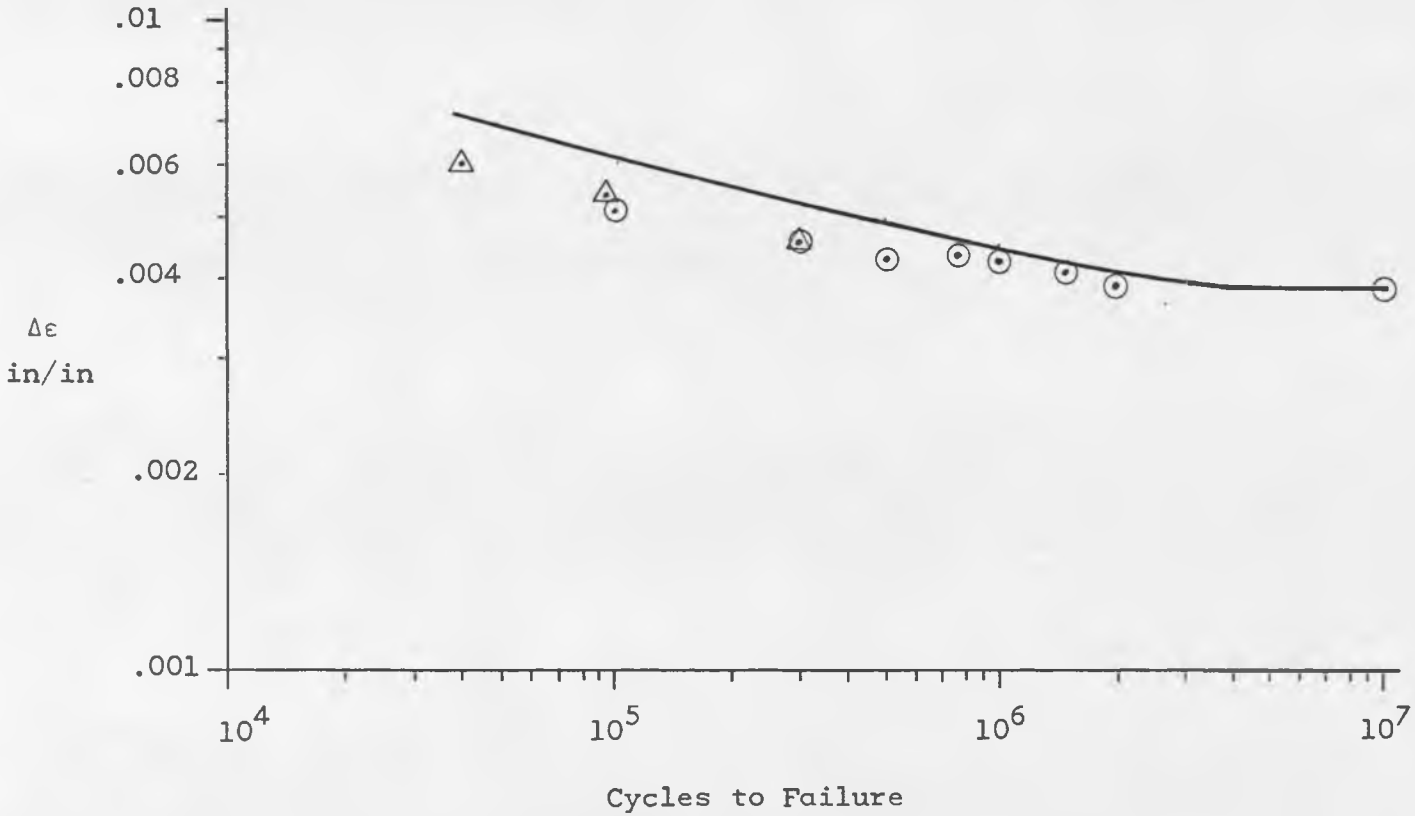

Figure 4-6. Comparison Between Reduced Data and Manson's Approximation of Total Strain Range Versus Cycles to Failure.

In Chapter 1 the general equation was given as:

$$\Delta\varepsilon = \frac{\Delta S}{E} + M\left(\frac{\Delta S}{E}\right)^{z/\gamma} \tag{1.8}$$

In numerical terms this becomes:

$$\Delta\varepsilon = \frac{\Delta S}{30 \times 10^6} + 0.5524\left(\frac{\Delta S}{380{,}200}\right)^{6.76798} \tag{4.8}$$

Utilizing a second computer program, presented in Appendix C, values for the total stress range were found for the corresponding total strain range. These are plotted in Figure 4-7.

We now have an approximate stress range-strain range curve. Notice that the curve departs from the ideal elastic line very near a stress range value of $2S_{end}$. The fact that the break does not occur at exactly this point indicates that the plastic strain range line is not actually zero at the endurance life (see Figure 4-4). However, the stress range-strain range curve (shown in Figure 4-7) can be assumed to be a good estimate of the actual cyclic stress range-strain range curves. This is certainly an improvement over use of any static stress-strain curves that might be available.

4-5. Statistical S-N Surface for Transition Zone

In Chapter 3 the assumption was made that, since the stress at any particular cycle life is usually considered to be normally distributed, the strain at any cycle life is also normally distributed. Knowing the strain range distribution, i.e., the mean and standard deviation estimators, it is a simple matter to check the validity of the assumption in Figure 4-7. If the assumption is true, the upper and lower three sigma limits will be equal

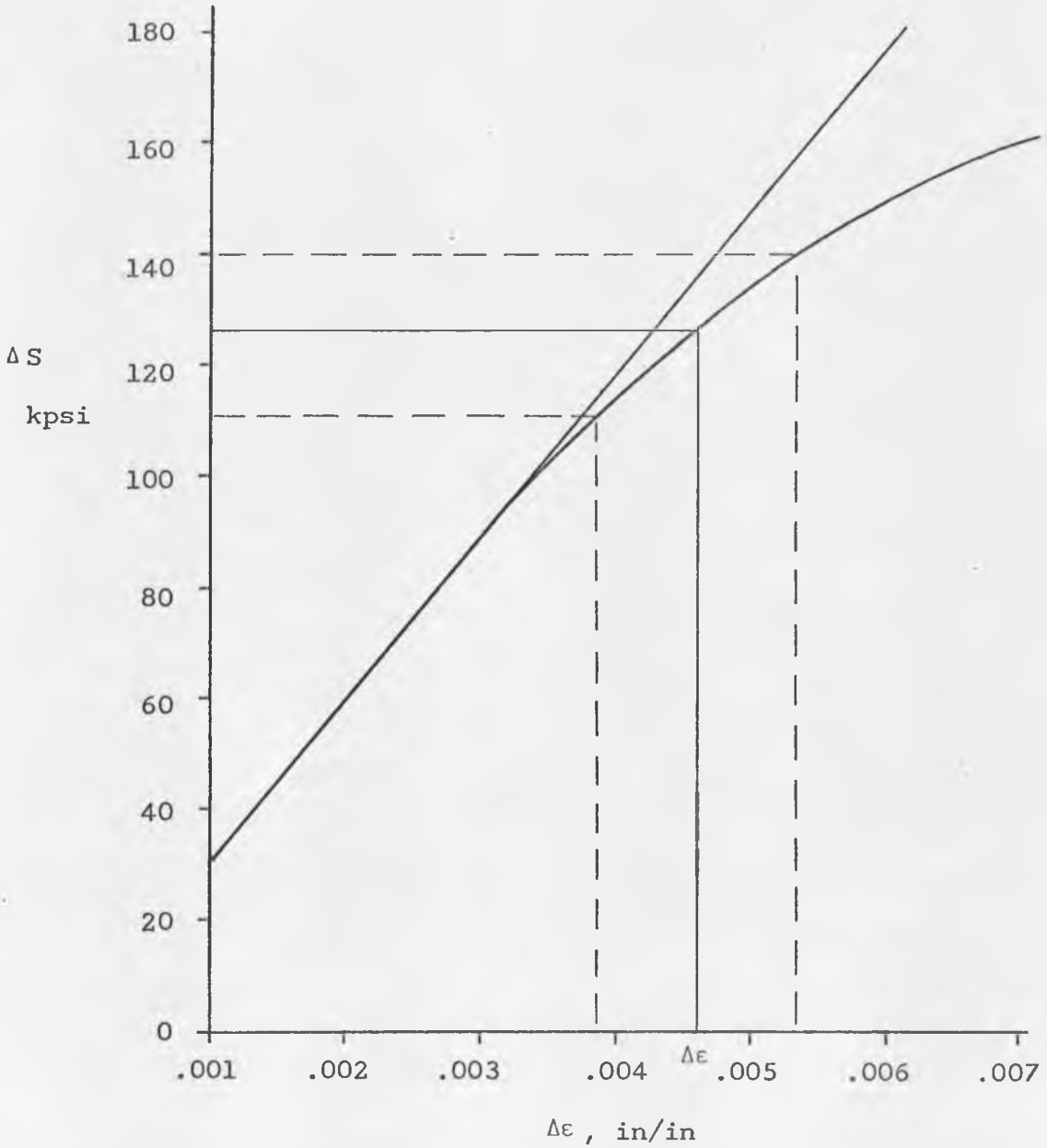

Figure 4-7. Approximate Cyclic Stress Range - Strain Range Curve For AISI 4340 Steel.

distances from the mean stress, for the corresponding strain. For example, take the point $\Delta\varepsilon_1$, which corresponds to the total strain range at 3×10^5 cycles, with a mean value of about 0.0046 in/in and with upper and lower three sigma limits of 0.00537 in/in and 0.00382 in/in. If we project these lines up to the curve and then over to the stress range axis, it is clear that the upper and lower three sigma stress range limits are the very nearly same distance from the mean stress range value. Therefore, the original assumption seems to be justified, in the nonlinear region of the stress range-strain range curve. The same is true in the linear region.

Having shown now that we can find the stress range distribution at any particular cycle life from our strain range reduced data, we have all of the necessary information from which to derive the final S-N surface of primary interest. The total stress range is twice the value of the maximum bending stress in the test member, and thus to find the mean maximum stress for any cycle life we divide the mean stress range at that point by two as in Equation 4.9.

$$\text{(Mean Maximum Stress)} = \text{(Mean Stress Range)}/2 \qquad (4.9)$$

This was shown to be true by the Algebra of Normal Functions in Chapter 3 (1, Chapter 3). By this same procedure the standard deviation of the maximum stress differs from the standard deviation of the total stress range by a factor of one-half also. See Equation 4.10.

$$\sigma_{\text{Max. Stress}} = (\sigma_{\text{Stress Range}})/2 \qquad (4.10)$$

This procedure was performed for each of the estimated strain range distributions that were established from tests made on the wire machines. The resulting final statistical S-N surface in the transition zone for cold drawn and annealed AISI 4340 steel wire is shown plotted log-log in Figure 4-8. Figure 4-9 shows superimposed on this derived curve the approximated S-N surface using Shigley's method described in Chapter 1 and shown in Figure 1-14. The mean line in the Shigley approximation is almost exactly the same as the experimental curve except, not unexpectedly, in the transition zone. Shigley's approximation defines the endurance limit fairly well, but is rather conservative as far as the endurance cycle life is concerned. It is also apparent from Figure 4-9 that the assumptions made about the stress distributions in constructing Figure 1-14 are everywhere conservative. Our data did not show as much variation at any point.

These, then, are the results of the experimental testing program that was carried out together with the application of these results to the theories of S. S. Manson. Further elaboration on the conclusions that were drawn and the subsequent recommendations are presented in Chapter 5.

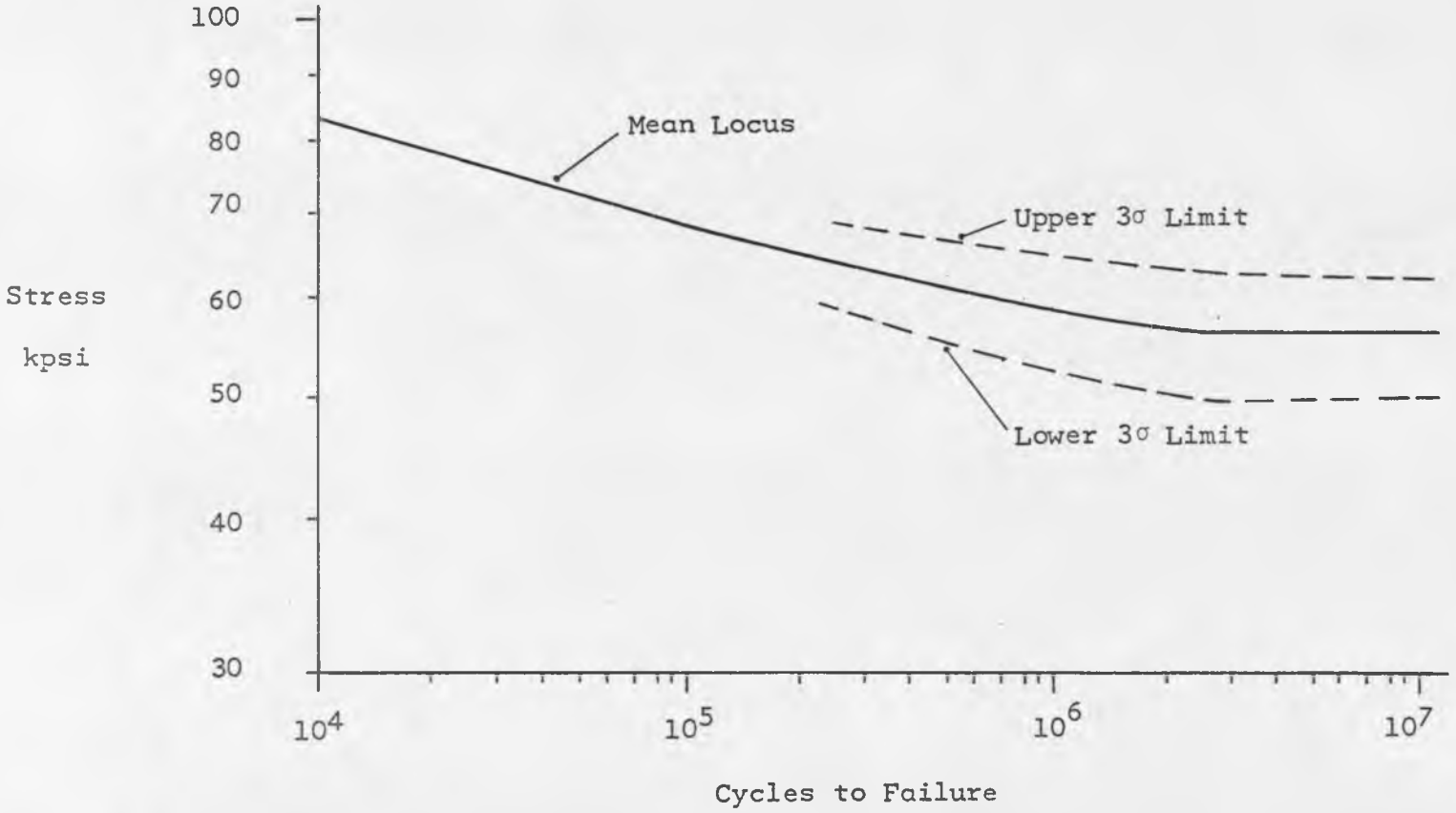

Figure 4-8. Statistical S-N Surface in the Transition Zone for AISI 4340 Steel.

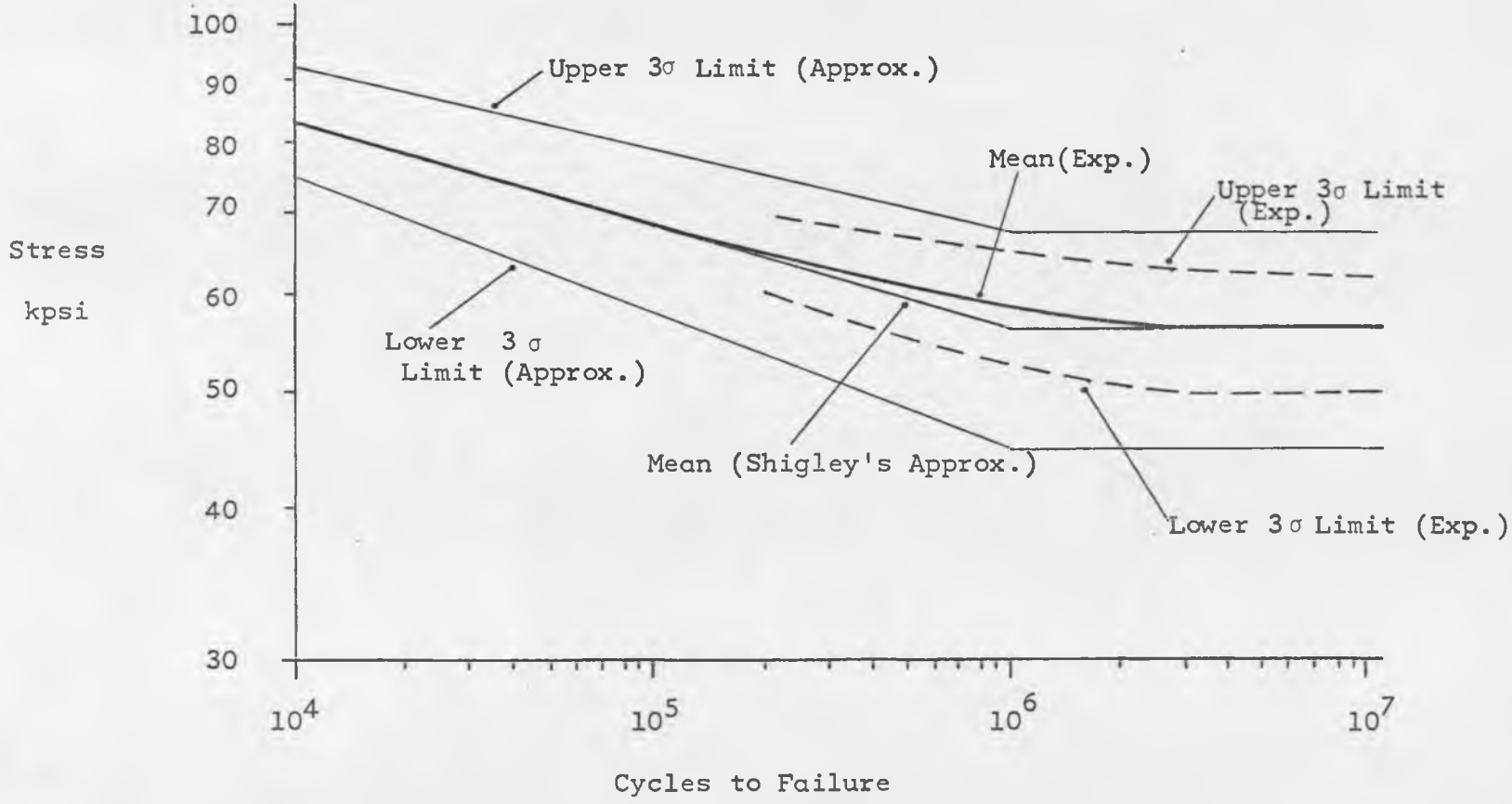

Figure 4-9. Comparison Between Reduced Experimental Data and Shigley's Approximation.

CHAPTER 5

CONCLUSIONS AND RECOMMENDATIONS

Looking at the results of the data reduction and the comparison with the approximations of Manson and Shigley there are several conclusions which can be drawn.

From all appearances, Manson's approximations, and therefore his theories, would seem to apply for our case. Our reduced data points were close to the final strain range versus cycles to failure curve of Manson. Judging from this, and similar results that Manson himself has obtained, his theories seem quite good. It is this author's opinion that Manson's approximations would be good in estimating the transition zone where there is little available data. If the designer is not necessarily interested in the transition zone of the S-N curve then Sigley's approximate line should be sufficient. This conclusion about Shigley's line is nothing new, however, because other authors have also shown this. In many cases, Shigley's approximate line is somewhat conservative and we found that the estimated S-N surface of Figure 1-14 was quite conservative expecially in the endurance region. The author found no references which offered any method of approximating the $+3\sigma$ to -3σ limits of a normal distribution and apparently the only method at this time of determining an S-N surface is through a process of testing.

Because Manson's total strain range versus cycles to failure curve is valid for our case we also determined that the cyclic stress range-strain range curve developed is also valid. Without any methods to find a cyclic stress-strain curve though testing Manson's curve is probably a reasonable approximation. It is almost certainly better to employ this curve for cyclic conditions, such as those incurred in fatigue than to use the static stress-strain curve. Unfortunately, a static stress-strain curve for our material was not available for comparison with our Manson approximation in this report. However, the cyclic curve usually varies greatly from the static in the region of plastic strain.

Although the final S-N surface presented in Figure 4-8 can be used with a reasonable degree of confidence it should be repeated that this was developed for a small diameter wire. How much the size of the specimen will effect the S-N curve is something which remains to be proven. Even so, the results might be applied cautiously. The procedure outlined in this thesis should, at any rate, be applicable to a great number of situations.

APPENDIX A

CALIBRATION DATA

All of the data that was taken in the calibration of wire fatigue machines #3 and #4 is contained in this appendix. Data was taken in the form of strain measured versus the bend angle, α , and is shown in its final form in Table 2-2 and graphically in Figure 2-3 and 2-4.

The angle was measured in two degree increments from 2 degrees to 12 degrees. Ten strain measurements were taken at each angle on each machine and then the average value was used. For similar calibration data on machines #1 and #2, see reference 13.

CALIBRATION DATA SHEET

Machine No. 3 0.0625 Diameter Wire

Bend Angle 2 degrees

Strain Indicator Reading		Strain Difference, micro in/in
0 Degrees	Bend Angle	
3,763	3,609	154
3,764	3,608	156
3,762	3,611	151
3,765	3,611	154
3,765	3,610	155
3,764	3,610	154
3,765	3,610	155
3,765	3,611	154
3,766	3,610	156
3,766	3,611	155

Average Strain 154.4

CALIBRATION DATA SHEET

Machine No. 3 0.0625 Diameter Wire

Bend Angle 4 degrees

Strain Indicator Reading		Strain Difference, micro in/in
0 Degrees	Bend Angle	
3,765	3,356	409
3,768	3,364	404
3,767	3,376	391
3,768	3,371	397
3,768	3,370	398
3,769	3,369	400
3,770	3,377	393
3,771	3,365	406
3,770	3,373	397
3,772	3,357	415

Average Strain 401.0

CALIBRATION DATA SHEET

Machine No. 3 0.0625 Diameter Wire

Bend Angle 6 degrees

Strain Indicator Reading		Strain Difference, micro in/in
0 Degrees	Bend Angle	
3,768	3,009	759
3,766	3,021	745
3,770	3,025	745
3,766	3,003	763
3,764	3,005	759
3,765	3,014	751
3,765	3,020	745
3,766	3,024	742
3,766	3,024	742
3,768	3,020	748

Average Strain 749.9

CALIBRATION DATA SHEET

Machine No. 3 0.0625 Diameter Wire

Bend Angle 8 degrees

Strain Indicator Reading		Strain Difference, micro in/in
0 Degrees	Bend Angle	
3,767	2,642	1,125
3,764	2,654	1,110
3,758	2,634	1,124
3,755	2,637	1,118
3,753	2,636	1,117
3,753	2,644	1,109
3,749	2,612	1,137
3,738	2,631	1,107
3,747	2,636	1,111
3,749	2,640	1,109

Average Strain 1,116.7

CALIBRATION DATA SHEET

Machine No. 3 0.0625 Diameter Wire

Bend Angle 10 degrees

Strain Indicator Reading		Strain Difference, micro in/in
0 Degrees	Bend Angle	
3,736	2,267	1,469
3,736	2,262	1,474
3,732	2,274	1,458
3,740	2,272	1,468
3,734	2,270	1,464
3,735	2,278	1,457
3,737	2,280	1,457
3,732	2,278	1,454
3,734	2,274	1,460
3,735	2,279	1,456

Average Strain 1,461.7

CALIBRATION DATA SHEET

Machine No. 3 0.0625 Diameter Wire

Bend Angle 12 degrees

Strain Indicator Reading		Strain Difference, micro in/in
0 Degrees	Bend Angle	
3,719	1,904	1,815
3,717	1,912	1,805
3,715	1,905	1,810
3,712	1,919	1,793
3,715	1,910	1,805
3,718	1,909	1,809
3,725	1,903	1,822
3,712	1,910	1,802
3,715	1,917	1,798
3,718	1,910	1,808

Average Strain 1,806.7

CALIBRATION DATA SHEET

Machine No. 4 0.0625 Diameter Wire

Bend Angle 2 degrees

Strain Indicator Reading		Strain Difference, micro in/in
0 Degrees	Bend Angle	
3,718	3,590	128
3,726	3,590	136
3,722	3,590	132
3,725	3,590	135
3,732	3,590	142
3,725	3,591	134
3,734	3,586	148
3,729	3,590	139
3,734	3,591	143
3,728	3,590	138

Average Strain 137.5

CALIBRATION DATA SHEET

Machine No. 4 0.0625 Diameter Wire

Bend Angle 4 degrees

Strain Indicator Reading		Strain Difference, micro in/in
0 Degrees	Bend Angle	
3,724	3,386	338
3,726	3,388	338
3,720	3,389	331
3,727	3,386	341
3,727	3,384	343
3,718	3,385	333
3,715	3,385	330
3,729	3,392	337
3,722	3,390	332
3,715	3,393	322

Average Strain 334.5

CALIBRATION DATA SHEET

Machine No. 4 0.0625 Diameter Wire

Bend Angle 6 degrees

Strain Indicator Reading		Strain Difference, micro in/in
0 Degrees	Bend Angle	
3,725	3,074	651
3,729	3,073	656
3,724	3,070	654
3,722	3,077	645
3,718	3,074	644
3,720	3,080	640
3,717	3,075	642
3,723	3,075	648
3,731	3,074	657
3,736	3,072	664

Average Strain 650.1

CALIBRATION DATA SHEET

Machine No. 4 0.0625 Diameter Wire

Bend Angle 8 degrees

Strain Indicator Reading		Strain Difference, micro in/in
0 Degrees	Bend Angle	
3,739	2,737	1,002
3,731	2,740	991
3,722	2,746	976
3,731	2,746	985
3,730	2,748	982
3,723	2,750	973
3,725	2,751	974
3,721	2,737	984
3,736	2,740	996
3,727	2,736	991

Average Strain 985.4

CALIBRATION DATA SHEET

Machine No. 4 0.0625 Diameter Wire

Bend Angle 10 degrees

Strain Indicator Reading		Strain Difference, micro in/in
0 Degrees	Bend Angle	
3,730	2,388	1,342
3,717	2,390	1,327
3,714	2,383	1,331
3,712	2,383	1,329
3,711	2,384	1,327
3,709	2,387	1,322
3,723	2,388	1,335
3,715	2,387	1,328
3,714	2,388	1,326
3,727	2,387	1,340

Average Strain 1,330.7

CALIBRATION DATA SHEET

Machine No. 4 0.0625 Diameter Wire

Bend Angle 12 degrees

Strain Indicator Reading		Strain Difference, micro in/in
0 Degrees	Bend Angle	
3,723	2,033	1,690
3,734	2,039	1,695
3,726	2,031	1,685
3,738	2,034	1,704
3,735	2,037	1,698
3,735	2,039	1,696
3,740	2,038	1,702
3,734	2,039	1,695
3,735	2,042	1,693
3,732	2,042	1,690

Average Strain 1,694.8

APPENDIX B

STAIRCASE FATIGUE DATA

All of the fatigue data generated for this thesis using the staircase method of testing is presented in this appendix. Copies of the original data sheets and the respective staircase plots are given for each cycle life from 10^5 to 10^7 cycles.

Each data sheet notes the number of cycles being tested and the machine used. For each specimen run the following information was recorded: date of the run, number of cycles actually run, and a note mentioning whether the specimen was a failure or success in the given number of cycles. Reduced data and calculations are found in Chapter 3.

STAIRCASE FATIGUE DATA SHEET

Machine No. 3 0.0625 diameter wire

Cutoff: 10^5 cycles

Date	Spec. No.	Bend Angle, Degrees	Cycles to Failure x 10^{-5}	Remarks
4/23/70	1	15.0	1.227	No Failure
4/23/70	2	15.5	1.056	No Failure
4/24/70	3	16.0	0.865	Failure
4/24/70	4	15.5	1.002	No Failure
4/24/70	5	16.0	1.007	No Failure
4/24/70	6	16.5	1.228	No Failure
4/24/70	7	17.0	0.898	Failure
4/24/70	8	16.5	1.553	No Failure
4/24/70	9	17.0	0.890	Failure
4/24/70	10	16.5	0.921	Failure
4/24/70	11	16.0	0.875	Failure
4/24/70	12	15.5	0.997	Failure
4/24/70	13	15.0	1.019	No Failure
4/24/70	14	15.5	1.608	No Failure
4/24/70	15	16.0	0.930	Failure
4/24/70	16	15.5	1.113	No Failure
4/24/70	17	16.0	1.387	No Failure
4/24/70	18	16.5	0.843	Failure
4/24/70	19	16.0	1.106	No Failure
4/24/70	20	16.5	0.765	Failure

STAIRCASE FATIGUE DATA SHEET

Machine No. 3 0.0625 diameter wire

Cutoff: 10^5 cycles

Date	Spec. No.	Bend Angle, Degrees	Cycles to Failure x 10^{-5}	Remarks
4/24/70	21	16.0	1.264	No Failure
4/24/70	22	16.5	1.013	No Failure
4/24/70	23	17.0	0.658	Failure
4/24/70	24	16.5	0.683	Failure
4/24/70	25	16.0	1.015	No Failure
4/25/70	26	16.5	0.791	Failure
4/25/70	27	16.0	1.144	No Failure
4/25/70	28	16.5	0.983	Failure
4/25/70	29	16.0	1.167	No Failure
4/25/70	30	16.5	1.100	No Failure
4/25/70	31	17.0	0.845	Failure.
4/25/70	32	16.5	0.699	Failure
4/25/70	33	16.0	0.968	Failure
4/25/70	34	15.5	1.013	No Failure
4/25/70	35	16.0	0.872	Failure
4/25/70	36	15.5	1.042	No Failure
4/25/70	37	16.0	0.871	Failure
4/25/70	38	15.5	1.005	No Failure
4/25/70	39	16.0	0.860	Failure
4/26/70	40	15.0	1.014	No Failure

STAIRCASE FATIGUE DATA SHEET

Machine No. 3 — 0.0625 diameter wire

Cutoff: 10^5 cycles

Date	Spec. No.	Bend Angle, Degrees	Cycles to Failure x 10^{-5}	Remarks
4/26/70	41	16.0	1.338	No Failure
4/26/70	42	16.5	0.702	Failure
4/26/70	43	16.0	1.033	No Failure
4/26/70	44	16.5	1.025	No Failure
4/26/70	45	17.0	0.532	Failure
4/26/70	46	16.5	1.011	No Failure
4/26/70	47	17.0	0.514	Failure
4/26/70	48	16.5	1.339	No Failure
4/26/70	49	17.0	0.678	Failure
4/26/70	50	16.5	1.133	No Failure
4/26/70	51	17.0	0.530	Failure
4/26/70	52	16.5	0.936	Failure
4/27/70	53	16.0	1.012	No Failure
4/27/70	54	16.5	0.605	Failure
4/27/70	55	16.0	0.904	Failure
4/27/70	56	15.5	1.235	No Failure
4/27/70	57	16.0	1.027	No Failure
4/27/70	58	16.5	0.582	Failure
4/27/70	59	16.0	1.006	No Failure
4/27/70	60	16.5	0.819	Failure

STAIRCASE FATIGUE DATA SHEET

Machine No. 3 0.0625 diameter wire

Cutoff: 10^5 cycles

Date	Spec. No.	Bend Angle, Degrees	Cycles to Failure x 10^{-5}	Remarks
4/27/70	61	16.0	0.991	Failure
4/27/70	62	15.5	1.437	No Failure
4/27/70	63	16.0	1.018	No Failure
4/27/70	64	16.5	1.027	No Failure
4/27/70	65	17.0	0.557	Failure
4/27/70	66	16.5	0.937	Failure
4/27/70	67	16.0	1.004	No Failure
4/27/70	68	16.5	0.788	Failure
4/27/70	69	16.0	0.888	Failure
4/27/70	70	15.5	1.450	No Failure
4/28/70	71	16.0	2.745	No Failure
4/28/70	72	16.5	1.022	No Failure
4/28/70	73	17.0	0.585	Failure
4/28/70	74	16.5	0.955	Failure
4/28/70	75	16.0	1.780	No Failure
4/28/70	76	16.5	0.618	Failure
4/28/70	77	16.0	1.844	No Failure
4/28/70	78	16.5	0.647	Failure
4/28/70	79	16.0	1.154	No Failure
4/28/70	80	16.5	0.864	Failure

STAIRCASE FATIGUE DATA SHEET

Machine No. 3 — 0.0625 diameter wire

Cutoff: 10^5 cycles

Date	Spec. No.	Bend Angle, Degrees	Cycles to Failure x 10^{-5}	Remarks
4/28/70	81	16.0	1.844	No Failure
4/28/70	82	16.5	1.016	No Failure
4/28/70	83	17.0	0.937	Failure
4/28/70	84	16.5	1.077	No Failure
4/29/70	85	17.0	0.532	Failure
4/29/70	86	16.5	0.748	Failure
4/29/70	87	16.0	1.013	No Failure
4/29/70	88	16.5	0.930	Failure
4/29/70	89	16.0	0.875	Failure
4/29/70	90	15.5	1.190	No Failure
4/29/70	91	16.0	1.008	No Failure
4/29/70	92	16.5	0.787	Failure
4/29/70	93	16.0	1.270	No Failure
4/29/70	94	16.5	0.785	Failure
4/29/70	95	16.0	1.085	No Failure
4/29/70	96	16.5	0.768	Failure
4/29/70	97	16.0	1.019	No Failure
4/29/70	98	16.5	0.814	Failure
4/29/70	99	16.0	1.764	No Failure
4/29/70	100	16.5	0.556	Failure

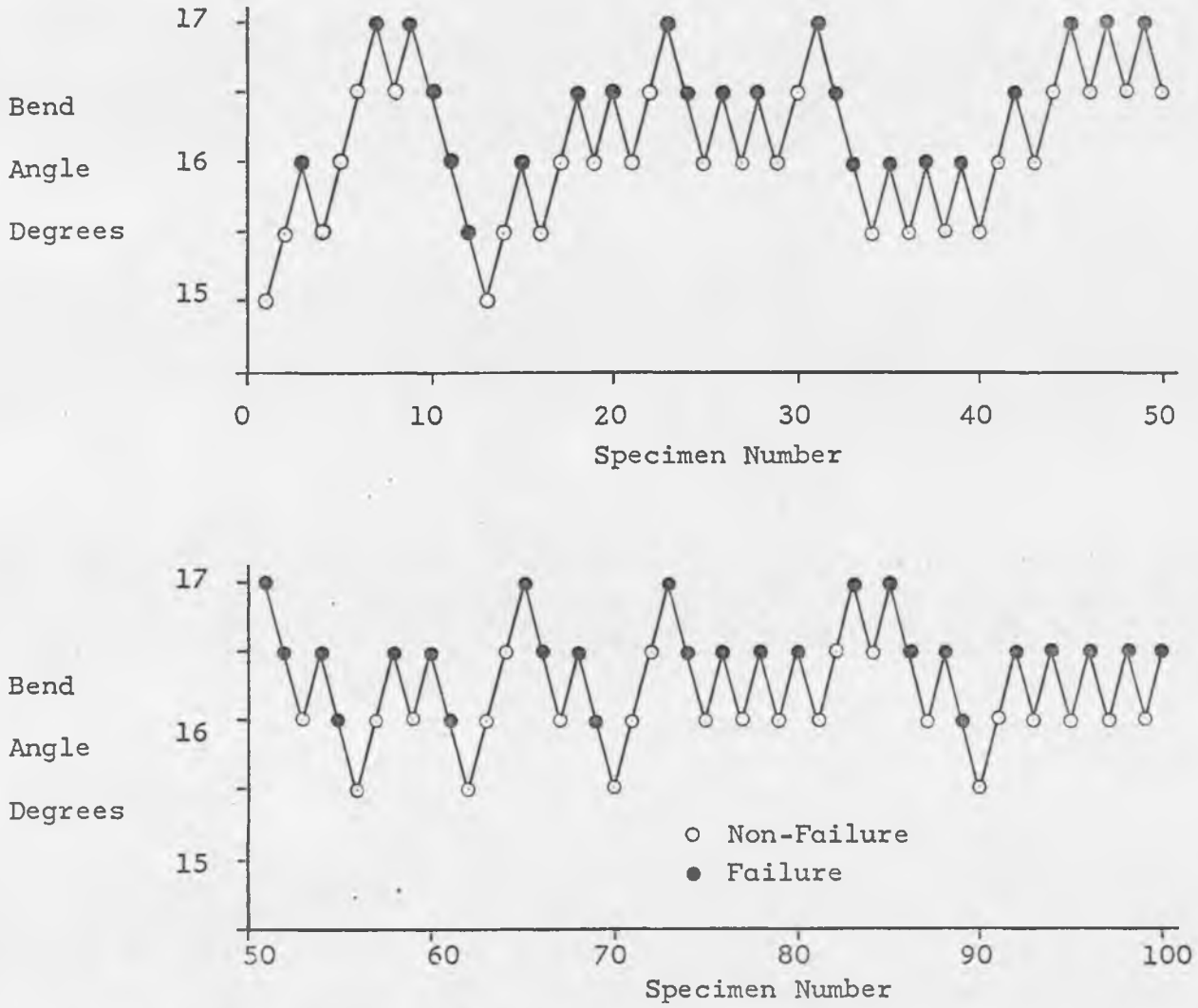

Figure B-1. Staircase Plot, 10^5 Cycles.

STAIRCASE FATIGUE DATA SHEET

Machine No. 3 0.0625 diameter wire

Cutoff: 3×10^5 cycles

Date	Spec. No.	Bend Angle, Degrees	Cycles to Failure $\times 10^{-5}$	Remarks
2/23/70	1	14.0	4.173	No Failure
2/23/70	2	14.5	3.069	No Failure
2/23/70	3	15.0	1.298	Failure
2/23/70	4	14.5	4.212	No Failure
2/23/70	5	15.0	3.480	No Failure
2/23/70	6	15.5	2.017	Failure
2/23/70	7	15.0	2.498	Failure
2/23/70	8	14.5	1.813	Failure
2/24/70	9	14.0	7.823	No Failure
2/24/70	10	14.5	3.052	No Failure
2/24/70	11	15.0	2.182	Failure
2/24/70	12	14.5	4.281	No Failure
2/24/70	13	15.0	4.662	No Failure
2/25/70	14	15.5	1.911	Failure
2/25/70	15	15.0	3.107	No Failure
2/25/70	16	15.5	2.437	Failure
2/27/70	17	15.0	8.004	No Failure
2/27/70	18	15.5	1.482	Failure
2/27/70	19	15.0	3.660	No Failure
2/28/70	20	15.5	2.236	Failure

STAIRCASE FATIGUE DATA SHEET

Machine No. 3 0.0625 diameter wire

Cutoff: 3×10^5 cycles

Date	Spec. No.	Bend Angle, Degrees	Cycles to Failure $\times 10^{-5}$	Remarks
3/1/70	21	15.0	3.554	No Failure
3/2/70	22	15.5	1.935	Failure
3/2/70	23	15.0	5.780	No Failure
3/2/70	24	15.5	1.584	Failure
3/3/70	25	15.0	2.229	Failure
3/4/70	26	14.5	2.591	Failure
3/4/70	27	14.0	7.946	No Failure
3/5/70	28	14.5	2.957	Failure
3/5/70	29	14.0	4.752	No Failure
3/5/70	30	14.5	3.151	No Failure
3/5/70	31	1 5.0	2.468	Failure
3/6/70	32	14.5	2.213	Failure
3/6/70	33	14.0	3.342	No Failure
3/6/70	34	14.5	3.140	No Failure
3/6/70	35	15.0	3.000	No Failure
3/6/70	36	15.5	0.729	Failure
3/6/70	37	15.0	2.412	Failure
3/6/70	38	14.5	1.848	Failure
3/7/70	39	14.0	3.054	No Failure
3/8/70	40	14.5	2.404	Failure

STAIRCASE FATIGUE DATA SHEET

Machine No. 3 0.0625 diameter wire

Cutoff: 3×10^5 cycles

Date	Spec. No.	Bend Angle, Degrees	Cycles to Failure $\times 10^{-5}$	Remarks
3/8/70	41	14.0	2.951	Failure
3/8/70	42	13.5	3.084	No Failure
3/8/70	43	14.0	3.414	No Failure
3/8/70	44	14.5	3.638	No Failure
3/8/70	45	15.0	0.617	Failure
3/8/70	46	14.5	1.284	Failure
3/8/70	47	14.0	2.376	Failure
3/8/70	48	13.5	3.020	No Failure
3/9/70	49	14.0	3.660	No Failure
3/10/70	50	14.5	1.754	Failure
3/10/70	51	14.0	4.272	No Failure
3/10/70	52	14.5	2.559	Failure
3/10/70	53	14.0	3.484	No Failure
3/10/70	54	14.5	2.175	Failure
3/10/70	55	14.0	4.159	No Failure
3/10/70	56	14.5	2.569	Failure
3/10/70	57	14.0	5.031	No Failure
3/10/70	58	14.5	3.621	No Failure
3/10/70	59	15.0	4.102	No Failure
3/11/70	60	15.5	2.224	Failure

STAIRCASE FATIGUE DATA SHEET

Machine No. 3 0.0625 diameter wire

Cutoff: 3×10^5 cycles

Date	Spec. No.	Bend Angle, Degrees	Cycles to Failure $\times 10^{-5}$	Remarks
3/11/70	61	15.0	2.497	Failure
3/11/70	62	14.5	4.467	No Failure
3/11/70	63	15.0	2.840	Failure
3/12/70	64	14.5	2.975	Failure
3/12/70	65	14.0	4.608	No Failure
3/12/70	66	14.5	3.000	No Failure
3/12/70	67	15.0	3.021	No Failure
3/12/70	68	15.5	1.603	Failure
3/12/70	69	15.0	1.511	Failure
3/16/70	70	14.5	5.073	No Failure
3/16/70	71	15.0	4.510	No Failure
3/16/70	72	15.5	1.005	Failure
3/17/70	73	15.0	3.632	No Failure
3/17/70	74	15.5	1.744	Failure
3/17/70	75	15.0	3.364	No Failure
3/17/70	76	15.5	2.396	Failure
3/17/70	77	15.0	2.809	Failure
3/17/70	78	14.5	2.052	Failure
3/17/70	79	14.0	6.339	No Failure
3/18/70	80	14.5	4.239	No Failure

STAIRCASE FATIGUE DATA SHEET

Machine No. 3 0.0625 diameter wire

Cutoff: 3×10^5 cycles

Date	Spec. No.	Bend Angle, Degrees	Cycles to Failure $\times 10^{-5}$	Remarks
3/18/70	81	15.0	2.821	Failure
3/18/70	82	14.5	4.753	No Failure
3/18/70	83	14.0	3.577	No Failure
3/18/70	84	15.5	0.984	Failure
3/18/70	85	15.0	3.020	No Failure
3/18/70	86	15.5	1.330	Failure
3/18/70	87	15.0	1.807	Failure
3/18/70	88	14.5	3.022	No Failure
3/18/70	89	15.0	6.387	No Failure
3/18/70	90	15.5	1.811	Failure
3/19/70	91	15.0	2.173	Failure
3/19/70	92	14.5	5.056	No Failure
3/19/70	93	15.0	4.295	No Failure
3/19/70	94	15.5	1.115	Failure
3/19/70	95	15.0	4.379	No Failure
3/19/70	96	15.5	2.413	Failure
3/19/70	97	15.0	4.660	No Failure
3/19/70	98	15.5	3.085	No Failure
3/19/70	99	16.0	1.041	Failure
3/19/70	100	15.5	1.929	Failure

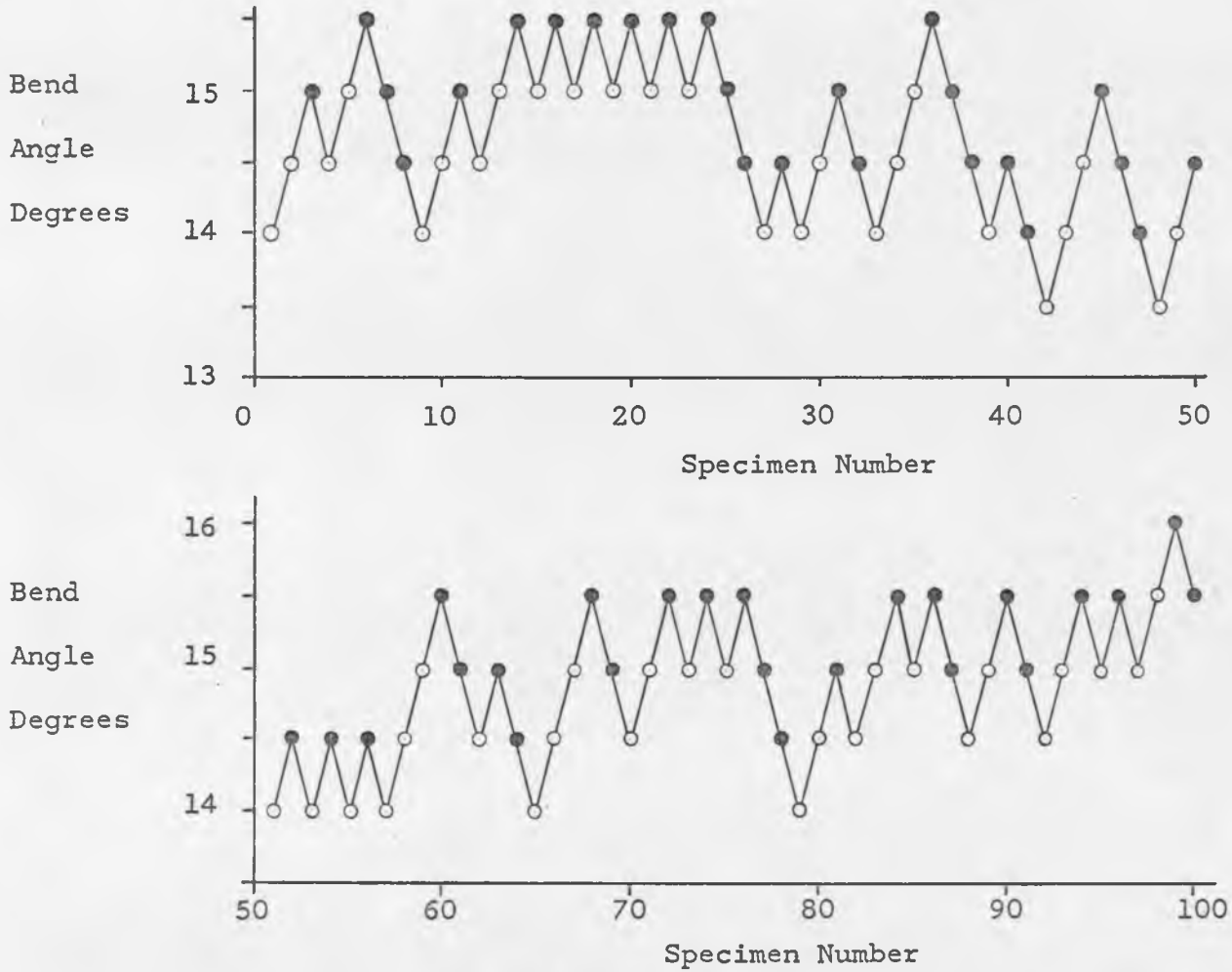

Figure B-2. Staircase Plot, 3×10^5 Cycles.

STAIRCASE FATIGUE DATA SHEET

Machine No. 3 0.0625 diameter wire

Cutoff: 5×10^5 cycles

Date	Spec. No.	Bend Angle, Degrees	Cycles to Failure $\times 10^{-5}$	Remarks
1/17/70	1	12.0	5.380	No Failure
1/17/70	2	12.5	5.526	No Failure
1/17/70	3	13.0	5.156	No Failure
1/18/70	4	13.5	5.018	No Failure
1/30/70	5	14.0	3.706	Failure
1/31/70	6	13.5	5.030	No Failure
2/2/70	7	14.0	2.037	Failure
2/2/70	8	13.5	2.132	Failure
2/2/70	9	13.0	3.801	Failure
2/2/70	10	12.5	5.793	No Failure
2/3/70	11	13.0	9.229	No Failure
2/3/70	12	13.5	2.590	Failure.
2.4.70	13	13.0	2.791	Failure
2/4/70	14	12.5	5.797	No Failure
2/4/70	15	13.0	3.920	Failure
2/4/70	16	12.5	7.717	No Failure
2/5/70	17	13.0	4.284	Failure
2/5/70	18	12.5	5.178	No Failure
2/5/70	19	13.0	2.697	Failure
2/5/70	20	12.5	5.185	No Failure

STAIRCASE FATIGUE DATA SHEET

Machine No. 3 — 0.0625 diameter wire

Cutoff: 5×10^5 cycles

Date	Spec. No.	Bend Angle, Degrees	Cycles to Failure x 10^{-5}	Remarks
2/5/70	21	13.0	5.027	No Failure
2/5/70	22	13.5	5.750	No Failure
2/6/70	23	14.0	4.540	Failure
2/6/70	24	13.5	2.931	Failure
2/6/70	25	13.0	2.202	Failure
2/6/70	26	12.5	5.066	No Failure
2/6/70	27	13.0	4.935	Failure
2/6/70	28	12.5	5.977	No Failure
2/8/70	29	13.0	5.016	No Failure
2/8/70	30	13.5	5.075	No Failure
2/8/70	31	14.0	2.970	Failure
2/8/70	32	13.5	5.211	No Failure
2/9/70	33	14.0	3.976	Failure
2/9/70	34	13.5	1.693	Failure
2/9/70	35	13.0	5.973	No Failure
2/9/70	36	13.5	5.240	No Failure
2/9/70	37	14.0	5.428	No Failure
2/9/70	38	14.5	3.019	Failure
2/9/70	39	14.0	5.293	No Failure
2/9/70	40	14.5	5.015	No Failure

STAIRCASE FATIGUE DATA SHEET

Machine No. 3 — 0.0625 diameter wire

Cutoff: 5×10^5 cycles

Date	Spec. No.	Bend Angle, Degrees	Cycles to Failure $\times 10^{-5}$	Remarks
2/10/70	41	15.0	3.386	Failure
2/10/70	42	14.5	5.150	No Failure
2/10/70	43	15.0	2.817	Failure
2/10/70	44	14.5	2.895	Failure
2/10/70	45	14.0	5.098	No Failure
2/10/70	46	14.5	9.022	No Failure
2/10/70	47	15.0	5.672	No Failure
2/11/70	48	15.5	3.398	Failure
2/11/70	49	15.0	1.503	Failure
2/11/70	50	14.5	4.702	Failure
2/11/70	51	14.0	4.486	Failure
2/12/70	52	13.5	5.892	No Failure
2/12/70	53	14.0	9.337	No Failure
2/12/70	54	14.5	4.025	Failure
2/12/70	55	14.0	5.025	No Failure
2/12/70	56	14.5	4.253	Failure
2/12/70	57	14.0	8.995	No Failure
2/12/70	58	14.5	3.560	Failure
2/12/70	59	14.0	7.781	No Failure
2/13/70	60	14.5	3.330	Failure

STAIRCASE FATIGUE DATA SHEET

Machine No. 3 0.0625 diameter wire

Cutoff: 5×10^5 cycles

Date	Spec. No.	Bend Angle, Degrees	Cycles to Failure $\times 10^{-5}$	Remarks
2/13/70	61	14.0	11.200	No Failure
2/13/62	62	14.5	3.911	Failure
2/13/70	63	14.0	8.576	No Failure
2/13/70	64	14.5	1 .919	Failure
2/14/70	65	14.0	7.031	No Failure
2/14/70	66	14.5	3.745	Failure
2/15/70	67	14.0	9.234	No Failure
2/15/70	68	14.5	3.634	Failure
2/15/70	69	14.0	3.445	Failure
2/15/70	70	13.5	5.035	No Failure
2/15/70	71	14.0	5.427	No Failure
2/16/70	72	14.5	3.603	Failure
2/16/70	73	14.0	4.482	Failure
2/17/70	74	13.5	6.000	No Failure
2/17/70	75	14.0	5.015	No Failure
2/17/70	76	14.5	2.623	Failure
2/17/70	77	1 4.0	5.424	No Failure
2/17/70	78	14.5	4.725	Failure
2/18/70	79	14.0	3.031	Failure
2/18/70	80	13.5	8.453	No Failure

STAIRCASE FATIGUE DATA SHEET

Machine No. 3 — 0.0625 diameter wire

Cutoff: 5×10^5 cycles

Date	Spec. No.	Bend Angle, Degrees	Cycles to Failure $\times 10^{-5}$	Remarks
2/18/70	81	14.0	4.309	Failure
2/18/70	82	13.5	7.004	No Failure
2/18/70	83	14.0	4.574	Failure
2/18/70	84	13.5	7.680	No Failure
2/19/70	85	14.0	7.649	No Failure
2/19/70	86	14.5	6.226	No Failure
2/19/70	87	15.0	1.667	Failure
2/19/70	88	14.5	5.289	No Failure
2/19/70	89	15.0	3.169	Failure
2/21/70	90	14.5	5.252	No Failure
2/21/70	91	15.0	4.277	Failure
2/21/70	92	14.5	5.660	No Failure
2/21/70	93	15.0	4.430	Failure
2/21/70	94	14.5	5.029	No Failure
2/21/70	95	15.0	4.134	Failure
2/21/70	96	14.5	4.814	Failure
2/22/70	97	14.0	3.297	Failure
2/22/70	98	13.5	5.487	No Failure
2/22/70	99	14.0	5.029	No Failure
2/23/70	100	14.5	4.659	Failure

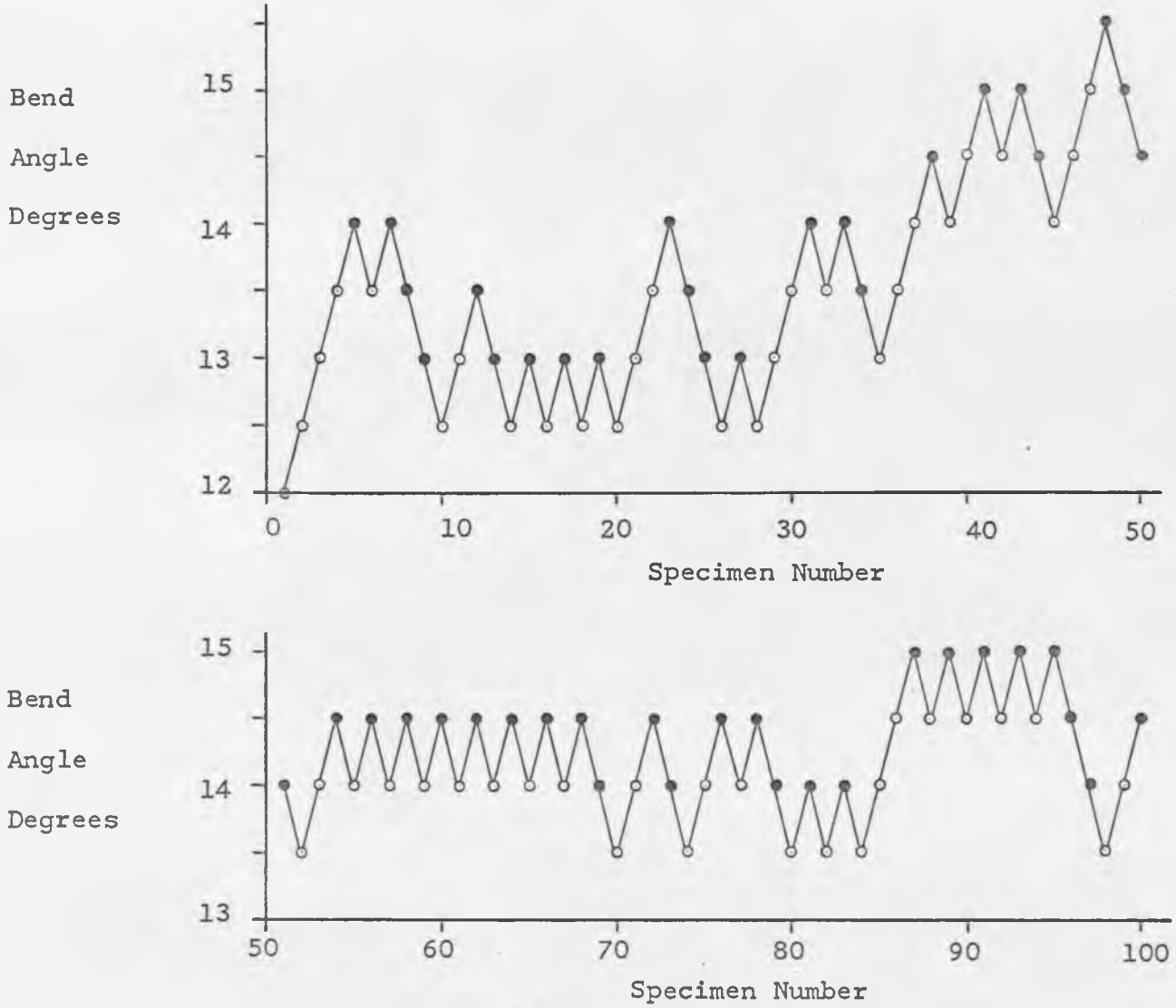

Figure B-3. Staircase Plot, 5×10^5 Cycles.

STAIRCASE FATIGUE DATA SHEET

Machine No. 2 0.0625 diameter wire

Cutoff: 7.5×10^5 cycles

Date	Spec. No.	Bend Angle, Degrees	Cycles to Failure $\times 10^{-5}$	Remarks
4/4/70	1	13.5	4.984	Failure
4/5/70	2	13.0	15.788	No Failure
4/5/70	3	13.5	8.044	No Failure
4/5/70	4	14.0	15.739	No Failure
4/5/70	5	14.5	3.119	Failure
4/5/70	6	14.0	4.550	Failure
4/6/70	7	13.5	7.374	Failure
4/6/70	8	13.0	11.867	No Failure
4/6/70	9	13.5	3.674	Failure
4/7/70	10	13.0	11.089	No Failure
4/7/70	11	13.5	8.698	No Failure
4/7/70	12	14.0	5.045	Failure
4/7/70	13	13.5	6.078	Failure
4/9/70	14	13.0	28.315	No Failure
4/9/70	15	13.5	5.291	Failure
4/9/70	16	13.0	7.671	No Failure
4/9/70	17	13.5	13.471	No Failure
4/10/70	18	14.0	4.461	Failure
4/10/70	19	13.5	21.087	No Failure
4/11/70	20	14.0	7.621	No Failure

STAIRCASE FATIGUE DATA SHEET

Machine No. 2 0.0625 diameter wire

Cutoff: 7.5×10^5 cycles

Date	Spec. No.	Bend Angle, Degrees	Cycles to Failure $\times 10^{-5}$	Remarks
4/11/70	21	14.5	5.328	Failure
4/11/70	22	14.0	6.631	Failure
4/11/70	23	13.5	4.239	Failure
4/11/70	24	13.0	7.612	No Failure
4/12/70	25	13.5	17.286	No Failure
4/12/70	26	14.0	4.360	Failure
4/13/70	27	13.5	6.327	Failure
4/13/70	28	13.0	24.601	No Failure
4/13/70	29	13.5	2.985	Failure
4/13/70	30	13.0	14.681	No Failure
4/13/70	31	13.5	5.736	Failure
4/13/70	32	13.0	8.570	No Failure
4/14/70	33	13.5	11.197	No Failure
4/14/70	34	14.0	4.061	Failure
4/14/70	35	13.5	2.846	Failure
4/14/70	36	13.0	8.149	No Failure
4/14/70	37	13.5	9.010	No Failure
4/14/70	38	14.0	9.093	No Failure
4/15/70	39	14.5	7.772	No Failure
4/15/70	40	15.0	8.999	No Failure

STAIRCASE FATIGUE DATA SHEET

Machine No. 2 0.0625 diameter wire

Cutoff: 7.5×10^5 cycles

Date	Spec. No.	Bend Angle, Degrees	Cycles to Failure x 10^{-5}	Remarks
4/15/70	41	15.5	1.885	Failure
4/15/70	42	15.0	2.398	Failure
4/16/70	43	14.5	4.771	Failure

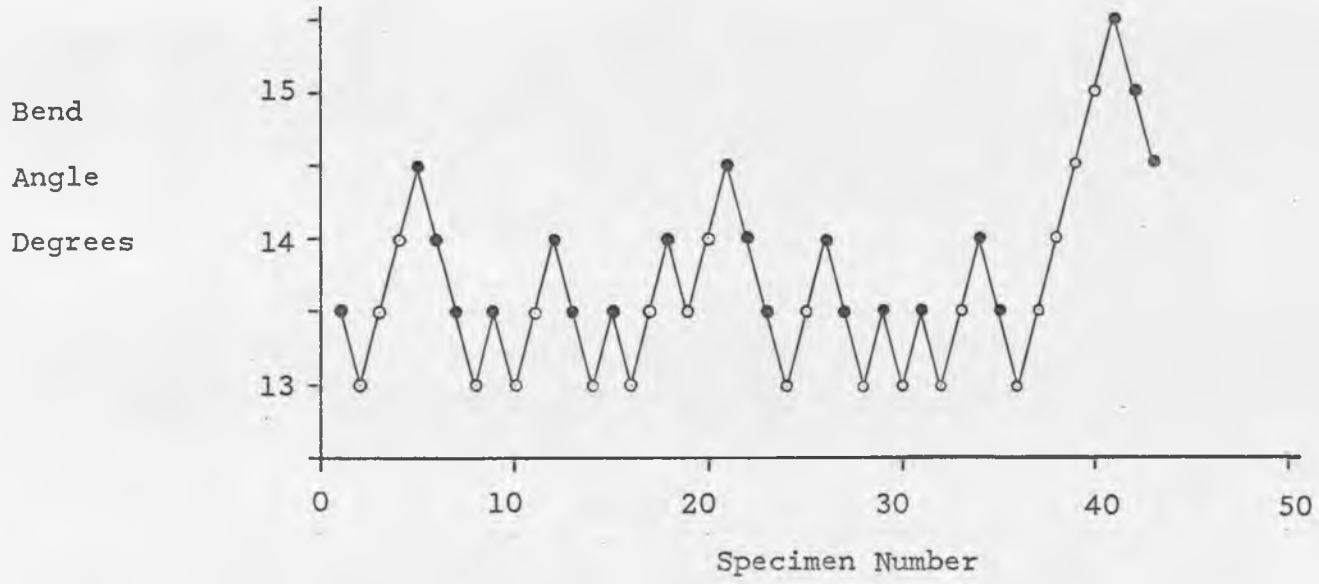

Figure B-4. Staircase Plot, 7.5×10^5 Cycles.

STAIRCASE FATIGUE DATA SHEET

Machine No. 3 — 0.0625 diameter wire

Cutoff: 10^6 cycles

Date	Spec. No.	Bend Angle, Degrees	Cycles to Failure x 10^{-5}	Remarks
3/31/70	1	12.0	13.698	No Failure
3/31/70	2	12.5	10.192	No Failure
3/31/70	3	13.0	14.984	No Failure
3/31/70	4	13.5	29.331	No Failure
4/1/70	5	14.0	8.350	Failure
4/1/70	6	13.5	10.438	No Failure
4/1/70	7	14.0	3.739	Failure
4/1/70	8	13.5	4.513	Failure
4/1/70	9	13.0	20.345	No Failure
4/2/70	10	13.5	3.990	Failure
4/2/70	11	13.0	17.232	No Failure
4/2/70	12	13.5	21.352	No Failure
4/2/70	13	14.0	1.962	Failure
4/2/70	14	13.5	58.784	No Failure
4/2/70	15	14.0	18.986	No Failure
4/3/70	16	13.5	11.926	No Failure
4/3/70	17	14.0	10.293	No Failure
4/3/70	18	14.5	2.573	Failure
4/3/70	19	14.0	13.146	No Failure
4/3/70	20	14.5	3.896	Failure

STAIRCASE FATIGUE DATA SHEET

Machine No. 3 — 0.0625 diameter wire

Cutoff: 10^6 cycles

Date	Spec. No.	Bend Angle, Degrees	Cycles to Failure x 10^{-5}	Remarks
4/4/70	21	14.0	6.007	Failure
4/4/70	22	13.5	11.597	No Failure
4/6/70	23	14.0	11.805	No Failure
4/6/70	24	14.5	5.728	Failure
4/6/70	25	14.0	5.333	Failure
4/6/70	26	13.5	14.451	No Failure
4/6/70	27	14.0	4.117	Failure
4/6/70	28	13.5	6.655	Failure
4/6/70	29	13.0	16.622	No Failure
4/7/70	30	13.5	8.429	Failure
4/7/70	31	13.0	13.051	No Failure
4/7/70	32	13.5	12.462	No Failure
4/7/70	33	14.0	10.704	No Failure
4/7/70	34	14.5	2.484	Failure
4/8/70	35	14.0	12.521	No Failure
4/8/70	36	14.5	2.145	Failure
4/8/70	37	14.0	19.153	No Failure
4/8/70	38	14.5	3.338	Failure
4/8/70	39	14.0	2.443	Failure
4/8/70	40	13.5	11.250	No Failure

STAIRCASE FATIGUE DATA SHEET

Machine No. 3 0.0625 diameter wire

Cutoff: 10^6 cycles

Date	Spec. No.	Bend Angle, Degrees	Cycles to Failure x 10^{-5}	Remarks
4/8/70	41	14.0	15.110	No Failure
4/8/70	42	14.5	4.611	Failure
4/8/70	43	14.0	6.969	Failure
4/9/70	44	13.5	12.907	No Failure
4/9/70	45	14.0	4.121	Failure
4/9/70	46	13.5	10.274	No Failure
4/9/70	47	14.0	10.240	No Failure
4/9/70	48	14.5	3.693	Failure
4/9/70	49	14.0	4.941	Failure
4/9/70	50	13.5	31.152	No Failure
4/9/70	51	14.0	13.433	No Failure
4/9/70	52	14.5	3.439	Failure
4/9/70	53	14.0	12.899	No Failure
4/9/70	54	14.5	5.114	Failure
4/10/70	55	14.0	15.293	No Failure
4/10/70	56	14.5	3.826	Failure
4/10/70	57	14.0	10.274	No Failure
4/10/70	58	14.5	3.237	Failure
4/10/70	59	14.0	4.037	Failure
4/10/70	60	13.5	19.903	No Failure

STAIRCASE FATIGUE DATA SHEET

Machine No. 3 0.0625 diameter wire

Cutoff: 10^6 cycles

Date	Spec. No.	Bend Angle, Degrees	Cycles to Failure x 10^{-5}	Remarks
4/10/70	61	14.0	2.668	Failure
4/10/70	62	13.5	10.097	No Failure
4/10/70	63	14.0	3.250	Failure
4/11/70	64	13.5	13.268	No Failure
4/11/70	65	14.0	10.959	No Failure
4/11/70	66	14.5	2.595	Failure
4/11/70	67	14.0	3.656	Failure
4/12/70	68	13.5	11.860	No Failure
4/12/70	69	14.0	5.252	Failure
4/12/70	70	13.5	6.223	Failure
4/13/70	71	13.0	11.799	No Failure
4/13/70	72	13.5	12.420	No Failure
4/13/70	73	14.0	36.971	No Failure
4/13/70	74	14.5	2.291	Failure
4/13/70	75	14.0	1.834	Failure
4/13/70	76	13.5	8.752	Failure
4/14/70	77	13.0	11.425	No Failure
4/14/70	78	13.5	19.031	No Failure
4/14/70	79	14.0	0.968	Failure
4/14/70	80	13.5	26.672	No Failure

STAIRCASE FATIGUE DATA SHEET

Machine No. 3 0.0625 diameter wire

Cutoff: 10^6 cycles

Date	Spec. No.	Bend Angle, Degrees	Cycles to Failure x 10^{-5}	Remarks
4/14/70	81	14.0	5.832	Failure
4/14/70	82	13.5	2.729	Failure
4/15/70	83	13.0	18.152	No Failure
4/15/70	84	13.5	11.205	No Failure
4/15/70	85	14.0	4.230	Failure
4/15/70	86	13.5	10.910	No Failure
4/15/70	87	14.0	3.966	Failure
4/15/70	88	13.5	19.397	No Failure
4/15/70	89	14.0	5.110	Failure
4/16/70	90	13.5	11.457	No Failure
4/16/70	91	14.0	17.593	No Failure
4/16/70	92	14.5	3.731	Failure
4/16/70	93	14.0	11.197	No Failure
4/16/70	94	14.5	11.225	No Failure
4/16/70	95	15.0	2.157	Failure
4/18/70	96	14.5	5.900	Failure
4/18/70	97	14.0	4.405	Failure
4/18/70	98	13.5	12.574	No Failure
4/18/70	99	14.0	2.290	Failure
4/18/70	100	13.5	27.525	No Failure

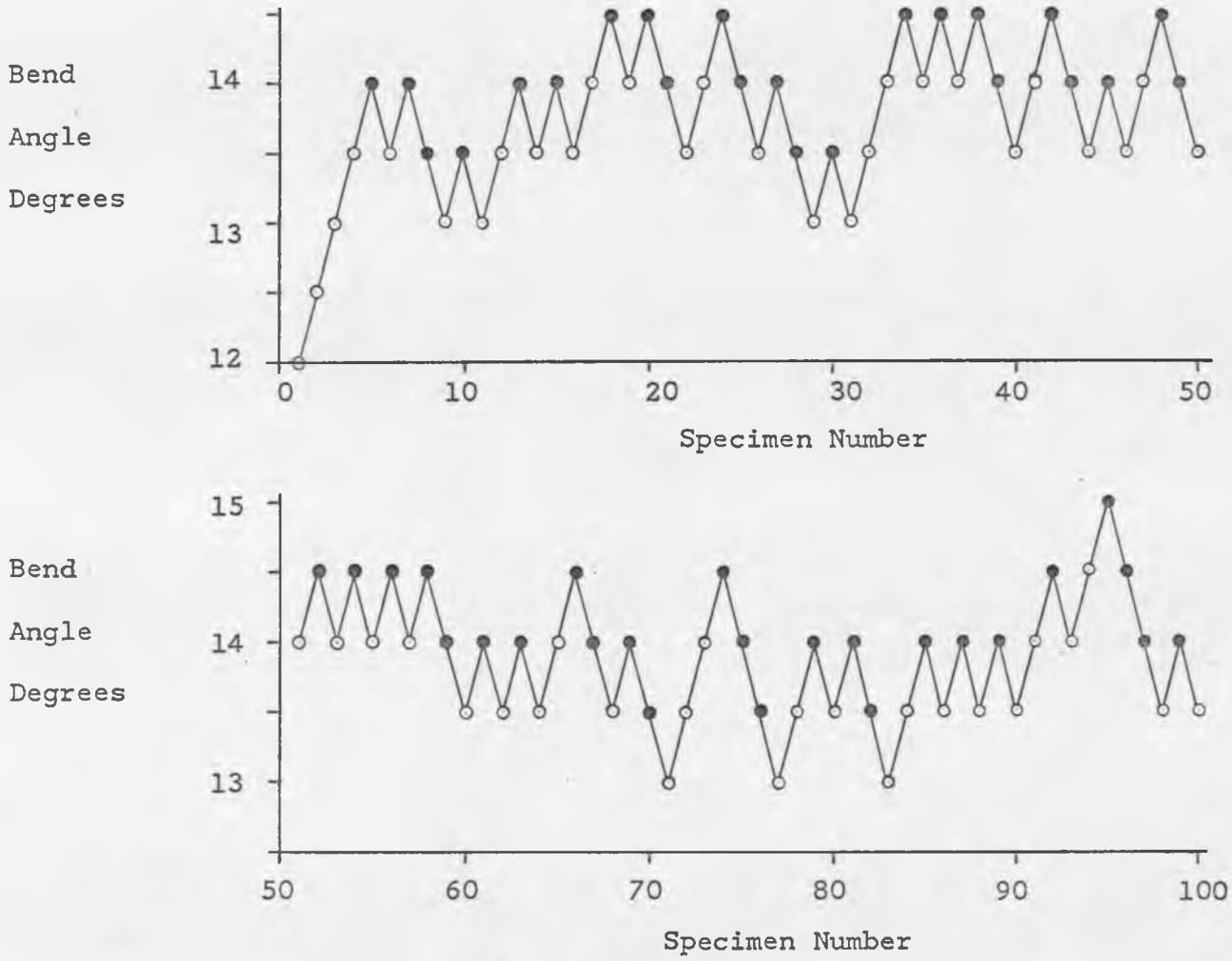

Figure B-5. Staircase Plot, 10^6 Cycles.

STAIRCASE FATIGUE DATA SHEET

Machine No. 1 0.0625 diameter wire

Cutoff: 1.5×10^6 cycles

Date	Spec. No.	Bend Angle, Degrees.	Cycles to Failure $\times 10^{-5}$	Remarks
3/23/70	1	13.0	16.950	No Failure
3/25/70	2	13.5	22.158	No Failure
3/25/70	3	14.0	15.012	No Failure
3/25/70	4	14.5	12.311	Failure
3/25/70	5	14.0	9.759	Failure
3/26/70	6	13.5	30.156	No Failure
3/26/70	7	14.0	7.768	Failure
3/26/70	8	13.5	15.018	No Failure
3/26/70	9	14.0	18.043	No Failure
3/27/70	10	14.5	59.865	No Failure
3/27/70	11	15.0	16.202	No Failure
3/27/70	12	15.5	2.525	Failure
3/27/70	13	15.0	3.074	Failure
3/28/70	14	14.5	4.850	Failure
3/30/70	15	14.0	27.665	No Failure
3/30/70	16	14.5	22.317	No Failure
3/30/70	17	15.0	3.884	Failure
3/31/70	18	14.5	6.546	Failure
3/31/70	19	14.0	25.247	No Failure
3/31/70	20	14.5	9.674	Failure

STAIRCASE FATIGUE DATA SHEET

Machine No. 1 0.0625 diameter wire

Cutoff: 1.5×10^6 cycles

Date	Spec. No.	Bend Angle, Degrees	Cycles to Failure $\times 10^{-5}$	Remarks
3/31/70	21	14.0	37.216	No Failure
4/1/70	22	14.5	24.212	No Failure
4/2/70	23	15.0	3.413	Failure
4/2/70	24	14.5	4.018	Failure
4/3/70	25	14.0	10.153	Failure
4/3/70	26	13.5	17.155	No Failure
4/4/70	27	14.0	4.381	Failure
4/4/70	28	13.5	19.709	No Failure
4/5/70	29	14.0	4.535	Failure
4/5/70	30	13.5	5.898	Failure
4/5/70	31	13.0	17.509	No Failure
4/5/70	32	13.5	25.138	No Failure
4/5/70	33	14.0	30.217	No Failure
4/6/70	34	14.5	3.320	Failure
4/7/70	35	14.0	15.296	No Failure
4/7/70	36	14.5	15.154	No Failure
4/7/70	37	15.0	4.008	Failure
4/9/70	38	14.5	4.513	Failure
4/9/70	39	14.0	24.246	No Failure
4/9/70	40	14.5	6.267	Failure

STAIRCASE FATIGUE DATA SHEET

Machine No. 1 — 0.0625 diameter wire

Cutoff: 1.5×10^6 cycles

Date	Spec. No.	Bend Angle, Degrees	Cycles to Failure $\times 10^{-5}$	Remarks
4/9/70	41	14.0	6.285	Failure
4/9/70	42	13.5	34.218	No Failure
4/10/70	43	14.0	33.793	No Failure
4/10/70	44	14.5	7.586	Failure
4/11/70	45	14.0	11.067	Failure
4/11/70	46	13.5	5.132	Failure
4/11/70	47	13.0	15.053	No Failure
4/11/70	48	13.5	15.002	No Failure
4/11/70	49	14.0	4.003	Failure
4/12/70	50	13.5	16.665	No Failure
4/12/70	51	14.0	29.619	No Failure
4/13/70	52	14.5	5.092	Failure
4/13/70	53	14.0	22.321	No Failure
4/13/70	54	14.5	7.109	Failure
4/13/70	55	14.0	50.950	No Failure
4/14/70	56	14.5	4.978	Failure
4/14/70	57	14.0	18.823	No Failure
4/14/70	58	14.5	12.891	Failure
4/14/70	59	14.0	13.064	Failure
4/14/70	60	13.5	15.083	No Failure

STAIRCASE FATIGUE DATA SHEET

Machine No. 1 0.0625 diameter wire

Cutoff: 1.5×10^6 cycles

Date	Spec. No.	Bend Angle, Degrees	Cycles to Failure $\times 10^{-5}$	Remarks
4/15/70	61	14.0	34.637	No Failure
4/15/70	62	14.5	24.382	No Failure
4/15/70	63	15.0	11.229	Failure
4/15/70	64	14.5	71.465	No Failure
4/16/70	65	15.0	18.689	No Failure
4/16/70	66	15.5	4.309	Failure
4/16/70	67	15.0	2.499	Failure
4/16/70	68	14.5	78.211	No Failure
4/17/70	69	15.0	23.387	No Failure
4/17/70	70	15.5	2.069	Failure
4/17/70	71	15.0	1.378	Failure
4/20/70	72	14.5	4.589	Failure
4/20/70	73	14.0	6.808	Failure

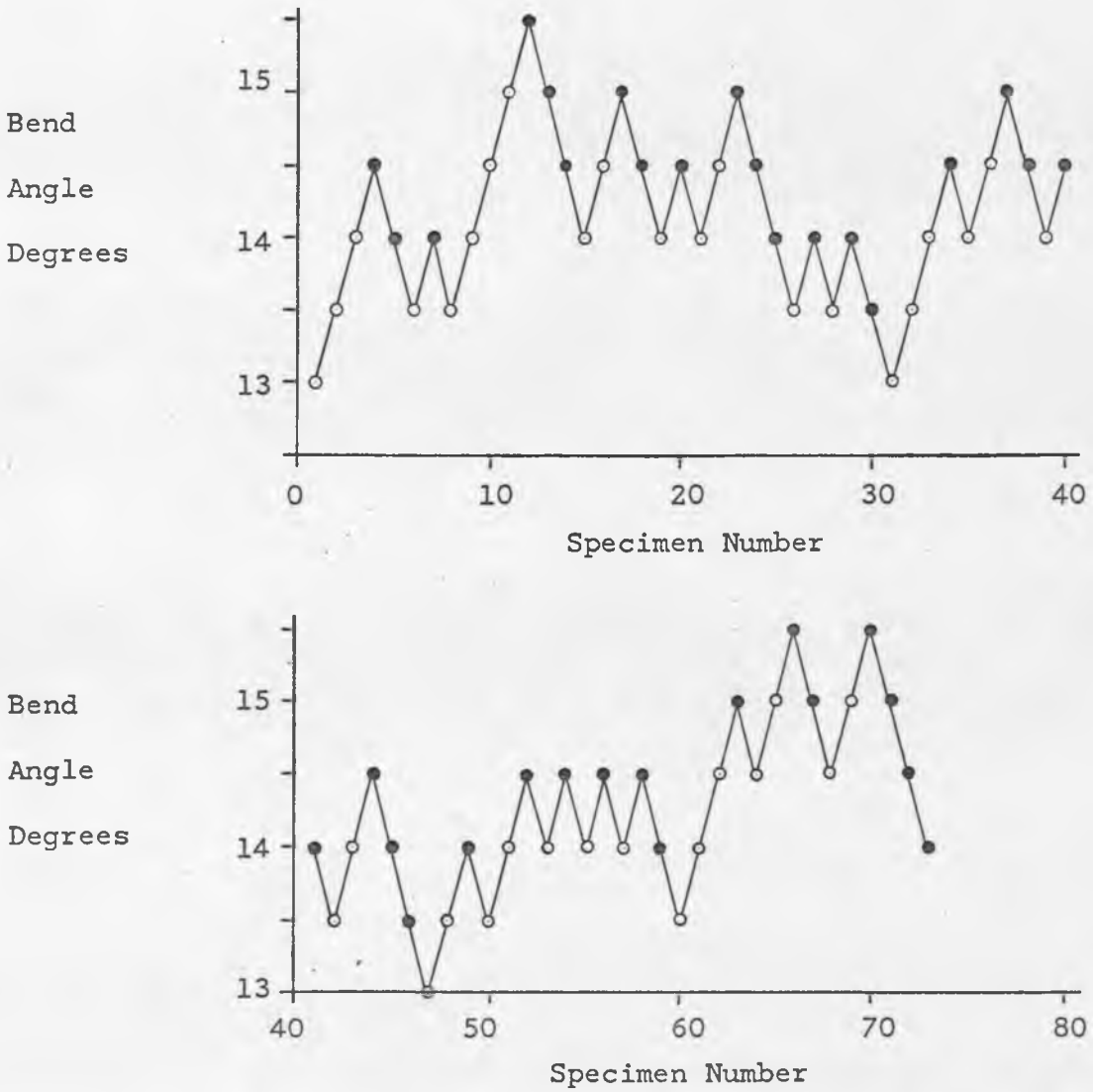

Figure B-6. Staircase Plot, 1.5 x 10^6 Cycles.

STAIRCASE FATIGUE DATA SHEET

Machine No. 3 — 0.0625 diameter wire

Cutoff: 2×10^6 cycles

Date	Spec. No.	Bend Angle, Degrees	Cycles to Failure $\times 10^{-5}$	Remarks
8/25/69	1	7.0	20.005	No Failure
8/25/69	2	7.5	20.068	No Failure
8/26/69	3	8.0	21.293	No Failure
8/27/69	4	8.5	20.126	No Failure
8/27/69	5	9.0	20.934	No Failure
8/28/69	6	9.5	20.037	No Failure
8/29/69	7	10.0	24.395	No Failure
8/29/69	8	10.5	20.112	No Failure
9/2/69	9	11.0	20.610	No Failure
9/2/69	10	11.5	20.173	No Failure
9/3/69	11	12.0	20.059	No Failure
9/5/69	12	12.5	20.059	No Failure
9/8/69	13	13.0	9.591	Failure
9/8/69	14	12.5	14.369	Failure
9/17/69	15	12.0	20.250	No Failure
9/26/69	16	12.5	20.513	No Failure
9/26/69	17	13.0	3.309	Failure
10/6/69	18	12.5	20.034	No Failure
10/6/69	19	13.0	2.244	Failure
10/8/69	20	12.5	9.432	Failure

STAIRCASE FATIGUE DATA SHEET

Machine No. 3 0.0625 diameter wire

Cutoff: 2×10^6 cycles

Date	Spec. No.	Bend Angle, Degrees	Cycles to Failure $\times 10^{-5}$	Remarks
10/9/69	21	12.0	14.846	Failure
10/10/69	22	11.5	20.233	No Failure
10/13/69	23	12.0	20.049	No Failure
10/13/69	24	12.5	20.168	No Failure
10/17/69	25	13.0	20.051	No Failure
10/17/69	26	13.5	1.109	Failure
10/17/69	27	13.0	3.839	Failure
10/20/69	28	12.5	20.071	No Failure
10/20/69	29	13.0	6.180	Failure
10/10/69	30	12.5	20.385	No Failure
10/21/69	31	13.0	22.173	No Failure
10/22/69	32	13.5	20.024	No Failure
10/22/69	33	14.0	20.292	No Failure
10/22/69	34	14.5	4.463	Failure
10/23/69	35	14.0	5.103	Failure
10/23/69	36	13.5	11.459	Failure
10/24/69	37	13.0	21.704	No Failure
10/27/69	38	13.5	21.494	No Failure
10/27/69	39	14.0	5.401	Failure
10/29/69	40	13.5	10.745	Failure

STAIRCASE FATIGUE DATA SHEET

Machine No. 3 0.0625 diameter wire

Cutoff: 2×10^6 cycles

Date	Spec. No.	Bend Angle, Degrees	Cycles to Failure $\times 10^{-5}$	Remarks
10/29/69	41	13.0	4.542	Failure
10/29/69	42	12.5	21.699	No Failure
10/29/69	43	13.0	32.348	No Failure
10/30/69	44	13.5	4.155	Failure
10/31/69	45	13.0	11.983	Failure
11/6/69	46	12.5	20.584	No Failure
11/7/69	47	13.0	7.576	Failure
11/11/69	48	12.5	20.109	No Failure
11/12/69	49	13.0	10.594	Failure
11/12/69	50	12.5	21.175	No Failure
11/13/69	51	13.0	7.676	Failure
11/14/69	52	12.5	21.700	No Failure
11/17/69	53	13.0	6.558	Failure
11/19/69	54	12.5	20.027	No Failure
11/19/69	55	13.0	20.807	No Failure
11/20/69	56	13.5	2.202	Failure
11/20/69	57	13.0	3.599	Failure
11/21/69	58	12.5	23.080	No Failure
11/29/69	59	13.0	6.373	Failure
11/24/69	60	12.5	7.379	Failure

STAIRCASE FATIGUE DATA SHEET

Machine No. 3 0.0625 diameter wire

Cutoff: 2×10^6 cycles

Date	Spec. No.	Bend Angle, Degrees	Cycles to Failure $\times 10^{-5}$	Remarks
11/26/69	61	12.0	20.531	No Failure
12/1/69	62	12.5	20.026	No Failure
12/1/69	63	13.0	3.321	Failure
12/3/69	64	12.5	20.537	No Failure
12/3/69	65	13.0	4.158	Failure
12/3/69	66	12.5	17.355	Failure
12/4/69	67	12.0	23.260	No Failure
12/5/69	68	12.5	6.823	Failure
12/5/69	69	12.0	25.894	No Failure
12/5/69	70	12.5	20.189	No Failure
12/8/69	71	13.0	10.017	Failure
12/8/69	72	12.5	24.919	No Failure
12/8/69	73	13.0	7.206	No Failure
12/9/69	74	12.5	13.001	Failure
12/9/69	75	12.0	24.183	No Failure
12/10/69	76	12.5	9.851	Failure
12/10/69	77	12.0	13.033	Failure
12/10/69	78	11.5	20.513	No Failure
12/11/69	79	12.0	20.572	No Failure
12/11/69	80	12.5	3.876	Failure

STAIRCASE FATIGUE DATA SHEET

Machine No. 3 0.0625 diameter wire

Cutoff: 2×10^6 cycles

Date	Spec. No.	Bend Angle, Degrees	Cycles to Failure $\times 10^{-5}$	Remarks
12/12/69	81	12.0	12.563	Failure
12/15/69	82	11.5	25.294	No Failure
12/15/69	83	12.0	22.802	No Failure
12/15/69	84	12.5	28.825	No Failure
12/17/69	85	13.0	7.523	Failure
12/17/69	86	12.5	3.482	Failure
12/18/69	87	12.0	22.567	No Failure
1/7/70	88	12.5	12.003	Failure
1/7/70	89	12.0	34.479	No Failure
1/7/70	90	12.5	32.376	No Failure
1/8/70	91	13.0	3.553	Failure
1/9/70	92	12.5	20.052	No Failure
1/9/70	93	13.0	12.582	Failure
1/9/70	94	12.5	12.852	Failure
1/12/70	95	12.0	21.455	No Failure
1/14/70	96	12.5	28.250	No Failure
1/14/70	97	13.0	24.984	No Failure
1/15/70	98	13.5	7.733	Failure
1/15/70	99	13.0	17.740	Failure
1/16/70	100	12.5	20.013	No Failure

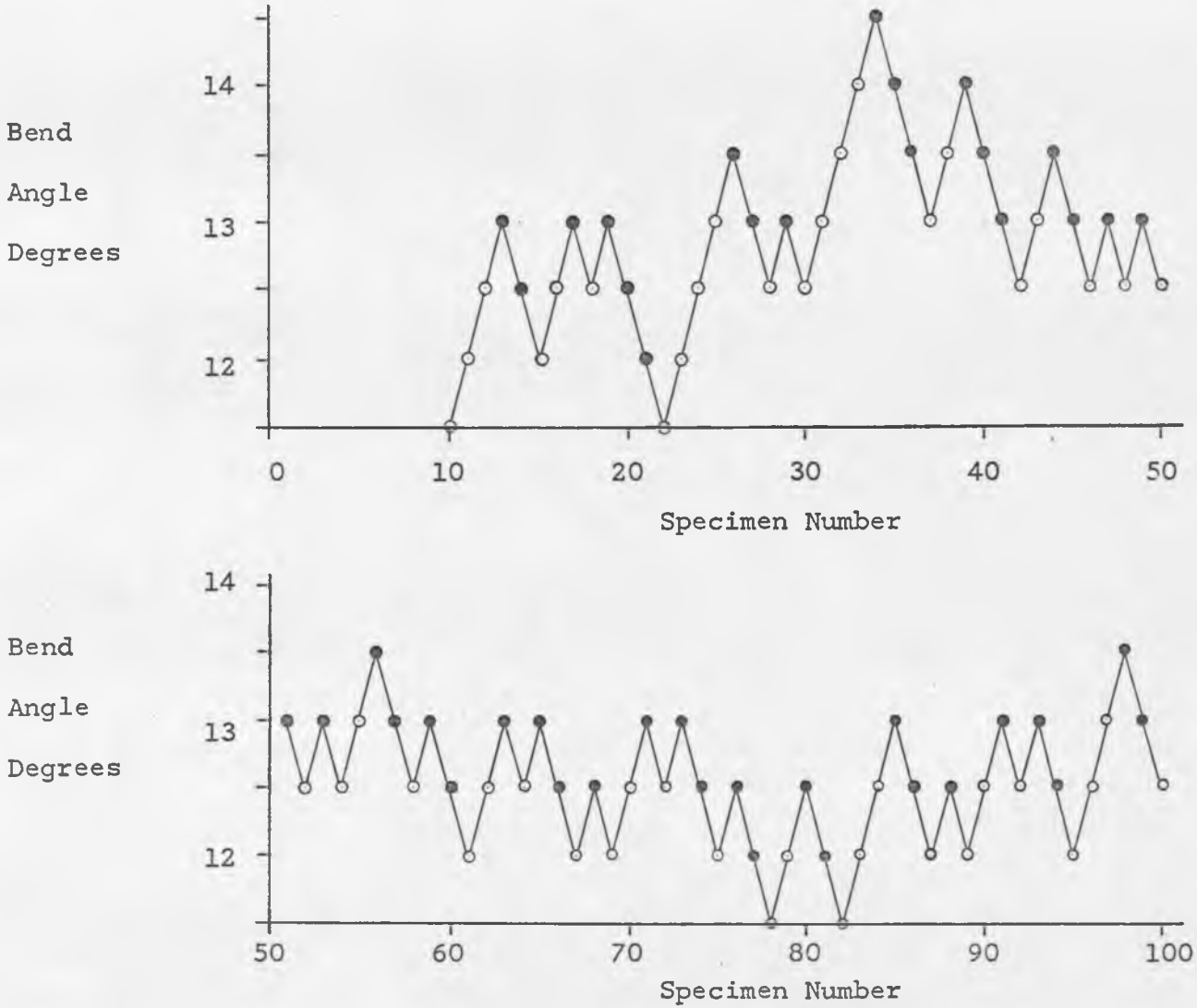

Figure B-7. Staircase Plot, Machine #3, 2 x 10^6 Cycles.

STAIRCASE FATIGUE DATA SHEET

Machine No. 4 0.0625 diameter wire

Cutoff: 2×10^6 cycles

Date	Spec. No.	Bend Angle, Degrees	Cycles to Failure $\times 10^{-5}$	Remarks
8/25/69	1	7.0	20.102	No Failure
8/25/69	2	7.5	20.191	No Failure
8/26/69	3	8.0	20.054	No Failure
8/27/69	4	8.5	22.016	No Failure
8/27/69	5	9.0	20.263	No Failure
8/28/69	6	9.5	20.210	No Failure
8/29/69	7	10.0	20.395	No Failure
8/29/69	8	10.5	20.048	No Failure
9/2/69	9	11.0	20.456	No Failure
9/2/69	10	11.5	20.274	No Failure
9/3/69	11	12.0	20.044	No Failure
9/5/69	12	12.5	20.305	No Failure
9/8/69	13	13.0	10.095	Failure
9/8/69	14	12.5	20.050	No Failure
9/11/69	15	13.0	11.041	Failure
9/26/69	16	12.5	27.767	No Failure
10/1/69	17	13.0	20.065	No Failure
10/1/69	18	13.5	6.432	Failure
10/1/69	19	13.0	16.209	Failure
10/6/69	20	12.5	20.424	No Failure

STAIRCASE FATIGUE DATA SHEET

Machine No. 4 0.0625 diameter wire

Cutoff: 2×10^6 cycles

Date	Spec. No.	Bend Angle, Degrees	Cycles to Failure $\times 10^{-5}$	Remarks
10/9/69	21	13.0	20.081	No Failure
10/10/69	22	13.5	5.602	Failure
10/10/69	23	13.0	3.510	Failure
10/13/69	24	12.5	20.167	No Failure
10/13/69	25	13.0	12.432	Failure
10/17/69	26	12.5	20.277	No Failure
10/17/69	27	13.0	28.360	No Failure
10/17/69	28	13.5	12.923	Failure
10/20/69	29	13.0	8.540	Failure
10/20/69	30	12.5	22.303	No Failure
10/20/69	31	13.0	20.067	No Failure
10/21/69	32	13.5	3.252	Failure
10/22/69	33	13.0	7.231	Failure
10/22/69	34	12.5	20.640	No Failure
10/22/69	35	13.0	2.862	Failure
10/23/69	36	12.5	20.329	No Failure
10/23/69	37	13.0	20.195	No Failure
10/24/69	38	13.5	14.021	Failure
10/27/69	39	13.0	21.513	No Failure
10/27/69	40	13.5	20.033	No Failure

STAIRCASE FATIGUE DATA SHEET

Machine No. 4 0.0625 diameter wire

Cutoff: 2×10^6 cycles

Date	Spec. No.	Bend Angle, Degrees	Cycles to Failure $\times 10^{-5}$	Remarks
10/29/69	41	14.0	6.155	Failure
10/29/69	42	13.5	1.783	Failure
10/29/69	43	13.0	22.967	No Failure
10/29/69	44	13.5	4.770	Failure
10/30/69	45	13.0	20.279	No Failure
10/31/69	46	13.5	11.620	Failure
11/6/69	47	13.0	13.598	Failure
11/7/69	48	12.5	25.815	No Failure
11/11/69	49	13.0	20.405	No Failure
11/12/69	50	13.5	2.067	Failure
11/12/69	51	13.0	10.883	Failure
11/13/69	52	12.5	30.328	No Failure
11/14/69	53	13.0	20.242	No Failure
11/19/69	54	13.5	20.106	No Failure
11/19/69	55	14.0	4.913	Failure
11/20/69	56	13.5	20.357	No Failure
11/20/69	57	14.0	13.656	Failure
11/21/69	58	13.5	10.432	Failure
11/24/69	59	13.0	24.795	No Failure
11/24/69	60	13.5	21.007	No Failure

STAIRCASE FATIGUE DATA SHEET

Machine No. 4 0.0625 diameter wire

Cutoff: 2×10^6 cycles

Date	Spec. No.	Bend Angle, Degrees	Cycles to Failure $\times 10^{-5}$	Remarks
11/26/69	61	14.0	3.732	Failure
12/1/69	62	13.5	5.510	Failure
12/1/69	63	13.0	21.364	No Failure
12/3/69	64	13.5	6.045	Failure
12/3/69	65	13.0	2.278	Failure
12/3/69	66	12.5	22.118	No Failure
12/4/69	67	13.0	6.783	Failure
12/5/69	68	12.5	20.488	No Failure
12/5/69	69	13.0	24.695	No Failure
12/8/69	70	13.5	20.788	No Failure
12/8/68	71	14.0	23.972	No Failure
12/8/69	72	14.5	1.864	Failure
12/9/69	73	14.0	2.826	Failure
12/9/69	74	13.5	23.177	No Failure
12/10/69	75	14.0	3.796	Failure
12/10/69	76	13.5	21.701	No Failure
12/10/69	77	14.0	3.792	Failure
12/11/69	78	13.5	4.928	Failure
12/11/69	79	130	20.423	No Failure
12/12/69	80	13.5	22.702	No Failure

STAIRCASE FATIGUE DATA SHEET

Machine No. 4 — 0.0625 diameter wire

Cutoff: 2×10^6 cycles

Date	Spec. No.	Bend Angle, Degrees	Cycles to Failure x 10^{-5}	Remarks
12/15/69	81	14.0	15.288	Failure
12/15/69	82	13.5	22.043	No Failure
12/15/69	83	14.0	28.646	No Failure
12/17/69	84	14.5	2.974	Failure
12/17/69	85	14.0	4.319	Failure
12/18/69	86	13.5	3.165	Failure
1/7/70	87	13.0	6.273	Failure
1/7/70	88	12.5	33.347	No Failure
1/7/70	89	13.0	13.563	Failure
1/8/70	90	12.5	20.019	No Failure
1/9/70	91	13.0	6.446	Failure
1/9/70	92	12.5	26.866	No Failure
1/9/70	93	13.0	22.633	No Failure
1/12/70	94	13.5	21.112	No Failure
1/14/70	95	14.0	21.731	No Failure
1/14/70	96	14.5	2.333	Failure
1/14/70	97	14.0	4.058	Failure
1/15/70	98	13.5	2.515	Failure
1/15/70	99	13.0	20.238	No Failure
1/16/70	100	13.5	9.001	Failure

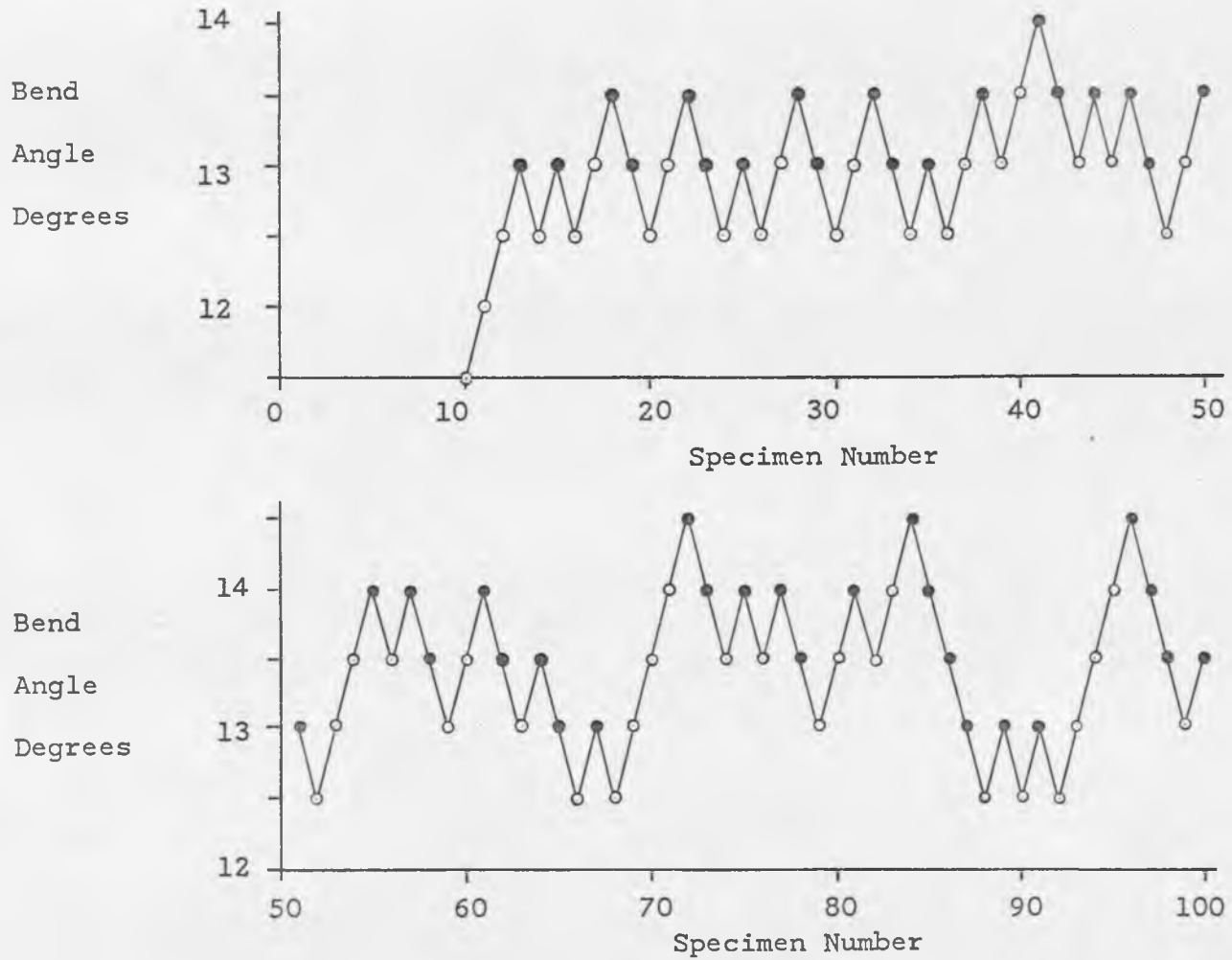

Figure B-8. Staircase Plot, Machine #4, 2 x 10^6 Cycles.

STAIRCASE FATIGUE DATA SHEET

Machine No. 4 0.0625 diameter wire

Cutoff: 1×10^7 cycles

Date	Spec. No.	Bend Angle, Degrees	Cycles to Failure $\times 10^{-5}$	Remarks
1/17/70	1	10.0	100.016	No Failure
1/18/70	2	10.5	100.108	No Failure
1/30/70	3	11.0	100.362	No Failure
1/31/70	4	11.5	101.006	No Failure
2/2/70	5	12.0	101.558	No Failure
2/3/70	6	12.5	8.509	Failure
2/4/70	7	12.0	100.000	No Failure
2/6/70	8	12.5	101.398	No Failure
2/7/70	9	13.0	96.219	Failure
2/9/70	10	12.5	100.602	No Failure
2/10/70	11	13.0	83.078	Failure
2/12/70	12	12.5	101.024	No Failure
2/14/70	13	13.0	107.081	No Failure
2/14/70	14	13.5	68.838	Failure
2/15/70	15	13.0	100.065	No Failure
2/16/70	16	13.5	7.976	Failure
2/18/70	17	13.0	102.604	No Failure
2/19/70	18	13.5	6.194	Failure
2/19/70	19	13.0	9.134	Failure
2/21/70	20	12.5	102.665	No Failure

STAIRCASE FATIGUE DATA SHEET

Machine No. 4 0.0625 diameter wire

Cutoff: 1×10^7 cycles

Date	Spec. No.	Bend Angle, Degrees	Cycles to Failure $\times 10^{-5}$	Remarks
2/22/70	21	13.0	6.258	Failure
2/22/70	22	12.5	121.912	No Failure
2/28/70	23	13.0	110.676	No Failure
2/28/70	24	13.5	6.166	Failure
3/1/70	25	13.0	101.512	No Failure
3/4/70	26	13.5	5.430	Failure
3/7/70	27	13.0	102.365	No Failure
3/8/70	28	13.5	4.401	Failure
3/8/70	29	13.0	10.157	Failure
3/10/70	30	12.5	103.889	No Failure
3/11/70	31	13.0	107.318	No Failure
3/12/70	32	13.5	109.024	No Failure
3/17/70	33	14.0	6.280	Failure
3/17/70	34	13.5	34.012	Failure
3/18/70	35	13.0	100.000	No Failure
4/1/70	36	13.5	13.614	Failure
4/3/70	37	13.0	100.527	No Failure
4/4/70	38	13.5	2.187	Failure
4/6/70	39	13.0	100.625	No Failure
4/7/70	40	13.5	129.056	No Failure

STAIRCASE FATIGUE DATA SHEET

Machine No. 4 0.0625 diameter wire

Cutoff: 1×10^7 cycles

Date	Spec. No.	Bend Angle, Degrees	Cycles to Failure $\times 10^{-5}$	Remarks
4/8/70	41	14.0	6.761	Failure
4/9/70	42	13.5	100.027	No Failure
4/9/70	43	14.0	3.392	Failure
4/10/70	44	13.5	7.812	Failure
4/10/70	45	13.0	4.614	Failure
4/11/70	46	12.5	28.635	Failure
4/11/70	47	12.0	144.304	No Failure
4/12/70	48	12.5	122.083	No Failure
4/12/70	49	13.0	7.488	Failure
4/13/70	50	12.5	19.058	Failure
4/14/70	51	12.0	100.287	No Failure
4/15/70	52	12.5	101.783	No Failure
4/15/70	53	13.0	20.993	Failure

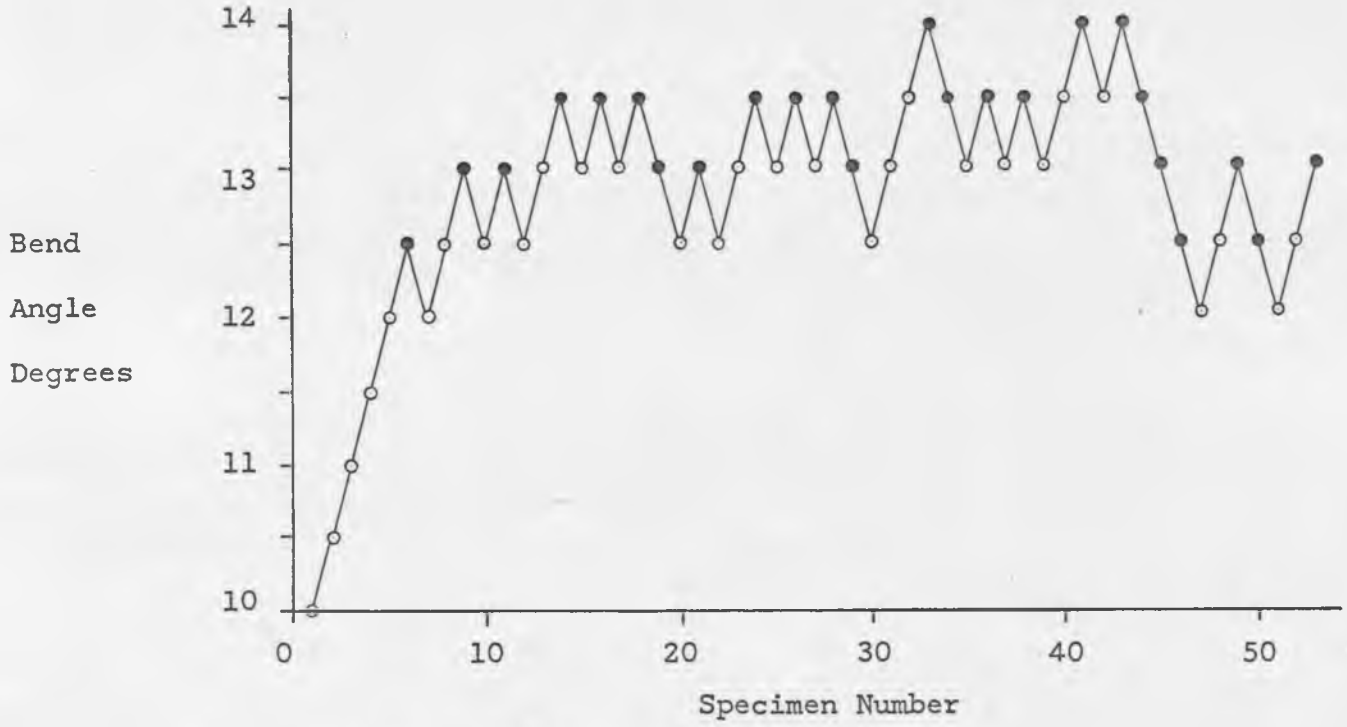

Figure B-9. Staircase Plot, 10^7 Cycles.

APPENDIX C

COMPUTER PROGRAMS

The computer programs mentioned in Chapter 4 will be presented here along with explanations of each including the meaning of all of the symbols and operations in the Focal-8 language for the PDP-8 computer.

The notations for the various operations in Focal-8 language are quire similar to those in Fortran. The operations that were used in both computer programs are contained in Table C-1 (19, Chapters 2 and 3).

Table C-1. Computer Operations.

Symbol	Operation
*	Multiplication
/	Division
+	Addition
-	Subtraction
FEXP(X)	e^x
FLOG(X)	ln (x)

The first computer program was used to determine the constants in Equations 1.3 and 1.4 and to evaluate the plastic,

Table C-2. Symbols for First Computer Program

Symbol	Definition of Symbol
E	Modulus of Elasticity, 30×10^6 psi
N1	0.25 Cycles
N2	Endurance Life, 2.5×10^6 Cycles
SF	Tensile Fracture Stress, 170,000 psi
E1	Elastic Strain Range at 0.25 Cycles
E2	Endurance Elastic Strain Range, 0.00388 in/in
GA	Material Constant, γ
G	Material Constant, G
D	Ductility
E3	Plastic Strain Range at 10 Cycles
N3	10 Cycles
N4	10,000 Cycles
E4	Elastic Strain Range at 10,000 Cycles
E5	Plastic Strain Range at 10,000 Cycles
Z	Material Constant, z
M	Material Constant, M
N	Cycle Life, N
EE	Elastic Strain Range at N Cycles
EP	Plastic Strain Range at N Cycles
ET	Total Strain Range at N Cycles

elastic and total strain ranges for the series of cycle lives using these constants. The meanings of the program variables are presented in Table C-2. This program was designed to print out the numerical values for G, γ, M and z. After performing this operation, the computer was programmed to ask for a value of N, the cycle life. The operator would give the computer a value for N and the computer would type the plastic, elastic and total strain ranges for that cycle life. The program repeated this process of asking for N for as long as desired by the operator. A copy of the program is shown in Figure C-1.

The second computer program was used to find the total strain range for various values of the total stress range, the result being Figure 4-7. The computer was instructed to ask for the stress range and then would type the strain range, repeating the process until told to stop by the operator. The symbols used in this program and the meaning of each is shown in Table C-3. The program itself is in Figure C-2.

Table C-3. Symbols for Second Computer Program

Symbol	Definition of Symbol
E	Modulus of Elasticity, 30 x 10^6 psi
G	G, 380,202 psi
M	M, 0.55242
Z	z, -0.541196
GA	γ, -0.080348
S	Stress Range
ER	Strain Range

```
C-FOCAL,1969

01.10 S E=30000000
01.20 S N1=.25
01.30 S N2-2500000
01.40 S SF=170000
01.50 S E1-2.5*SF/E
01.60 S E2=.00388
01.70 S GA=(FLOG(E1)-FLOG(E2))/(FLOG(N1)-FLOG(N2))
01.80 S G=E*E1/FEXP(GA*FLOG(N1))
01.90 S D=-FLOG(.58)

02.10 S E3=.25*FEXP(.75*FLOG(D))
02.20 S N3=10
02.30 S N4=10000
02.40 S E4=(G/E)*FEXP(GA*FLOG(N4))
02.50 S E5=(.0132-E4)/1.91
02.60 S Z=(FLOG(E3)-FLOG(E5))/(FLOG(N3)-FLOG(N4))
02.70 S M=(E3)/FEXP(Z*FLOG(N3))
02.80 T %, "G" G,!,"GAMMA" GA,!,"M" M,!, "Z" Z,!
02.90 FOR X=1,1,25;DO 3.0

03.10 A "CYCLES" N
03.20 S EE=(G/E)*FEXP(GA*FLOG(N))
03.30 S EP=M*FEXP(Z*FLOG(N))
03.40 S ET=EE+EP
03.50 T %, "ELASTIC STRAIN" EE,!
03.60 T %, "PLASTIC STRAIN" EP,!
03.70 T %, "TOTAL STRAIN" ET,!
*
```

Figure C-1. First Computer Program.

```
C-FOCAL,1969

01.10 S E=30000000
01.20 S G=380202
01.30 S M=.55242
01.40 S Z=-.542196
01.50 S GA=-.080348
01.60 FOR X=1,1,35; DO 2.0

02.10 A "STRESS RANGE" S
02.20 S ER=S/E+M*FEXP((Z/GA)*FLOG(S/G))
02.30 T %, "STRAIN RANGE" ER,!
```

Figure C-2. Second Computer Program.

For a more complete explanation of the procedures used in programming with Focal-8 language see reference 19 (Chapters 2 and 3).

NOMENCLATURE

A	First Moment of Frequency
a	Material Constant
α	Bend Angle
B	Second Moment of Frequency
b	Material Constant
C	Material Constant
c	Distance from Neutral Axis
D	Ductility
d	Staircase Increment
Δ	Deflection
E	Modulus of Elasticity
ε	Strain
ε_{el}	Elastic Strain Range
ε_{p}	Plastic Strain Range
$\Delta\varepsilon$	Total Strain Range
G	Material Constant
γ	Material Constant
I	Moment of Inertia
i	Staircase Ranking Subscript
K	Material Constant
L	Deflected Length of Wire Specimen
ℓ	Effective Length of Wire Specimen

M	Material Constant
m	Bending Moment
μ	Mean of a Normal Distribution
N	Total of Less Frequent Event in Staircase Test
N	Cycles of Failure
n_i	Frequency
P	Load
R.A.	Reduction in Area in a Tensile Test
S	Maximum Stress
S'	Minimum Stress
S_{end}	Endurance Stress
S_f	Tensile Fracture Stress
S_i	Internal Stress
S_{ut}	Ultimate Tensile Strength
S_t	Strength
ΔS	Total Stress Range
s	Estimate of Standard Deviation of Strain
s_t	Estimate of Standard Deviation of Strain Range
σ	Standard Deviation of a Normal Distribution
$\bar{y}$	Estimate of Mean Strain
$\bar{y}_t$	Estimate of Mean Strain Range
y'	Lowest Staircase Level
y_o	First Staircase Level
z	Material Constant

REFERENCES

1. Haugen, Edward B., Probabilistic Approaches to Design, John Wiley and Sons, Inc., N. Y., 1968.

2. Madayag, Angel F., Metal Fatigue: Theory and Design, John Wiley and Sons, Inc., N. Y., 1969.

3. Manson, S. S., Thermal Stress and Low-Cycle Fatigue, McGraw-Hill Book Co., Inc., N. Y., 1966.

4. Sines, George and Waisman, J. L., Metal Fatigue, McGraw-Hill Book Co., Inc., N. Y., 1959.

5. Van Vlack, Lawrence H., Elements of Materials Science, Addison-Wesley Pub. Co., Inc., Reading, Mass., 1964.

6. Byars, Edward F. and Snyder, Robert D., Engineering Mechanics, of Deformable Bodies, International Textbook Co., Scranton, Pa., 1963.

7. Johnson, Ray C., Optimum Design of Mechanical Elements, John Wiley and Sons, Inc., N. Y., 1961.

8. Juvinall, Robert C., Engineering Considerations of Stress, Strain and Strength, McGraw-Hill Book Co., Inc., N. Y., 1967.

9. Freudenthal, A. M. and Gumbel, E. J. "On the Statistical Interpretation of Fatigue Tests", The Proceedings of the Royal Society of London, Vol. 216A, 1952.

10. Shigley, Joseph E., Mechanical Engineering Design, McGraw-Hill Book Co., Inc., N. Y., 1963.

11. McLean, D., Mechanical Properties of Metals, John Wiley and Sons, Inc., N. Y., 1962.

12. Tweeddale, J. G., The Mechanical Properties of Metals, American Elsevier Pub. Co., N. Y., 1964.

13. Peterson, Gary J., Design Refinement and Experimental Research on Wire Fatigue Machines, Master's Report, University of Arizona, Tucson, 1970.

14. Corten, H. T. and Sinclair G. M., "A Wire Fatigue Machine for Investigation of the Influence of Complex Stress Histories", ASTM Proceedings, Vol. 56, American Society for Testing Materials, Philadelphia, 1956.

15. Chemical Rubber Co., Standard Mathematical Tables, 13th Edition, Cleveland, Ohio, 1964.

16. Dixon, W. J., and Mood, A. M., "A Method of Obtaining and Analyzing Sensitivity Data", Journal of the American Statistical Association, Vol. 43, 1948.

17. Finney, D. F., Probit Analysis, Cambridge at the University Press, 1962.

18. A Guide for Fatigue Testing and The Statistical Analysis of Fatigue Data, ASTM Special Technical Publication No. 91-A, 2nd Edition, American Society for Testing Materials, Philadelphia, 1963.

19. Digital Equipment Corp., Focal-8, PDP-8 Family Programming Manual, Maynard, Mass., 1970.

CORKEN PUMP COMPANY
A Subsidiary of Southwest Factories, Inc.
3805 N.W. 36TH STREET/P.O. BOX 12338/ OKLAHOMA CITY, OKLAHOMA 73112, U.S.A./PHONE 405—946-5576

Mrs. Kozan
Graduate College
University of Arizona
Tucson, Arizona 85721

August 5, 1970

Mrs. Kozan, this letter is to inform you that copyright application has been made for my Master's Thesis "A Statistical Analysis of the Transition Zone of the S-N Curve for AISI 4340 Steel". If you require any further information or have any questions please let me know. Unless I hear from you to the contrary, I assume I have fulfilled all graduation requirements.

Neal R. Kennedy

NRK:ww

State of Oklahoma
County of Oklahoma

Subscribed and sworn to before me this fifth day of August, 1970.
My Commission expires November 22, 1972.

Notary Public